

Institute of Geoecology

**An analysis of hydraulic, environmental and economic impacts
of flood polder management at the Elbe River**

A dissertation submitted to the Faculty of Mathematics and Natural Sciences at the
University of Potsdam, Germany
for the degree of Doctor of Natural Sciences (Dr. rer. nat.) in Geoecology

by
Saskia Förster

Potsdam, August 2008

Online published at the
Institutional Repository of the Potsdam University:
<http://opus.kobv.de/ubp/volltexte/2008/2726/>
[urn:nbn:de:kobv:517-opus-27260](#)
[<http://nbn-resolving.de/urn:nbn:de:kobv:517-opus-27260>]

Contents

Summary.....	7
Zusammenfassung	9
<hr/>	
Chapter I Introduction.....	11
1 Background	11
2 Objective and Research questions	12
3 Study areas.....	12
4 Outline of the thesis.....	14
<hr/>	
Chapter II Flood risk reduction by the use of retention areas at the Elbe River.....	15
1 Introduction	16
2 Description of the study area.....	16
3 Research approach	17
4 Modelling the inundation of the polder system.....	17
4.1 Outline of the CR Model	17
4.2 Application of the CR Model to the Lower Havel River	18
4.3 Aggregation of simulation results	20
5 Damage assessment in the polder system.....	20
6 Assessment of potential damage reduction in Wittenberge.....	21
6.1 Determination of flooded areas	21
6.2 Assessment of potential damage in Wittenberge.....	23
7 Cost-benefit analysis	23
8 Discussion and conclusions.....	24
<hr/>	
Chapter III Hydrodynamic simulation of the operational management of a proposed flood emergency storage area at the Middle Elbe River.....	27
1 Introduction	28
2 Study area.....	28
3 Hydrodynamic model setup.....	31
4 Considered flood scenarios and control strategies.....	32
4.1 Flood frequency analysis	32
4.2 Definition of flood scenarios.....	33

4.3 Definition of control strategies	33
5 Results	35
6 Conclusions and discussion	37
Chapter IV Comparison of hydrodynamic models of different complexities to model floods with emergency storage areas.....	39
1 Introduction	40
2 Study Area and Data Used.....	41
3 Methodology	42
3.1 One-dimensional model setup	42
3.1.1 Calibration and validation of model	43
3.2 One-/ two-dimensional model setup.....	43
3.3 Sensitivity analysis	44
3.3.1 Manning's n	44
3.3.2 DEM's of different resolutions	44
3.3.3 Number of cross-sections used	44
3.3.4 Gate opening time and opening/closing duration.....	45
4 Results and Discussions	45
4.1 Calibration and validation of the one-dimensional model	45
4.2 One-dimensional model results for flooding and emptying processes in the polder.....	46
4.3 Comparison of one- and one-/ two-dimensional model results.....	48
4.4 Computation time, storage space requirements and modelling effort	48
4.5 Sensitivity analysis	50
4.5.1 Manning's n	50
4.5.2 DEM's of different resolutions	51
4.5.3 Number of cross-sections used	53
4.5.4 Gate opening time and opening/closing duration.....	53
5 Conclusions	54
Chapter V Simulation of water quality in a flood detention area using models of different spatial discretisation	57
1 Introduction	58
2 Study site.....	58
3 Methods and data	59
3.1 Comparison of the 0D and the 2D approach.....	59
3.2 Water quality processes	60
3.3 Computational procedures.....	63
3.4 Boundary conditions, parameters, and initial values	63
3.5 Analysis of uncertainty	64
4 Results	66
4.1 Simulation results of the two models	66
4.2 Uncertainty of predictions	68

5 Discussion and conclusions	69
5.1 The impact of spatial discretisation	69
5.2 Conclusions from the uncertainty analysis	70
5.3 Implications and recommendations	70

Chapter VI Assessing flood risk for a rural detention area	73
1 Introduction	74
1.1 Damage estimation methods	74
1.2 Study site.....	76
2 Methodology	76
2.1 Damage estimation.....	77
2.2 Flood frequency analysis	79
3 Results	81
4 Sensitivity analysis	83
5 Discussion and Conclusions	84

Chapter VII Conclusions and recommendations	87
1 Conclusions	87
1.1 Hydrodynamic modelling.....	87
1.2 Water quality modelling.....	88
1.3 Vulnerability assessment.....	88
1.4 Model complexity.....	89
2 Recommendations.....	90
2.1 Flood polder management.....	90
2.2 Future research	92
References	95
Acknowledgements	101
Curriculum Vitae and list of publications	103
Author's declaration	105

SUMMARY

In recent years, extreme river floods have occurred in many European countries including Germany. These events have triggered a shift from traditional safety-oriented flood protection to a comprehensive flood risk management approach. Flood risk management comprises measures that aim at reducing the flood hazard as well as the vulnerability to floods.

Flood polders are part of the flood risk management strategy for many lowland rivers. They are used for the controlled storage of flood water so as to lower peak discharges of large floods. Consequently, the flood hazard in adjacent and downstream river reaches is decreased in the case of flood polder utilisation. Flood polders are dry or partially wet storage reservoirs that are typically characterised by agricultural activities or other land use of low economic and ecological vulnerability.

The objective of this thesis is to analyse hydraulic, environmental and economic impacts of the utilisation of flood polders in order to draw conclusions for their management. For this purpose, hydrodynamic and water quality modelling as well as an economic vulnerability assessment are employed in two study areas on the Middle Elbe River in Germany. One study area is an existing flood polder system on the tributary Havel, which was put into operation during the Elbe flood in summer 2002. The second study area is a planned flood polder, which is currently in the early planning stages. Accordingly, the studies can be addressed as ex-post and ex-ante investigations.

Hydrodynamic numerical models are applied in both study areas to investigate peak reduction and flooding characteristics under different flood scenarios and operational schemes. It is demonstrated that flood peak levels can effectively be capped by temporary water storage. However, the research also shows that the obtainable flood peak reduction strongly depends on the shape of the flood hydrograph. Flooding characteristics such as water depth, flow velocity and inundation duration exhibit a large spatial variation throughout the flood polder areas. This information provides input for the subsequent water quality modelling and vulnerability assessment.

Long water storage may have negative environmental effects. A major problem that has been observed in flood polders on the Elbe River during the August 2002 flood was the depletion of dissolved oxygen due to the strong oxygen demand imposed by organic material in the water body and on agricultural fields. Therefore, a numerical model is employed for the simulation of dissolved oxygen dynamics throughout the filling, stagnancy and emptying phases of the flood polder operation.

The economic vulnerability assessment focuses on agricultural land according to the prevailing land use in the flood polders. In contrast to other damage categories, losses on agricultural fields exhibit a strong seasonal pattern, while the flooding probability also has a seasonal variation. Both seasonal aspects are included in the estimation of annual losses on agricultural land.

Furthermore, numerical models of different spatial dimensionality, ranging from zero- to two-dimensional, are applied in order to evaluate their suitability for hydrodynamic and water quality simulations of flood polders in regard to performance and modelling effort. For many applications, models of lower dimensionality may deliver sufficiently accurate results, while providing the opportunity to investigate various scenarios and extensively test model sensitivity. In contrast, two-dimensional models require a considerably higher computational effort, but are inevitable for certain applications. Generally, two-dimensional approaches may be preferred in floodplain areas of complex topography and distinct spatial variations in hydraulic variables such as flow velocity and water depth. For practical applications, it is suggested to use a simplistic approach first and increase spatial dimensionality if the target variables show a large spatial variability.

The thesis concludes with overall recommendations on the management of flood polders, including operational schemes and land use. In view of future changes in flood frequency and further increasing values of private and public assets in flood-prone areas, flood polders may be effective and flexible technical flood protection measures that contribute to a successful flood risk management for large lowland rivers.

ZUSAMMENFASSUNG

In den vergangenen Jahren traten in vielen europäischen Ländern einschließlich Deutschland extreme Fluss-Hochwasser auf. Diese Ereignisse haben einen Wandel vom traditionellen auf Sicherheit ausgerichteten Hochwasserschutz zu einem übergreifenden Hochwasserrisikomanagement angestoßen. Das Hochwasserrisikomanagement umfasst sowohl Maßnahmen zur Verminderung der Hochwassergefährdung als auch der Vulnerabilität gegenüber Hochwassern.

Flutpolder sind Bestandteil des Hochwasserrisikomanagements an vielen Tieflandflüssen. Sie werden zum gesteuerten Rückhalt von Wasser eingesetzt, um Spitzenabflüsse von großen Hochwassern zu senken. Dadurch wird im Falle des Flutpoldereinsatzes die Hochwassergefährdung für benachbarte und unterstrom liegende Flussabschnitte verringert. Flutpolder sind trockene oder teilweise vernässte Staubecken, welche typischerweise durch landwirtschaftliche oder andere Landnutzung geringer ökonomischer und ökologischer Vulnerabilität gekennzeichnet sind.

Ziel dieser Dissertation ist die Analyse von hydraulischen, ökologischen und ökonomischen Auswirkungen des Einsatzes von Flutpoldern, um daraus Schlussfolgerungen für ihre Bewirtschaftung zu ziehen. Dazu werden hydrodynamische und Wassergütemodelle eingesetzt sowie erfolgt eine Abschätzung der ökonomischen Vulnerabilität in zwei Untersuchungsgebieten an der Mittleren Elbe in Deutschland. Ein Untersuchungsgebiet ist ein existierendes Flutpoldersystem am Nebenfluss Havel, welches während der Elbeflut im Sommer 2002 zum Einsatz kam. Das zweite Untersuchungsgebiet ist ein geplanter Flutpolder, welcher sich bisher noch in einem frühen Planungsstadium befindet. Entsprechend können die Studien als ex-post und ex-ante Untersuchungen bezeichnet werden.

Hydrodynamisch-numerische Modelle werden in beiden Untersuchungsgebieten angewandt, um die Hochwasserkappung und die Überflutungscharakteristik unter verschiedenen Hochwasserszenarien und Kontrollstrategien zu untersuchen. Es wird gezeigt, dass Hochwasserspitzen durch zeitweiligen Wasserrückhalt effektiv gekappt werden können. Jedoch belegen die Untersuchungen auch, dass der erzielbare Kappungsbetrag stark von der Form der Hochwasserwelle abhängt. Überflutungskenngrößen wie Wassertiefe, Fließgeschwindigkeit und Überflutungsdauer weisen eine große räumliche Variabilität innerhalb der Flutpolder auf. Diese Daten bilden eine Grundlage für die anschließende Wassergütemodellierung und Schadensabschätzung.

Eine lang anhaltende Wasserspeicherung kann negative ökologische Effekte hervorrufen. Ein großes Problem, welches in Flutpoldern an der Elbe während des Hochwassers im August 2002 beobachtet wurde, stellt die Zehrung von gelöstem Sauerstoff aufgrund des hohen Sauerstoffbedarfs dar, der durch organisches Material im Wasser und auf landwirtschaftlichen Feldern hervorgerufen wird. Daher wird die Dynamik des gelösten Sauerstoffes während der Flutungs-, Stagnations- und Entleerungsphase des Flutpoldereinsatzes mit einem numerischen Modell simuliert.

Die Abschätzung der ökonomischen Vulnerabilität konzentriert sich hauptsächlich auf landwirtschaftliche Flächen entsprechend der vorherrschenden Flächennutzung in den Flutpoldern. Im Gegensatz zu anderen Schadenkategorien weisen Verluste auf landwirtschaftlichen Feldern einen ausgeprägten saisonalen Verlauf auf, während sich die Hochwasserwahrscheinlichkeit auch im Jahresverlauf ändert. Beide saisonalen Aspekte werden bei der Abschätzung der jährlichen Verluste auf landwirtschaftlichen Flächen einbezogen.

Darüber hinaus werden numerische Modelle verschiedener räumlicher Dimensionalität von null- bis zwei-dimensional angewandt, um ihre Eignung für hydrodynamische und Wassergütesimulationen von Flutpoldern hinsichtlich der Leistungsfähigkeit und des Modellierungsaufwands zu bewerten. Für viele Anwendungen liefern Modelle geringere Dimensionalität ausreichend genaue Ergebnisse, während sie die Untersuchung von vielfältigen Hochwasserszenarien und eine ausführliche Überprüfung der Modellsensitivität ermöglichen. Im Gegensatz dazu benötigen zwei-dimensionale Modelle einen erheblich höheren Rechenaufwand, sind allerdings für bestimmte Anwendungen unumgänglich. Allgemein sollten zwei-dimensionale Modelle in Überflutungsgebieten mit komplexer Topographie und ausgeprägter räumlicher Variabilität von hydraulischen Größen wie Fließgeschwindigkeit und Wassertiefe bevorzugt

werden. Für die praktische Umsetzung wird vorgeschlagen, mit einem einfachen Ansatz zu beginnen und die räumliche Dimensionalität zu erhöhen, falls die Zielgrößen eine hohe räumliche Variabilität aufweisen.

Die Dissertation schließt mit übergreifenden Empfehlungen zur Bewirtschaftung von Flutpoldern einschließlich Kontrollstrategien und Landnutzung ab. Im Hinblick auf zukünftige Änderungen in der Auftretenshäufigkeit von Hochwassern und weiterhin ansteigenden Werten von privatem und öffentlichem Vermögen in überflutungsgefährdeten Gebieten stellen Flutpolder ein effektive und flexible Maßnahmen des technischen Hochwasserschutzes dar, welche zu einem erfolgreichen Hochwasserrisikomanagement großer Tieflandflüsse beitragen.

Chapter I

Introduction

1 BACKGROUND

In the last few decades, floods in Europe have become a growing issue of concern for citizens and authorities (Alphen et al., 2008) as several extreme river floods have occurred in many European countries including Germany. At the same time, the value of public and private assets in flood prone areas has further increased. Moreover, effects of climate change on flood frequency are projected in many studies. For instance, Christensen and Christensen (2003) state that the frequency of severe summer flooding over large parts of Europe is likely to increase, despite the general trend to drier summer conditions. Furthermore, regional changes in the seasonality of floods have already been observed in many areas of Europe as a result of changes in the flood-generating mechanisms (Kundzewicz, 2008). These developments have triggered a new comprehensive approach on flood risk management on a European level which finally led to the adoption of the Directive on the Assessment and Management of Flood Risk (EU, 2007). According to this directive, flood risk is defined as a combination of the probability of a flood event and of the potential adverse consequences to human health, the environment, cultural heritage and economic activity associated with a flood event. Flood risk management comprises measures that aim to reduce flood hazard and vulnerability to floods. Certain flood risk measures apply to floods of different recurrence intervals (DKKV, 2004). During rare floods with recurrence intervals between approximately 10 and 200 years, the flood hazard can be reduced by technical measures such as dikes, reservoirs or so-called flood polders, whereas during very rare floods with recurrence intervals larger than approximately 200 years, organisational meas-

ures such as hazard zoning, early warning systems or evacuations become most important.

Flood polders are embanked areas that are intentionally inundated during large floods so as to reduce peak flood flows and hence the hazard in adjacent and downstream river reaches. Flood polders contribute to the flood risk management strategy for many lowland rivers in Germany, other European countries and elsewhere (for examples, cf. Dijkman et al., 2003). The term “flood polder” originates from the equivalent German word. Other commonly used terms are flood detention area or off-stream flood storage reservoir. Figure 1 shows a schematic view of a flood polder. It is usually enclosed by a separation dike to the river and by an additional polder dike to the hinterland if an increasing topography does not limit the water flow (Fischer et al., 2005).

Ideally, the discharge up to a pre-defined level will be passed into the flood polder by use of adjustable control structures. For a maximum peak reduction, the flood wave needs to be cut horizontally. During the emptying process, the stored water should be released as soon as possible provided that water levels in the main river allow for safe discharges at the downstream river reaches (Hall et al., 1993). The land within the storage area may be used for agriculture or other low-intensity purposes, but is not suitable for buildings or similar investments (Smith and Ward, 1998).

The effectiveness of a flood protection measure refers to the extent to which the measure’s objectives are achieved (OECD, 2002). Flood peak reduction, being the main objective of flood polder utilisation, is influenced by several factors such as the storage capacity compared to the discharge volume of the flood wave, the operational scheme of the control structures, the quality of the flood forecast and the shape of the flood wave (Dijkman et al., 2003).

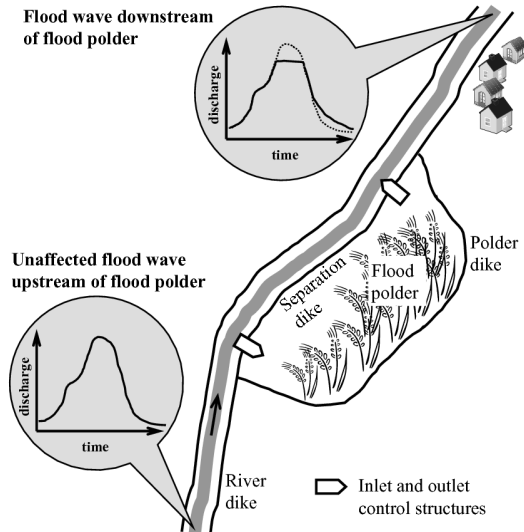


Fig. 1: Schematic of flood peak attenuation by the use of controlled water storage in flood polders

The efficiency is a measure of how economically resources are converted into results (OECD, 2002). In the case of flood polders, it is mostly affected by the prevented damage in the downstream areas or reduced expenses for flood management, the costs for construction and maintenance of the flood polder dikes and control structures, damage occurring due to the temporary water storage and the probability of utilisation (Gocht and Bronstert, 2006).

Apart from economic losses, utilisation of flood polders can lead to environmentally harmful situations. An environmental side effect that has been observed during long storage times is the depletion of dissolved oxygen in the water due to the strong oxygen demand imposed by organic material in the water body and on the agricultural fields. This may cause stress on terrestrial and aquatic ecosystems and in particular on fish populations in the storage area or in the river after release of stored water. After flood polder utilisation at a tributary of the Elbe River in summer 2002, an almost complete fish extinction in the adjacent river reach was observed, which was directly linked to the depletion of dissolved oxygen in the water (Böhme et al., 2005).

2 OBJECTIVE AND RESEARCH QUESTIONS

The overall objective of this thesis is to assess hydraulic, environmental and economic

impacts of the utilisation of flood polders for flood peak reduction during large flood events. It is addressed by applying models of different complexities in terms of spatial dimensionality (hydraulic and water quality modelling) and time frame (vulnerability assessment) in order to evaluate their suitability for flood polder studies.

To tackle the overall objective the following research questions are posed:

- How effective are the flood polders in terms of peak reduction for varying flood scenarios and operational schemes?
- How does the long water storage affect water quality and particularly dissolved oxygen levels in the flood polders?
- How can economic vulnerability be assessed when considering time-varying damage in agricultural areas?
- Which is the appropriate model complexity to simulate hydraulic and water quality processes in flood polders?

3 STUDY AREAS

To address the research questions, investigations are carried out in two study areas, both situated on the Middle Elbe River in Germany (Figure 2). The first study area is a flood polder system on the tributary Havel (hereinafter called “Havelpolder system”), which was constructed in the 1950s and was set in operation during the

Elbe flood in summer 2002. The Lower Havel floodplain and six flood polder reservoirs on both sides of the Havel River near its confluence with the Elbe River provide room for retaining the Elbe flood peak. The maximum storage capacity of the flood polder reservoirs amounts to 110 million m³, while the overall storage capacity of both the flood polder reservoirs and the floodplain is approximately 250 million m³. Adjustable inlet control structures are only installed in one of the reservoirs. Instead, the other reservoirs were opened by dike blasting or excavation during their utilisation in summer 2002.

The second study area is the planned flood polder system Axien, which is not yet existing but in the early planning stages by the federal water authorities. Its maximum storage capacity

is planned to be 40 million m³. The planned flood polder consists of two separate reservoirs. Adjustable gates will control the inflow from and outflow to the river and the flow between the two reservoirs.

Both flood polder systems are designed to reduce flood peaks having a return period of approximately 100 years or larger, i.e. they will only be operated during very large flood events. The two study areas have a similar land use, which is dominated by intensive arable land and grassland. The agricultural fields constitute a large source of degradable organic material when inundated. After designation as flood polder, the original land use is maintained and farmers are paid for their losses in the case of flood polder utilisation.



Fig. 2: Map of the Elbe catchment with locations and photographic impressions of the study areas (modified after IKSE, 2005)

The Elbe is the forth largest river in Central Europe, having a total length of 1092 km and a catchment area of nearly 150000 km², which is shared by Germany (65 %), the Czech Republic (34 %), Poland and Austria (together less than 1 %). The main tributaries are the Moldau/Vltava, Saale and Havel, each comprising a catchment area of approximately 25000 km² (Figure 2).

The runoff seasonality of the Elbe River is strongly influenced by the Czech and German middle-mountain regions which cover about 30 % of the catchment area. It can be characterised as a pluvio-nival regime with highest discharges in March and April and low discharges from June to November. Compared to the runoff behaviour of some other large European rivers, e.g. the River Rhine, discharge in the

Elbe River is not affected by stored water in glaciers and permanent snow. More than 80 % of the floods occur during the winter and spring season in consequence of snow melt associated with intense rainfall. Floods in winter or spring are characterised by long durations, while summer floods caused by heavy continuous rains typically only last a few days, but they usually have higher flood magnitudes (IKSE, 2005).

The present-day embankments confining most of the German part of the Elbe River date back to the second half of the 19th century. However, diking at the Elbe River started as early as the 12th century. The dike construction led to a reduction of the retention area on German territory from 6172 km² to 838 km² (13.6 % of the original area) (BfG, 2002). Today, the reactivation of floodplains by dike-shifting and the designation of flood polders are discussed. Several sites along the middle course of the Elbe River have already been suggested as potential locations for flood polders (IKSE, 2003) and were investigated in terms of flood peak reduction potential (Helms et al., 2002; Busch and Hammer, 2007).

4 OUTLINE OF THE THESIS

Figure 3 illustrates how the chapters are related to the main research subjects, i.e. the investigation of hydraulic, environmental and economic impacts of flood polder utilisation.

Chapter II deals with the hydraulic simulations and the economic analysis carried out in study area 1. Effects of different flood scenarios and operational schemes on flood polder utilisation in study area 2 are investigated in Chapter III, while Chapter IV focuses on the comparison of hydrodynamic models of different spatial dimensionality for the same study area. Chapter V investigates the impact of flood polder utilisation on dissolved oxygen dynamics in study area 2, whereas economic vulnerability is estimated in Chapter VI. And finally, chapter VII presents overall conclusions based on the several studied aspects and gives recommendations regarding flood polder management and future research.

Chapters II to VI were written as stand-alone manuscripts that are either published or awaiting publication in international peer-reviewed journals (for full reference, see front pages of the chapters).

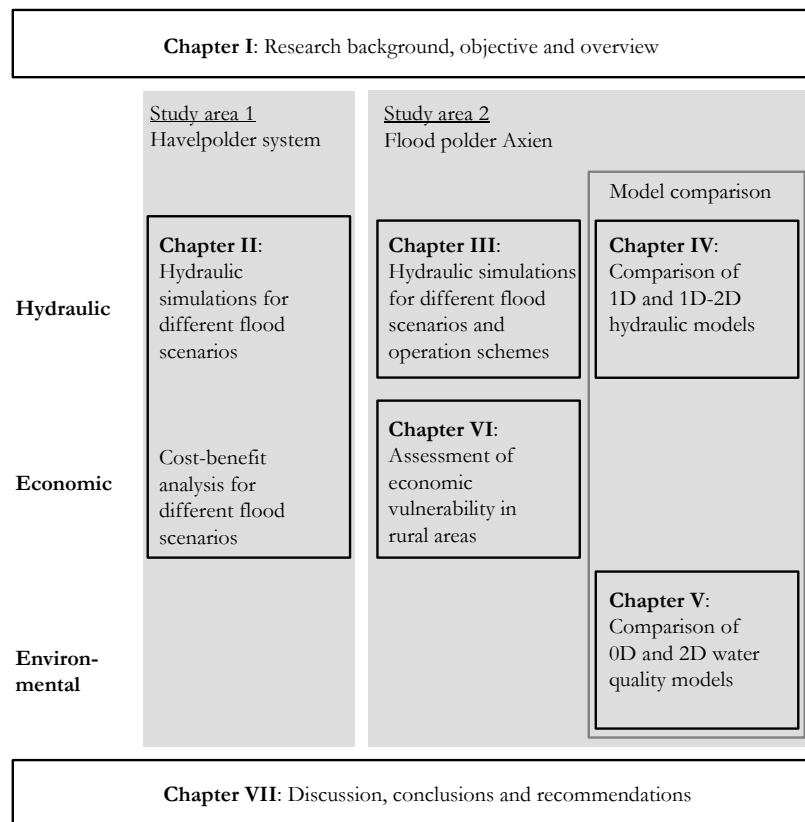


Fig. 3: Outline of the thesis

Chapter II

Flood risk reduction by the use of retention areas at the Elbe River

ABSTRACT:

The paper presents research results on flood risk mitigation by the controlled flooding of a retention area on the middle reaches of the Elbe River. The retention area consists of six large polders and the floodplain of a tributary, the Havel, and is located near the Havel's confluence with the Elbe River. The total retention volume of both the polders and the Havel floodplain amounts to approximately 250 million m³.

The controlled flooding of the retention area was simulated by the use of a conceptual model and assessed economically for two flood scenarios. In a cost-benefit analysis, the damage to agriculture, the road network, buildings and fishery caused by the flooding of the polders was compared with the resulting reduction in potential damage in the town of Wittenberge, 30 km downstream. On the basis of a monetary assessment it was concluded that the use of the retention area for flood protection is highly cost-effective in economic terms.

*Published as: Förster S, Kneis D, Gocht M and Bronstert A. 2005. Flood Risk Reduction by the Use of Retention Areas at the Elbe River. *Intl. Journal of River Basin Management*, 3 (1), 21-29.*

1 INTRODUCTION

In the last few years, floods have caused enormous damage in Central Europe. The flood of the Elbe River and its tributaries during the summer of 2002 was accompanied by the highest water levels ever measured at many gauging stations. The overall damage in Germany amounted to about 10 billion € (DKKV, 2004).

Flood risk management aims at minimising the impact of flood disasters (Plate, 2002). The use of retention areas can be an efficient measure in modern flood risk management. By controlled flooding of sparsely or non-populated areas with relatively low damage potential, the risk of inundation for downstream areas with higher vulnerability can be reduced.

The largest retention area along the Elbe River is situated on the tributary Havel near its confluence with the Elbe. This retention area consists of six large polders and the floodplain of the Lower Havel River which together have a potential retention volume of up to 250 million m³.

The system was constructed in the 1950s, but was used operationally for the first time during the Elbe flood in 2002. By controlled flooding of the retention area the peak stages were attenuated by approximately 40 cm at the gauge of Wittenberge (BfG, 2002). Consequently, the risk of inundation for the town of Wittenberge and areas further downstream was significantly reduced.

The flood peak reduction resulting from the use of the retention area was considered very successful by the water authorities. However, this assessment was not based on an economic evaluation including costs and benefits of the measure. Therefore, the aim of this study was to assess economically the use of the polders described above for flood protection in order to gain valuable information for their further use.

2 DESCRIPTION OF THE STUDY AREA

In the case of an extreme flood event along the middle stretches of the Elbe River, both the floodplain and the polders at either side of the Havel River provide storage capacity for retaining the Elbe flood peak (see Figure 1). The six polders comprise an area of 100 km² with a volume of 110 million m³. The overall potential retention

volume of the Havel floodplain and polders together amounts to approximately 250 million m³.

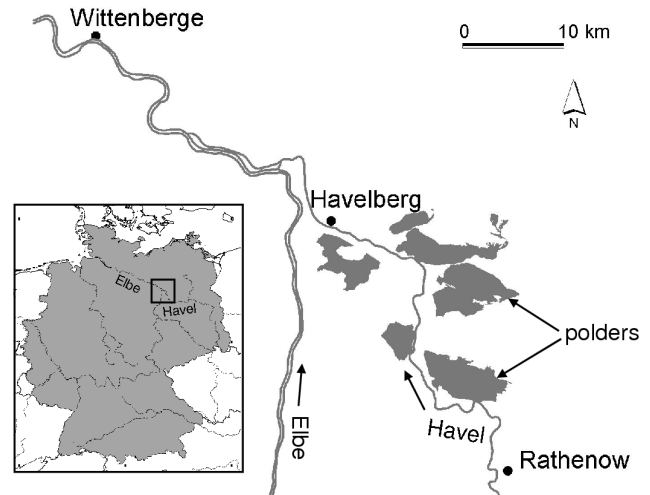


Fig. 1: Simplified map of the retention area near the confluence of the Havel and the Elbe River

Before the extensive construction of dikes and water-engineering works, the whole Lower Havel River floodplain was a natural retention area for the Elbe River and was characterised by frequent inundations. The dikes were constructed in order to protect settlements and agricultural areas from flooding. Extensive melioration and deforestation in the last centuries have enabled an intensive agricultural use of the polder area. The farmland is used as arable land and grassland in approximately equal shares. The main crops are winter grain and corn. The polders are only sparsely populated.

The discharge of the Havel into the Elbe River is controlled by several gates. In the case of an extreme flood along the Elbe River, the gates are closed in order to prevent the uncontrolled inflow of water from the Elbe into the Havel River. However, in time of peak discharge on the Elbe River, an emergency gate can be opened in order to divert and temporarily retain the Elbe flood peak in the retention area. The resulting flood peak reduction mitigates the flood risk for areas further downstream. Within this study the benefit of flooding the retention area for the town of Wittenberge was investigated. This town is situated on the Elbe about 30 km downstream of the confluence, and has a population of approximately 25 000 inhabitants. The lower parts of the town are protected against floods by embankments and mobile walls (see Figure 7).

3 RESEARCH APPROACH

Two different flood scenarios were analysed in this study. As a reference scenario the Elbe flood of August 2002 with a maximum discharge of $4225 \text{ m}^3/\text{s}$ at the gauge at Wittenberge was selected, since detailed hydrological observation data were available. Using these data, a conceptual inundation model (section 4) was calibrated and tested. The model provides a means to simulate the flooding of the retention area for the 2002 event but it also allows further user-defined flood scenarios to be investigated. The return period of the reference scenario was estimated to be about 180 years based on the discharge series 1900–2002.

A more extreme scenario (referred to as “scenario II”) was derived from the 2002 flood event by increasing the ordinates of the observed discharge hydrograph by a factor of 1.05. This transformation not only raises the peak discharge from 4225 to $4440 \text{ m}^3/\text{s}$ but also increases the total volume of the flood wave. The intention of scenario II was to design the largest possible flood that would not cause embankment failures in the town of Wittenberge provided that the polder system is used for flood peak retention. The return period of the second flood scenario was estimated to be about 300 years.

In the first step of the economic assessment it was assumed that the polder system is used for flood peak retention and consequently embankment failures in the town Wittenberge do not occur. For both flood scenarios stage hydrographs for the Havel River and the adjacent polders were deduced either from observed data (for the flood in 2002) or model simulations (for scenario II). The inundation extent and duration of flooding were determined from these hydrographs. Combining the results with data on agricultural land use and on the asset of houses and roads enabled the calculation of damage within the polders for both scenarios (section 5).

In a subsequent step it was hypothesised that the polders are not flooded, resulting in a partial inundation of Wittenberge. Therefore, potential damage in this town was determined for the two flood scenarios (section 6).

Finally, a cost-benefit analysis was carried out (section 7). Within this analysis losses resulting from controlled flooding of the polder system were compared with the potential damage in the town of Wittenberge that would occur if the Elbe

flood peak was not attenuated. Figure 2 shows the overall investigation scheme of the study.

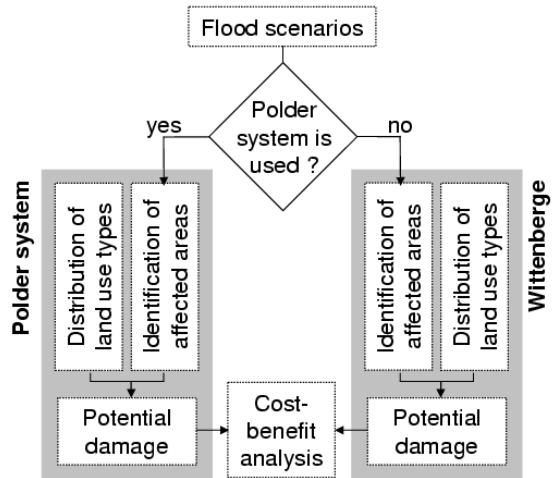


Fig. 2: Investigation scheme used within this study

4 MODELLING THE INUNDATION OF THE POLDER SYSTEM

The estimation of damage in the polders primarily requires information on the inundated area and the duration of flooding. While for the 2002 reference scenario these data could be derived from gauge observations and aerial views, the investigation of scenario II requires a simulation of the inundation process. For that purpose a simple but robust conceptual model, the “Coupled Reservoirs Model” (short: CR Model), was developed. Section 4.1 introduces the general outline of this model whereas section 4.2 deals with its application to the retention area on the Lower Havel River.

4.1 Outline of the CR Model

In the CR Model, the natural system consisting of river sections, floodplains and polders is discretised into a number of reservoirs. It is assumed that the water surface slope within each reservoir is negligible. Hence, reservoirs are described by simple storage functions relating water surface elevation to storage volume, mean depth and inundated area. Each reservoir may be linked to one or more adjacent reservoirs, allowing water to be exchanged. Boundary conditions can be assigned to reservoirs in order to account for external inflows and outflows of the modelled system.

Figure 3 exemplifies the model outline showing two polders connected to a river. The river

reach with its associated floodplain is subdivided into sections, each represented by a discrete but interconnected reservoir. The system's in- and outflows are associated with the most upstream and downstream river section, respectively. Two auxiliary reservoirs allow for the storage of water in the polders' soil zones.

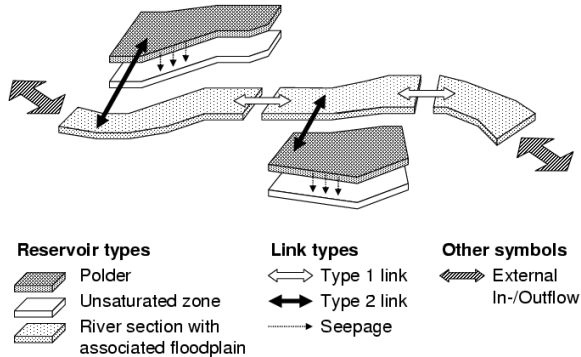


Fig. 3: Scheme of a simple polder system illustrating the outline of the Coupled Reservoirs Model. See text for explanation of individual elements.

The flow between coupled surface water reservoirs may be calculated by two different approaches. The first option is to compute flow rates from both slope and water surface elevation at the interface cross section of adjacent reservoirs. The underlying assumption is that a continuous slope exists between the coupled reservoirs, though in the model each reservoir is represented by a single stage only. Hence, the water surface elevation at the interface cross section can be estimated from the reservoirs' stages. This option provides a simple means to compute the flow between river sections, each of them represented by a separate reservoir (see "Type 1 link" in Figure 3). During the simulation, pre-processed lookup tables are used to determine the current flow rate depending on gradient and stage. A second option is used if adjacent reservoirs are connected by hydraulic control structures. Because the water surface profile changes rapidly at these locations, flows are directly calculated from the reservoirs' stages. Control structures like breaches, weirs and culverts usually provide the link between polders and the river (see "Type 2 link" in Figure 3). Again, lookup tables are used to derive the flow from stage information during a model run.

A special type of reservoir was implemented to account for the storage of water in the unsaturated soil zone (see Figure 3). Seepage from surface water reservoirs to the aquifer is estimated using a leakage approach (Eq. 1):

$$Q_S = A \cdot L \cdot \begin{cases} (h_O - h_B) & \text{if } h_{GW} < h_B \\ (h_O - h_{GW}) & \text{if } h_{GW} \geq h_B \end{cases} \quad (1)$$

where Q_S = seepage flow ($\text{m}^3 \text{s}^{-1}$), A = inundated area of the surface water reservoir (m^2), h_O = surface water elevation (m), h_{GW} = groundwater surface elevation (m), h_B = average terrain elevation of the inundated area (m). The leakage factor L (s^{-1}) is subject to calibration. For reasons of simplicity it is assumed that seepage causes the ground water surface to rise instantaneously with the soil water content of the above layer remaining unchanged. Furthermore the groundwater surface is assumed to be horizontal and lateral groundwater flow between reservoirs is not simulated.

Two types of boundary conditions are available in the CR Model for representing inflows and outflows of the modelled system. On the one hand external in-/outflows can be assigned to a reservoir by directly specifying a discharge time series. On the other hand stage hydrographs can be used as boundary condition. In the latter case the reservoir's in-/outflow rates are derived from a pre-processed lookup table, relating the flow to both the external stage given by a time series and the stage in the modelled reservoir itself.

The output files of the CR Model provide time series of water level and storage volume for each reservoir. Furthermore, flow rates between reservoirs (link flows) and boundary conditions are continuously recorded.

4.2 Application of the CR Model to the Lower Havel River

The retention area at the Lower Havel River was modelled as a system of 17 reservoirs (see Figure 4). The Havel River with its associated floodplain was discretised into six subsections H1 to H6. The remaining 11 reservoirs include the six large emergency polders, two of them subdivided into two separate basins (P1–P8). The labels P9 to P11 mark three smaller polders separated from the floodplain by small dams only. Storage functions for all reservoirs were deduced from digital elevation models in a pre-processing step with the results being stored as lookup tables for subsequent use by the CR Model. Auxiliary reservoirs (not shown in Figure 4) represent the unsaturated soil zone of polders and floodplains

sections. Relationships between ground water level and storage volume for these reservoirs were estimated from the soil's air-filled porosity at field capacity and terrain elevation data.

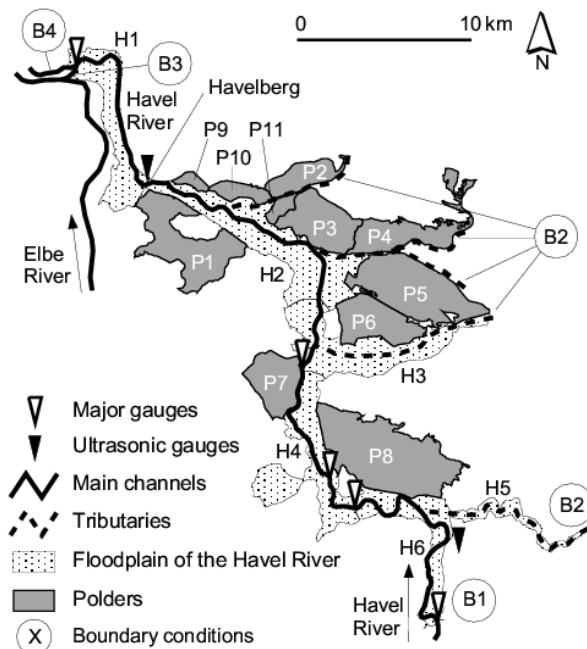


Fig. 4: Coupled Reservoirs Model of the retention area on the Lower Havel River. Reservoirs that correspond to polders and floodplain sections of the Havel River are labelled P1–P11 and H1–H6, respectively. Dikes separate the polders from the floodplain. Boundary conditions are labelled B1 to B4. The actual confluence of the rivers Elbe and Havel (not shown on the map) is located 8 km northwest of symbol B4. Further details are given in the text.

All boundary conditions are shown in Figure 4. The inflow of the Havel River into the modelled system is labelled B1. Discharge is constantly measured by an ultrasonic flow meter at this location providing reliable input data for the simulation of the 2002 reference scenario. For simplicity, a constant inflow at B1 was assumed for the simulation of scenario II. All minor tributaries of the Havel River are labelled B2. Due to the lack of flow gauges, their discharges had to be estimated from catchment size using mean specific discharges of nearby river basins. B3 marks the emergency gate through which water from the Elbe can be diverted into the Havel River. During the 2002 flood event, water levels were recorded by the operators and the flow through the gate was computed using a weir equation. For scenario II a corresponding flow series was generated which reflected the desired discharge reduction in the Elbe River as well as basic hydraulic features of the inlet structure and the overall storage capacity of the retention area. Whereas the boundary conditions B1 to B3 were imple-

mented by assigning inflow hydrographs to the corresponding reservoirs, a stage boundary condition was used to simulate the system's outflow through a constructed channel (label B4 in Figure 4). This was necessary as the outflow depends on both the stage at the channel's confluence with the Elbe River and the simulated stage at the channel's upstream end (reservoir H1). In addition, evaporation losses were taken into account in the simulation of the reference scenario to reflect the evaporation caused by the exceptionally hot weather conditions in August 2002.

As depicted in section 4.1, the CR Model accesses pre-processed lookup tables to compute the flow between adjacent reservoirs. The creation of appropriate tables was a major challenge in setting up the model. Connections between the floodplain sections H1 to H6 (Figure 4) were represented by links of "Type 1" (see section 4.1). Hence, relations between flow, water surface gradient and stage at the interface of the reservoirs had to be identified. For the reservoirs H1 and H2 a regression model was fitted, since stage and discharge are continuously recorded at the Havelberg gauge (Figure 4) and stage information is also available from adjacent gauges. The regression is of the type:

$$Q = P(h) \cdot \sqrt{S} \quad (2)$$

where Q = flow ($\text{m}^3 \text{s}^{-1}$), S = slope of the water surface ($-$) estimated from the stage difference of adjacent gauges, and $P(h)$ is a polynomial with the stage h (m) as argument. The goodness of fit is shown in Figure 5.

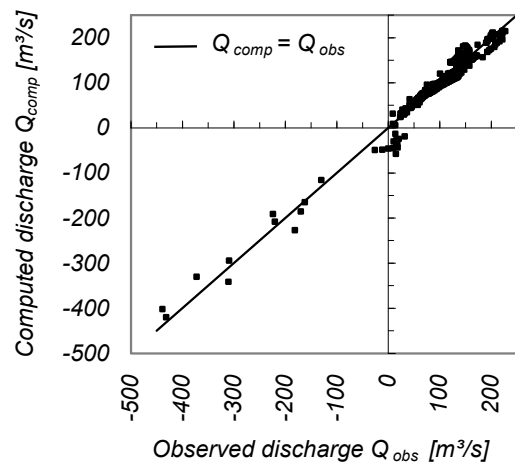


Fig. 5: Observed and computed discharge at the Havelberg gauge (see Figure 4) using multiple regression

Figure 5 indicates that the flow rate may be predicted from the regression with an acceptable level of error. This is true for both normal conditions ($Q > 0$) and reverse flow. The observed negative discharges at Havelberg occurred when the emergency gate (label B3 in Figure 4) was opened for flood peak attenuation in 2002. Lookup tables which are required to predict the flow between the remaining floodplain sections H2 to H6 (Figure 4) were derived from cross section geometry data using Manning's law. Roughness coefficients were taken from previous applications of a 1D hydrodynamic model. However, the computed flow rates should be considered as rough estimates only.

Since the polders P2–P11 (Figure 4) are flooded either through dike breaches or weirs, their connection to the corresponding floodplain sections was implemented using "Type 2" links (see section 4.1). The flow through either inlet structure was calculated using the POLENI equation:

$$Q = c \cdot \frac{2}{3} \cdot \sqrt{2g} \cdot \mu \cdot w \cdot h_u^{3/2} \quad (3)$$

where Q = flow ($\text{m}^3 \text{s}^{-1}$), μ = overflow coefficient (-), c = submergence correction factor (-), w = width of the inlet (m) and h_u = upstream energy head (m) above the crest. Appropriate values of μ were taken from (FAS, 1975) or calibrated in case of the breaches. The submergence correction factor c was estimated according to Schmidt (1957), using the ratio of downstream to upstream water level above the crest. Approaches of pipe hydraulics were used to create the required lookup table for polder P1 (Figure 4) since culverts provide the link to the Havel River at this location.

Simulations were carried out with a computational time step of 15 min. Since flow rates integrated over the length of a time step are small compared to the reservoirs' storage volumes, the CR Model uses a simple explicit solution technique.

4.3 Aggregation of simulation results

Since damage assessment in the polders (section 5) is based on inundation maps only, hydrographs and further results of the scenario simulations using the CR Model are not presented here. Figure 6 gives an example of a flood duration

map for a single polder. The map was generated from a simulated stage hydrograph in a two step procedure. Firstly, grid maps of the inundated area were created for each day by reclassifying the polder's digital elevation model. A value of 1 was assigned to inundated grid cells and the remaining dry cells were set to zero. Secondly, the grid maps of all successive days were summed up to yield the spatial pattern of flood duration. Similar maps as shown in Figure 6 were produced for all polders P1–P8.

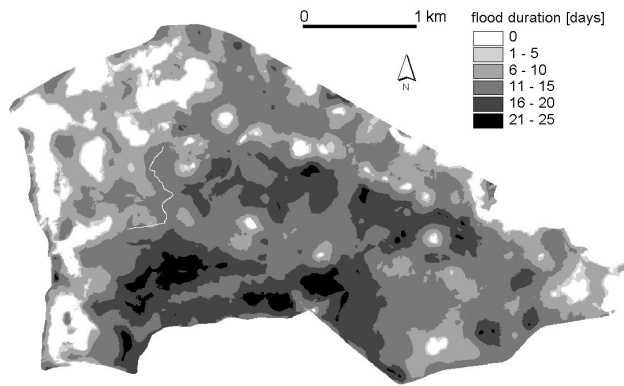


Fig. 6: Flood duration map of the polder Twerl (label P6 in Figure 4) for scenario II as it was derived from a stage hydrograph simulated by the CR Model. The dike breach through which the polder was flooded is located in the middle of its southern boundary.

5 DAMAGE ASSESSMENT IN THE POLDER SYSTEM

Damage to agriculture, the road network, housing and fishery was assessed on a monetary basis as described in the following.

Agricultural damage strongly depends on the time of occurrence of the flood event within a year (see Table 1). In general, floods occurring before the sowing of the spring grain cause least damage whereas maximum losses are caused by flood events occurring shortly before harvest. Also, losses vary greatly between the agricultural land use types. Therefore, the damage to agriculture was calculated for both flood scenarios depending on the extent and duration of inundation, the spatial distribution of the land use types and the timing of flood occurrence.

Damage to roads depends on the extent of the inundated area, the spatial distribution of road construction types and the degree of damage. Unfortunately, cost assessments for the 2002 event were not made available by the communities affected by the flood. Therefore, costs for

repair or reconstruction of the total road network within the polder area had to be calculated on the basis of bid prices (see Table 2). In the cost-benefit analysis (section 7) calculated repair and reconstruction costs were used as lower and upper bounds of the total damage to the road network, respectively.

Tab. 1: Calculated agricultural losses in the polders for the two flood scenarios (million €)

Flood occurrence	Scenario I	Scenario II
Before sowing of spring grain (mid April)	1.47	2.26
After sowing of spring grain (mid April)	2.40	3.70
Before harvest (mid July)	3.08	4.73
After harvest (mid July)	2.20	3.39

Tab. 2: Calculated damage to roads in the polders for the two flood scenarios (million €)

Type of costs	Scenario I	Scenario II
Repair costs	3.26	3.59
Reconstruction costs	5.16	5.66

Due to the small number of houses in the retention area, damage to buildings was estimated to be low compared to the other damage categories. On the basis of observation and experience, estimates range from 0.17 to 0.22 million € for scenario I and from 0.32 to 0.39 million € for scenario II. Losses to fishery were ascertained by the appropriate authorities for compensation purposes. The costs amounted to 0.47 million € for the reference scenario.

The damage categories described above were considered to be most relevant in terms of a monetary damage assessment. The effort involved in assessing the damage to further catego-

ries appeared inappropriate given the low expected amount of loss. Thus, further categories were not included in this study.

6 ASSESSMENT OF POTENTIAL DAMAGE REDUCTION IN WITTENBERGE

The benefits of using the polders appear downstream in the form of prevented damage. There is a large range of damage types to be considered. Generally, direct damage resulting from the physical contact of the floodwaters with humans or properties and indirect damage like disruption of traffic and trade can be distinguished (Smith and Ward, 1998). Further differentiation into tangible and intangible damage is possible. Besides the prevention of flood damage, changes in defence and evacuation effort as well as dike restoration costs can be taken into account.

The scope of this investigation was rather the development of a comprehensive approach towards assessing the use of polders for flood retention than a detailed study of all damage and benefit categories. Therefore, only prevented direct damage to industry, trade and services, public facilities and housing in the downstream town of Wittenberge was considered, which is referred to as “potential damage” in the following.

The first step in the assessment was to determine the extent of inundated areas for both flood scenarios (section 6.1). Subsequently, the corresponding damage was calculated as described in 6.2.

6.1 Determination of flooded areas

The town of Wittenberge is protected against floods by embankments. Over a total length of 1100 m in the harbour area of Wittenberge, these embankments do not reach the full height required by the design flood for reasons of amenity. As a makeshift, mobile walls are used for flood protection at this location. These walls are estimated to have a larger failure probability than the embankments.

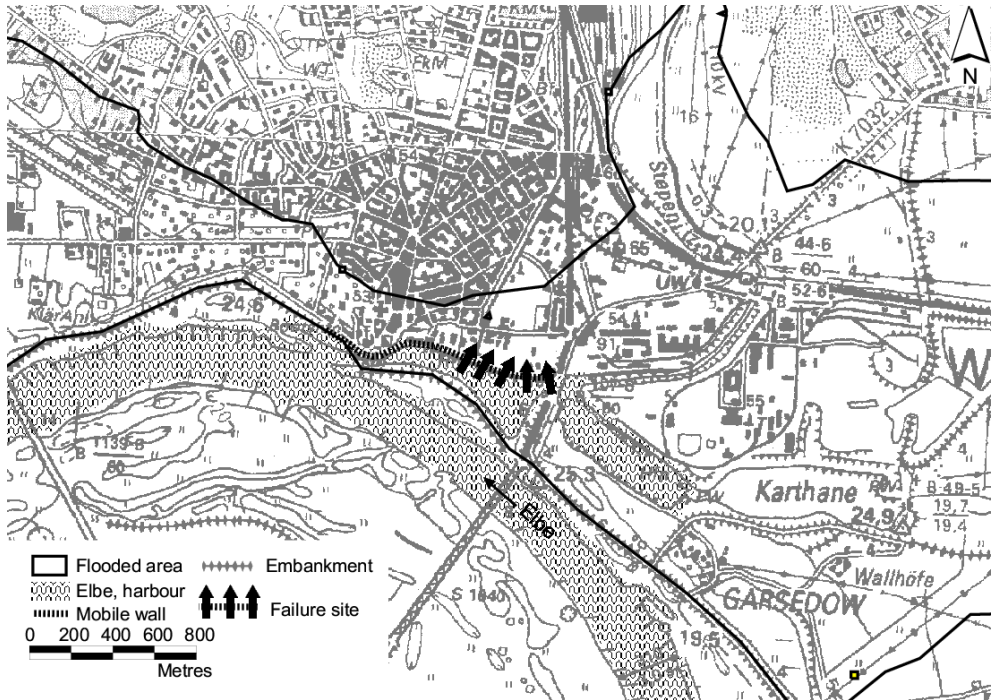


Fig. 7: Flood hazard map for the town of Wittenberge (flood scenario II with an estimated return period of about 300 years)

The use of flood polders reduces the failure probability of flood protection measures downstream. In a simplified scenario it was assumed that the mobile flood protection walls would fail over a length of 500 m in the harbour of Wittenberge and that overtopping of the embankments would occur unless the polders were used for flood peak retention. The volume of the flood wave exceeding the embankment's crest level was assumed to flow through the lower parts of Wittenberge. The failure site and the flooded area for scenario II are shown in Figure 7. Because occurrence probability and intensity of flooding are known for the scenario given in the map, it is referred to as hazard map (Merz et al., 2005).

The volume of the embankment overflow at the failure site was calculated using the weir formula of POLENI (Eq. 3). For the flood scenarios defined in section 3, volumes of 7.4 million m^3 for the reference scenario and 21.6 million m^3 for scenario II were estimated.

In order to determine the affected area in the town of Wittenberge a relationship between the water level and the corresponding storage volume was established from the digital elevation model. Using this relation the inundated area and the water level behind the failure site was derived for the estimated outflow volumes of 7.4 and 21.6 million m^3 (Figure 8).

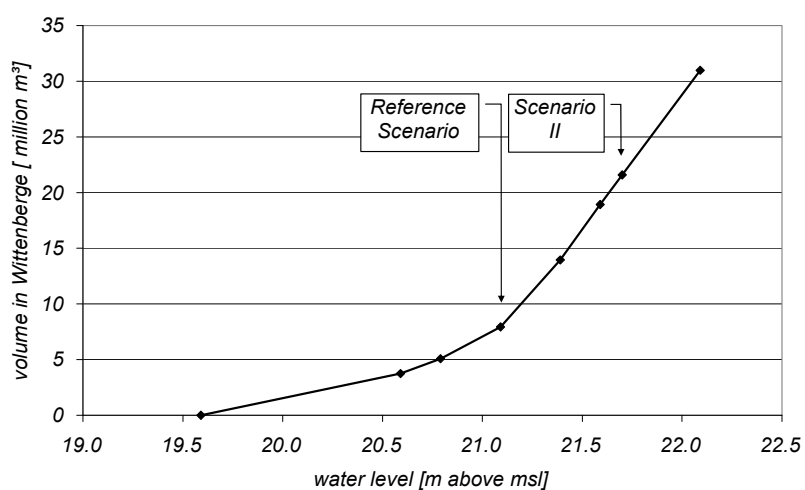


Fig. 8: Inundation volume in the town of Wittenberge against inundation water level behind the failure site as result of hydraulic calculations

6.2 Assessment of potential damage in Wittenberge

Direct damage to industry, trade and services, public facilities and housing was estimated on the basis of land use. The German land register ATKIS served as the spatial basis for land use information. An analysis of the national accounts delivered specific economic values ($\text{€}/\text{m}^2$) for

each land use type. The potential damage per land use unit depends on the water depth. Relative stage-damage functions, giving flood damage as a percentage of an area's total value against water depth, were used to determine damage in currency units. The applied method was based on a reference study from the German federal state of North Rhine-Westphalia (MULR, 2000). A more detailed description of the approach is included in the project report (Bronstert, 2004).

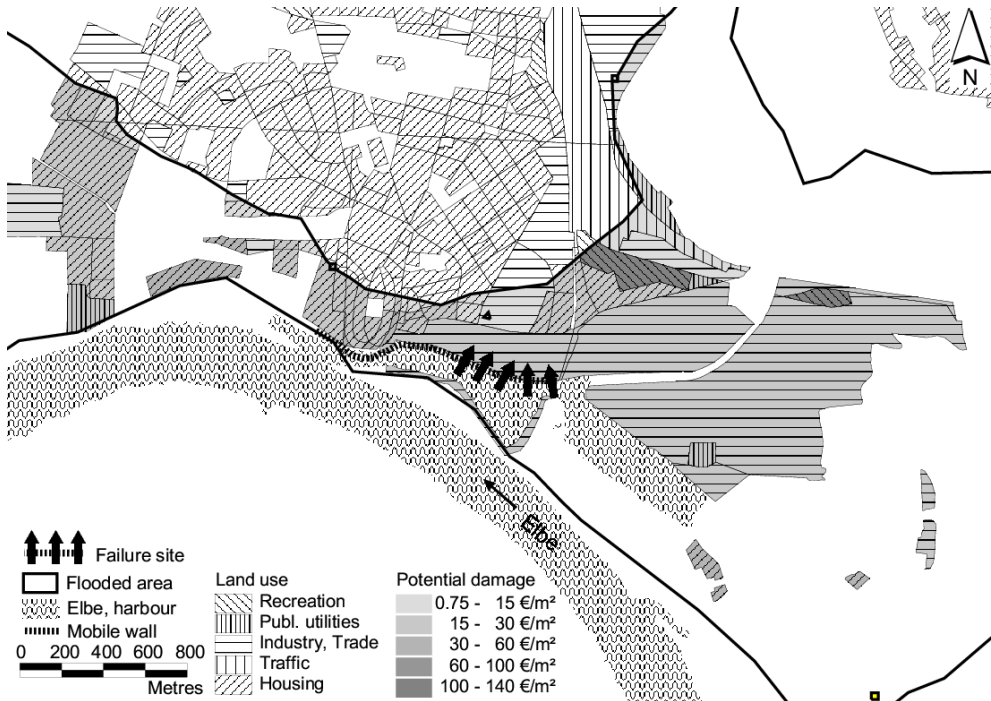


Fig. 9: Flood risk map for the town of Wittenberge (flood scenario II). Potential damage is given for each flood affected land use unit.

The intersection of land register and water depth enabled the calculation of the potential damage for the areas affected by flooding.

Figure 9 shows a risk map where potential damage for each land use unit is mapped. Because hazard and vulnerability are known for the scenario shown in the map, it is referred to as risk map (Merz et al., 2005).

Uncertainty of damage assessment was considered by varying the specific economic values for each land use type on the basis of an on-site inspection of the area, yielding a lower and upper boundary of the potential damage.

The result of the damage assessment in the form of a graphical representation of potential flood damage against inundation volume is given in Figure 10. For the reference scenario, a poten-

tial flood damage of about 17 million € was estimated. Scenario II resulted in potential damage of about 31 million €.

7 COST-BENEFIT ANALYSIS

The cost-benefit analysis aggregates those project results which are expressed in monetary units into a cost-benefit ratio. Because a complete monetary account of all benefit and cost positions could not be elaborated within the project, the ratio cannot serve as the only decision criterion. However, a comprehensive assessment should be based on a decision support taking all relevant perspectives into account.

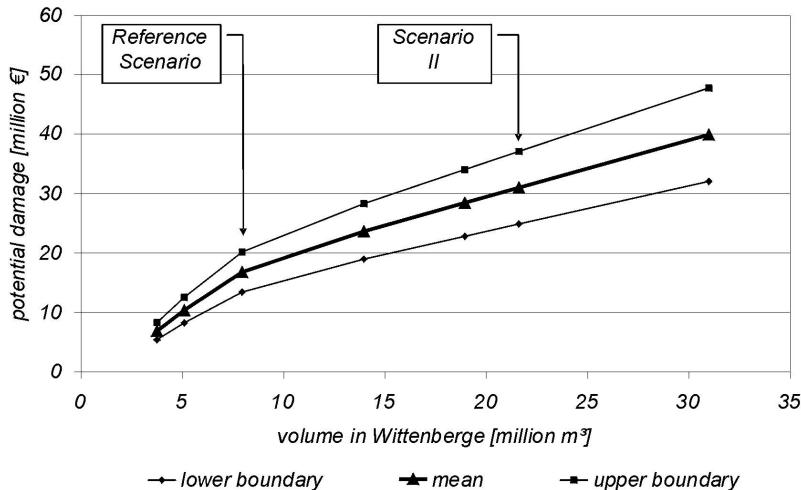


Fig. 10: Potential damage against inundation volume in the town of Wittenberge

The polders on the Lower Havel River were built as a multi-purpose system. Besides flood protection of downstream riparian areas they enable agricultural land use and protect infrastructural facilities. For the performance of a cost-benefit analysis a clear decision as to which costs are to be associated with a certain purpose is required. Therefore, costs are differentiated into event-dependent ones and event-independent ones where “event” refers to “flood protection of downstream riparian areas”.

Event-dependent costs are damage to agriculture, road network, buildings and fishery. Furthermore, the costs of blowing up and reconstructing the dikes fall into this category as most of the polders are not equipped with inlets. Event-independent costs arise from constructing and maintaining the dikes. Only event-dependent costs were included in the efficiency assessment of using the polders for flood protection.

The lifetime of the system was assumed to be 90 years. A discount rate of 3 % was selected for taking time preference into account. As Table 3 indicates, the benefit-cost ratio calculated for scenario II is significantly higher than for the reference scenario.

Tab. 3: Calculated benefit-cost ratios of using the polder system for attenuation of the Elbe flood peak

Benefit-cost ratio	Scenario I	Scenario II
Lower estimate	1.5	2.2
Upper estimate	4.0	5.8
Mean	2.8	4.0

The large spread of the benefit-cost ratio is a result of combining low benefit and high cost estimates and vice versa. The use of lower and upper estimates of cost (section 5) and benefit (6.2) in the calculation of the benefit-cost ratio serves as a pragmatic means to provide an idea of the associated uncertainty.

The high benefit-cost ratios indicate that for the investigated scenarios the use of the polders for flood protection is economically highly beneficial. Because both benefits and costs are event-dependent, a variation in the anticipated lifetime of the system or discount rate would not affect the result.

It can be argued that each of the above-mentioned purposes should carry a certain portion of construction and maintenance costs of the polder dikes. A partial inclusion of these event-independent costs would lower the benefit-cost ratio. Furthermore, the result would become sensitive to changes in anticipated lifetime or discount rate.

8 DISCUSSION AND CONCLUSIONS

The aim of the study was to assess economically the use of a polder system for flood protection. For this purpose an interdisciplinary research approach was essential since aspects of hydraulics, agricultural science and economics had to be accounted for.

From our investigation, it can be concluded that for the two extreme flood scenarios under consideration, the controlled flooding of the retention area on the Lower Havel River is highly cost-effective. For scenario II a higher benefit-cost ratio was calculated than for the reference

scenario. This is mainly due to the fact that the total potential damage in the town of Wittenberge varies greatly between the two flood scenarios. The higher inundation depth in scenario II results in greater damage compared to the reference scenario, since loss is strongly correlated to inundation depth for most urban land use categories. However, losses in the polders show less variation between the two flood scenarios. The larger volume retained in the polders in scenario II results in a higher inundation depth rather than in an enlargement of the flood-affected area. Since damage to agriculture and the road network depends on the extent of the flooded area rather than on the inundation depth, the difference in total damage for the two flood scenarios is comparatively low.

Experiences from the 2002 flood event as well as from the conducted study proved that polders of large storage capacity are essential to effectively attenuate an extreme flood peak of the Elbe River. However, the full benefit of the storage capacity can only be achieved by controlled operation and good timing.

Modelling the inundation dynamics in the polder area for the two considered flood scenarios was an essential part of the research. The CR Model, which was developed for this purpose (section 4), proved to be an adequate simulation tool adapted to the system's complexity and the data availability. Apart from the two scenarios focused on in this study, the model is applicable to various other flood scenarios. Thus, the effects of initial and boundary conditions (e.g. varying discharge of the Havel River) and of model configuration (e.g. exclusion of selected polders) on the inundation dynamics could be investigated.

Throughout this study it emerged that further research is required towards assessing the use of

polders as a flood protection measure in a holistic way. In the analysis of costs and benefits (section 7) it was assumed that the mobile wall in the harbour of Wittenberge would fail unless the polders were used for flood peak retention. However, a more comprehensive approach would entail a probabilistic failure assessment based on the reliability of flood defences downstream of the confluence of Elbe and Havel.

Future research work should account for further damage categories than were included in the current cost-benefit analysis. In this study only direct tangible damage was considered. However, for a comprehensive evaluation of flood management strategies indirect as well as intangible damage should be taken into account. Whereas approaches exist for the inclusion of indirect damage like disruption to traffic, production or trade, an appropriate assessment of intangible damage such as damage to human health and ecological side effects is a major challenge for further research.

ACKNOWLEDGEMENTS

We thank Werner Sauer (state office for environment of the federal state of Brandenburg), Gert Neubert and Ronald Thiel (state office for agriculture of the federal state of Brandenburg), Holger Ellmann and Burkhard Schulze (Ellmann&Schulze GbR) for their contribution to the joint research project, which was funded by the German Federal Ministry of Education and Research.

Comments by two anonymous referees on an earlier version of this paper are gratefully acknowledged.

Chapter III

Hydrodynamic simulation of the operational management of a proposed flood emergency storage area at the Middle Elbe River

ABSTRACT:

Emergency storage areas can be an effective structural flood protection measure. By their controlled flooding the risk of inundation for downstream areas with higher vulnerability can be reduced.

In the present study, the flooding and emptying process of a proposed storage area at the Middle Elbe River is simulated. The storage area has a maximum capacity of 40 million m³ and is divided into two polder basins. It is designed for the attenuation of extreme floods of 100 years or more return period.

A one-dimensional hydrodynamic model is set up for a 20 km reach of the Elbe River, wherein the storage area is schematised by two storage cells each representing one polder basin. Flow between the storage cells and the Elbe River is controlled by adjustable gates which operate based on pre-defined conditions.

Four flood scenarios which differ in flood magnitude and hydrograph shape are simulated. The scenarios are derived from analyses of a 70 years discharge record. Furthermore, for each flood scenario two gate control strategies are investigated.

The results show that during large floods the utilisation of the storage area with controlled gate operations significantly reduces the Elbe River peak discharges. However, the magnitude of the attenuation depends on the steepness of the flood hydrograph and the applied control strategy with well-timed gate operations.

Published as: Förster S, Chatterjee C and Bronstert A. 2008. Hydrodynamic Simulation of the Operational Management of a Proposed Flood Emergency Storage Area at the Middle Elbe River. River Research and Applications. Published online, DOI: 10.1002/rra.1090.

1 INTRODUCTION

Flood emergency storage areas serve the primary purpose of temporary water storage during large flood events in order to reduce the flood peak levels and thus alleviate the risk of inundation in downstream areas with higher vulnerability. Such storage areas are typically located along the middle reaches of large rivers. As a structural flood protection measure they can form part of a modern flood risk management system.

Storage is most effective if it is controlled, while the time of opening of the control gates is crucial for a successful operation. This aspect has been pointed out by several authors (Jaffe and Sanders, 2001, Aureli et al., 2005, Galbáts, 2006, Rátkey and Szlávík, 2001). If the storage is utilised too early, most of the detained volume is taken from the rising limb. If the inlet gate is opened too late, the volume is merely taken from the falling limb. In both cases the obtained peak lowering will be less than potentially possible (Silva et al., 2004). Ideally the flood hydrograph should be cut to a constant discharge level while using the full storage capacity (Figure 1). After the flood peak has passed by, the storage area should be cleared of stored water as soon as water levels in the main river allow for a safe release (Hall et al., 1993). Besides a well-timed gate operation, the amount of peak attenuation depends on the characteristics of the flood wave.

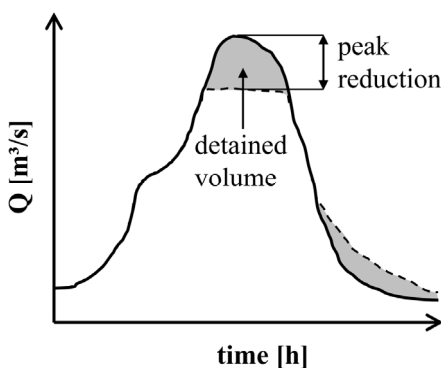


Fig. 1: Effect of ideal peak capping by controlled detention on hydrograph (dashed line). The unaffected hydrograph is shown by a solid line.

During the large Elbe flood in summer 2002 the effectiveness of emergency storage was evident. By temporary water detention in the large storage area at the confluence of Havel and Elbe Rivers, the Elbe flood peak was lowered by approximately 40 cm (Förster et al., 2005). Locations for further controlled and non-controlled

potential detention areas along the Elbe have been proposed by the International Commission of the Protection of the Elbe (2003) and their general suitability in terms of peak attenuation has been investigated (Helms et al., 2002, Büchel et al., 2004).

One of these proposed detention sites has been chosen for a detailed investigation in the present study as it seemed especially suitable for flood water storage because of its topography and location. It is situated in a river reach where several major dike failures occurred during the flood in August 2002 resulting in a flooded area of more than 200 km². Due to the dike failures the flood peak was reduced by 11 cm (corresponding to 220 m³/s) at the town of Wittenberg, situated about 30 km downstream of the proposed detention site (IKSE, 2004). This demonstrates the potential of controlled water storage at this location in reducing the risk of dike failures as well as lowering the water level in inundated areas just downstream along the river, where sites of cultural and industrial importance are situated.

The objective of the present study is therefore to determine the maximum peak attenuation which can be obtained by the investigated potential storage area and to study the effect of different floods and operation schemes on the peak attenuation. This is done by detailed simulations of the filling and emptying process using the hydrodynamic model MIKE 11. Based on an analysis of the 70 years discharge record at the Torgau gauging station different flood scenarios with regard to flood magnitude and hydrograph shape are derived for further investigation. Furthermore, for each flood scenario two gate control strategies are considered. Finally, general aspects of controlled detention in emergency storage areas are discussed.

2 STUDY AREA

The proposed emergency storage area is located in the lowland area at the Middle Elbe River in Germany between the gauges Torgau and Wittenberg. Figures 2 to 4 show an overview map of the study area, a cross sectional view of the modelled river stretch and of the polder basin, respectively. The storage area extends 7 km along the right bank of the Elbe River. The overall area amounts to 17 km² with a maximum storage capacity of approximately 40 million m³.

The storage area is divided into a northern and a southern polder basin by an already existing dike road running through the area. Both basins are connected by a sluice gate of 50 m width. The filling and emptying process of the storage

area is controlled by two adjustable overflow weirs of 25 m width each. Both weirs are divided into four parts of 6.25 m width, which can be operated independently.

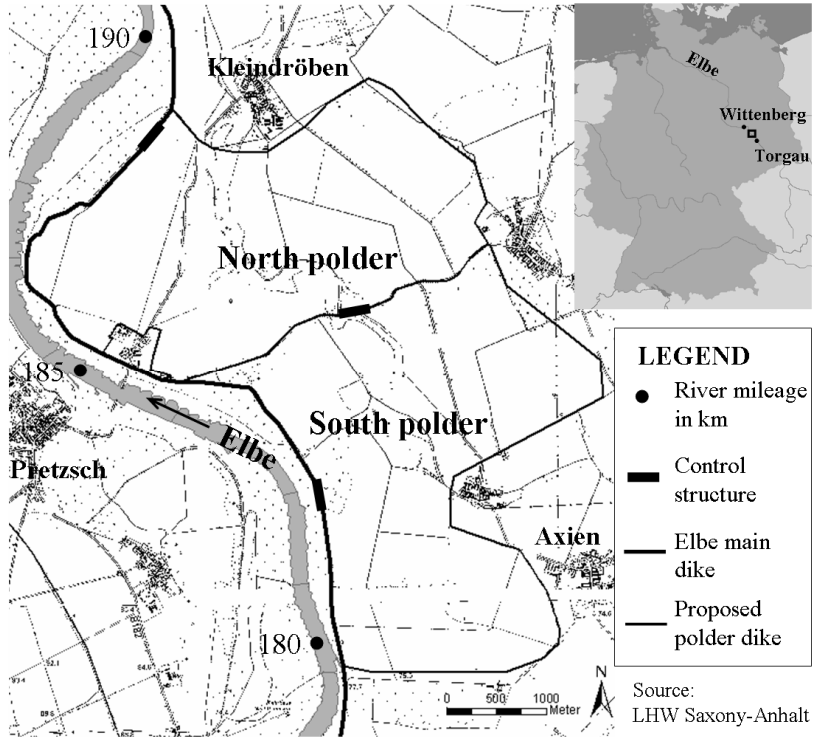


Fig. 2: Map of the proposed flood emergency storage area. The Elbe-km information refers to the river mileage in German territory (starting at Elbe-km 0.0 at the Czech-German border)

Discharge characteristics of the gauges Torgau and Wittenberg are given in Table 1. Dikes running along both sides of most of the Middle Elbe River are designed for a 100 year flood plus one metre freeboard. Accordingly, the proposed emergency storage area is to be designed for reducing flood peaks of 100 years return period or larger as the dikes are expected to withstand floods of smaller magnitude. However, very large floods in the range of 200 years recurrence time or larger are very likely to cause dike overtopping or dike failure at upstream locations along the

Elbe River and hence are not expected to arrive at the storage area.

The national flood forecasting system provides water level information with lead-times of 48 hours plus another two to three days trend at the river stretch of interest. The accuracy of the flood forecast model is given with a standard error of 5 cm (BfG, 2006). Unless unexpected events such as dike failures occur just upstream of the storage area, the flood forecast information is accurate enough and gives sufficient time to enable an optimised operation of the control structures.

Tab. 1: Discharge statistics for the gauges Torgau and Wittenberg (LHW, 2003). Lower discharge values recorded at the downstream gauge Wittenberg are due to several dike failures that occurred between the two gauges during the flood in 2002.

Gauge (Elbe-km)	Mean annual discharge [m ³ /s]	Mean annual peak discharge [m ³ /s]	Maximum discharge recorded [m ³ /s] (date)	Series
Torgau (154.2)	344	1420	4420 (18.08.2002)	1936-2003
Wittenberg (214.1)	369	1410	4110 (18.08.2002)	1936-2003

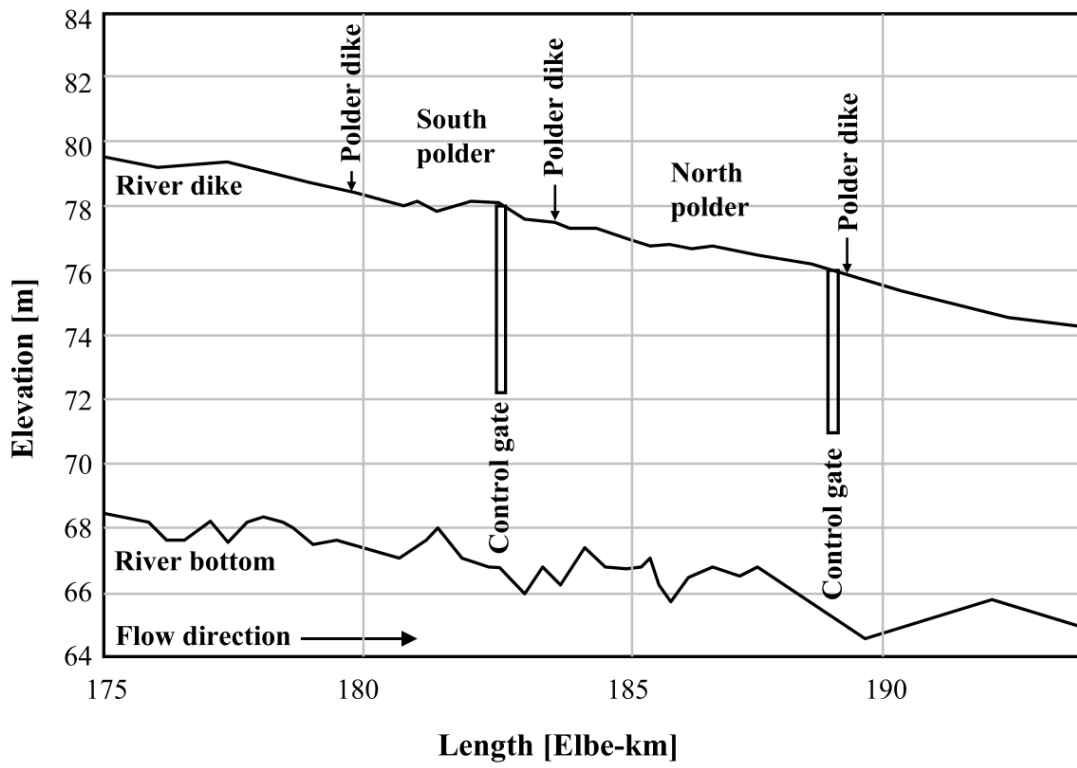


Fig 3: Longitudinal cross-section along the modelled river stretch showing Elbe river bottom, and proposed polder dikes as well as control structures

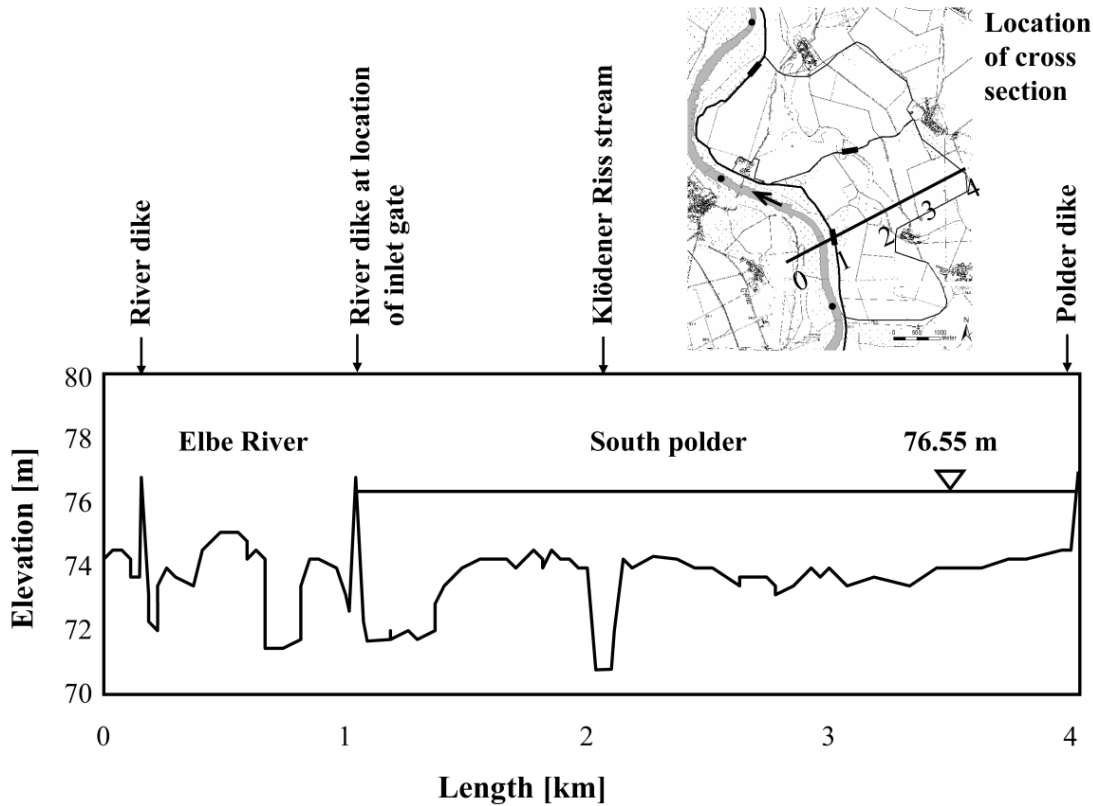


Fig 4: Cross-sectional view of the southern polder basin

It may be noted that the emergency storage area under study is a potential detention site and hence, at present neither the dikes surrounding the polder basins nor any control structures exist. Topographic data and information on control structures and polder dikes were provided by the local water authorities according to the current planning stage.

Currently about 90 % of the area is under intensive agricultural use. The rest is taken up by watercourses and forests, most of which are under nature protection. It is expected that the land will retain its original purpose after designation as emergency storage area.

3 HYDRODYNAMIC MODEL SETUP

Models of different complexities may be applied for the hydrodynamic simulation of floodplains and storage areas (Bates et al., 2005, Hesselink et al., 2003). An appropriate modelling approach should be chosen depending on the objective of the study, the available data and the amount of accuracy required (Bates and De Roo, 2000). A two-dimensional or quasi-two-dimensional hydrodynamic model of the storage area is essential if the propagation of the inundation flow in the storage area as prerequisite for the simulation of erosion and sedimentation processes or the subsequent estimation of flood damage is of interest (Huang et al., 2007, Chatterjee et al., 2007). However, if one is only interested in studying the effectiveness of the storage area in capping the peak discharge in the river, a simple one-dimensional model for the river coupled with a storage cell may be sufficient. The latter approach was chosen for this study where the simulation of the filling and emptying process of the emergency storage area is made by the practical application of the modelling package MIKE 11 developed at the Danish Hydraulic Institute, Denmark (DHI, 1997). MIKE 11 has been applied in several similar studies (Faganelllo and Attewill, 2005, Hammersmark, 2002). It uses an implicit finite difference scheme for computation of unsteady flow based on the vertically integrated equations of conservation of continuity and momentum (the Saint Venant equations).

MIKE 11 is set up to represent a 18.6 km reach of the Elbe River, which is described by a series of 34 cross sections that stem from recent sonar measurements and airborne laser altimetry (see Figure 5). In view of future bed erosion as

well as other processes and measures that lead to a modification of the river cross section it should be ensured that up-to-date cross section data is used.

The boundary condition at the upstream end of the reach at 175.00 Elbe-km is a discharge hydrograph of the Torgau gauging station. Although this gauge is located approximately 20 km upstream of the upper model boundary, utilisation of these discharge data is justified as there are only minor tributaries to the Elbe River between Torgau and the modelled river stretch. The downstream boundary condition at 193.60 Elbe-km is provided as a rating curve.

The emergency storage area is schematised in the model by two storage cells each representing one polder basin. The storage cells are described by their area-elevation curves. The curves are derived from a high-resolution Digital Elevation Model that was obtained from airborne LiDAR survey. The gates are implemented as control structures that operate due to pre-set conditions according to the control strategies described in section 4.3.

The model is carefully calibrated and validated against water levels recorded at the gauging station at 184.4 Elbe-km. Because of the different nature of bed materials two hydraulic roughness classes are distinguished, one for the main channel and one for the floodplain. Initially, the roughness information in the form of Manning's n values is taken from the literature (Chow, 1959) and similar studies (Horritt and Bates, 2002). A two stage calibration and validation procedure is adopted in order to find the appropriate roughness coefficients. In the first stage the coefficient for the river bed is identified by considering two smaller flood events during which the water did not spill over to the floodplains. In the second stage the roughness coefficient for the floodplain is found by use of two larger flood events which also affected the floodplains. In this stage the coefficient for the main river is kept to the value that was identified to fit the data best during the first stage. Finally, Manning's n values of 0.038 for the river channel and 0.050 for the floodplain were found to fit the observation data best on the basis of a goodness of fit criterion. Due to lack of calibration data for the emergency storage area, the floodplain roughness value obtained in the calibration process is also applied to the polder basins. This assumption seems acceptable, since land use in both the floodplains and the detention areas are comparable. For a detailed descrip-

tion of the model setup, calibration process and

sensitivity analysis see Chatterjee et al. (2008).

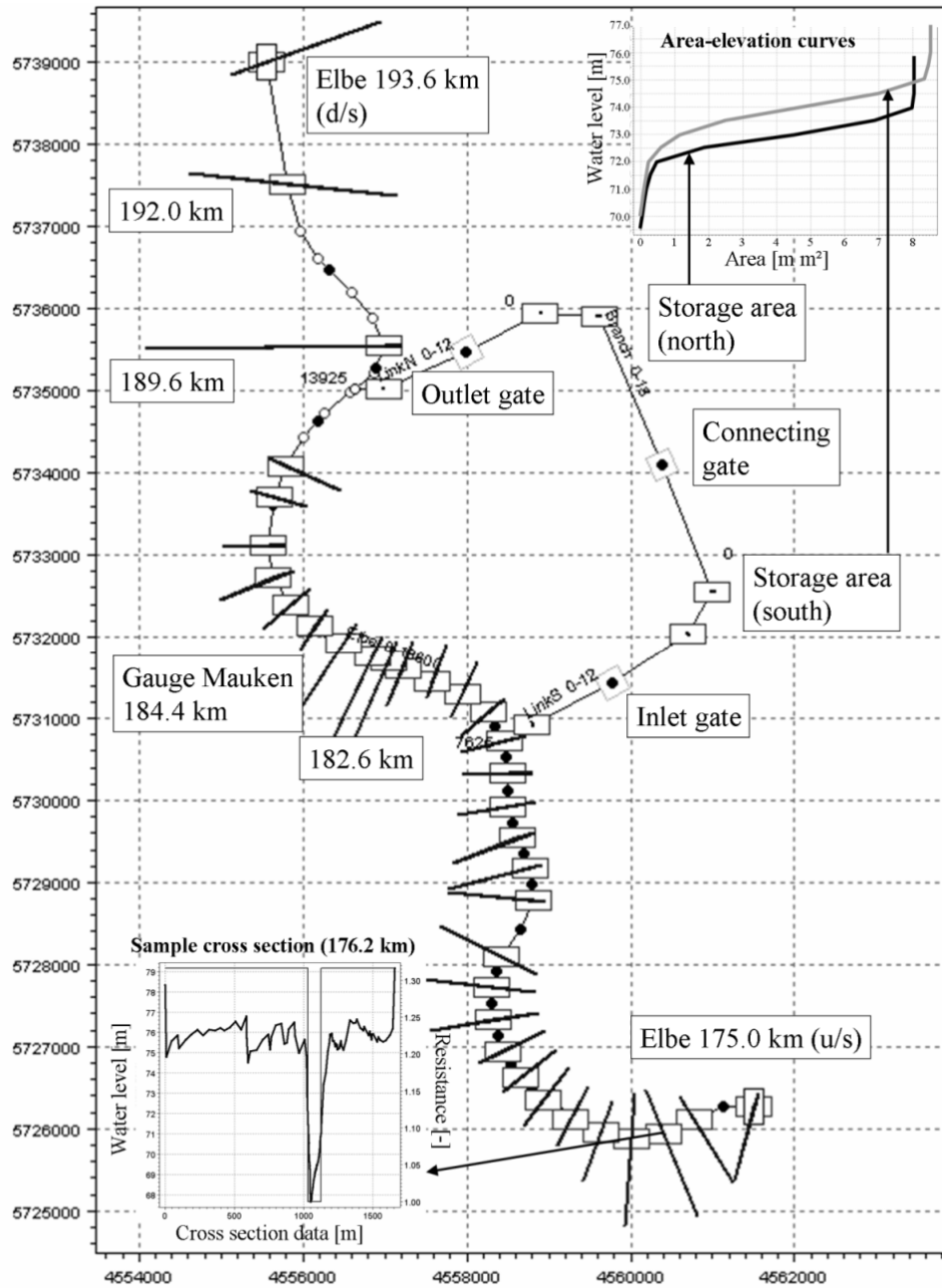


Fig. 5: Cross-sectional view of the southern polder basin

4 CONSIDERED FLOOD SCENARIOS AND CONTROL STRATEGIES

A primary objective of this study is to investigate the effect of magnitude and shape of a flood wave on the peak attenuation. Rather than studying a single past flood event with a specific magnitude and hydrograph shape, in the present study flood scenarios were derived in such a way that they cover a broad range of potential flood situations to be expected at the storage area. The

flood scenarios are found by analysing peak flows observed at Torgau gauge.

For the management of the emergency storage area different control strategies may be adopted with respect to timing, sequence and number of gate operations. Out of these two most promising control strategies are chosen for further investigation.

4.1 Flood frequency analysis

An at-site flood frequency analysis is carried out in order to relate the magnitude of extreme

flood events to their frequency of occurrence. The analysis is based on the annual maximum series (AMS) of the 1936-2005 discharge record at the Torgau gauging station. Torgau gauge is situated approximately 20 km upstream of the storage area along the Elbe River.

Preliminary tests for independence and homogeneity as well as tests for outliers are carried out. The best fit distribution was identified on the basis of the L-moment ratio diagram and the Z-dist statistic criteria (Hosking and Wallis, 1997). Among several 2- and 3-parameter distribution functions the Generalised Logistic Distribution was found to fit the data best. Based on the selected distribution function, the 100 and 200 year return period floods are found to have a discharge of 4022 and 4775 m³/s, respectively. The maximum discharge observed at Torgau station on 18th August 2002 was 4420 m³/s (Table 1) which corresponds to a return period of approximately 180 years.

4.2 Definition of flood scenarios

According to the water authority the flood storage area will be utilised to reduce large flood peaks ranging between 100 and about 200 years recurrence time. This range is a result of the current dike heights as described above. Consequently, flood magnitudes of 100 and 200 years return period are considered in this investigation.

The hydrograph shapes have been obtained by analysing the ten largest floods in the 70 year discharge record at the Torgau gauging station. Among them the flood event of summer 2002 was the only one exceeding the discharge corresponding to a return period of 100 years. In a non-dimensional analysis the peaks of these hydrographs were scaled to a uniform ordinate value of 1. The scenario hydrographs were then constructed by selecting the steepest and widest hydrographs considering the top portion of the flood wave that is relevant for the diversion of water into the storage area (above approximately 3500 m³/s, see Table 2). Subsequently, each discharge ordinate was multiplied by an amplifier, which is the design peak corresponding to the 100 and 200 year return period. Besides the increase in peak discharge the described transformation lead to an enhanced flood wave volume and duration in the top portion of the hydrograph that is relevant for peak capping. Figure 6 shows all four considered flood scenarios.

Several two or multiple peaked floods can be found in the Torgau discharge record. This is also the case with the selected steep flood hydrograph where a second flood peak follows the larger peak. However, the second peak is much smaller than the discharge threshold relevant for water diversion into the storage area and hence, does not have an effect on the operation of the storage area.

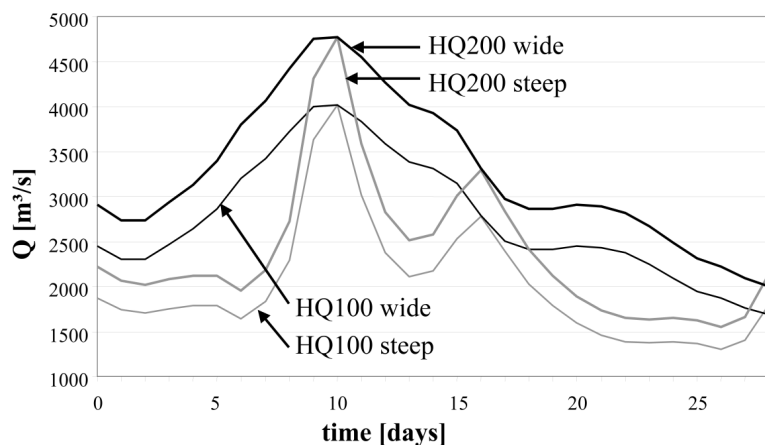


Fig. 6: Hydrographs of investigated flood scenarios as derived from the discharge record at the Torgau gauge. Hydrographs of the flood events of April 1941 (steep) and March/April 1988 (wide) were rescaled to the peak discharge corresponding to the 100 and 200 return period, respectively

4.3 Definition of control strategies

The type of control strategies refers to the timing, sequence and number of gate operations,

which have an effect on the flood peak attenuation as well as on the flooding dynamics within the storage area.

Two control strategies are considered in the study as schematised in Figure 7. Flow direction

of the Elbe River is from left to right. The current state of opening of the three gates is marked by black and white arrows. As can be seen, the south basin has a higher design water level than the north basin. Consequently, both polder basins cannot be completely filled up solely through the north gate.

In the simulation runs the gates are operated according to pre-defined event-specific conditions of Elbe discharge and polder water level. In control strategy I the north gate (NG) and the south gate (SG) are initially closed whereas the sluice gate connecting both polder basins (CG) is open (1), as shown in Figure 7. When a certain Elbe threshold discharge is reached during a large flood event the first part of the SG is opened leading to a momentary drop followed by an increase in Elbe water levels. The remaining SG parts are then opened every time the Elbe threshold level is reached (2).

The selection of this threshold value corresponding to the maximum achievable attenuation is governed by the available volume in the storage area, the discharge capacity of the inlet gates and their opening/closure duration. It was assumed that the gates take 30 minutes for a complete opening process, which is a realistic duration for such type of gates according to the water authorities. Once the process is started it continues until the gate is fully open. The same applies to the

gate closure process. The threshold value is determined for each individual flood hydrograph.

To complete the filling process, the CG and afterwards the SG are closed as soon as the north basin and the south basin, respectively, reach their full capacity (3, 4).

On the contrary, in control strategy II the emergency storage area is filled through the NG as well as the SG. Following the same initial gate status (1), a pre-defined number of NG parts is opened first upon reaching a certain Elbe threshold discharge and hence the filling process starts from the low lying areas (2). The number of gate parts which open depends on the required discharge capacity of the gate, which will be high for rather steep flood hydrographs and lower for wide hydrographs. After opening the SG upon reaching a threshold Elbe discharge, the storage area is filled from both sides (3). This process continues until the NG is closed because the water flow through the gate reverses due to decreasing Elbe water levels compared to increasing water levels in the storage area (4). Similar to control strategy I the CG and the SG are closed as soon as the design water levels in the polder basins are reached (5, 6).

In both control strategies the emptying process starts as soon as the Elbe water level falls below a level that allows for safe discharge at the downstream river reaches. The storage area is drained out through NG and SG.

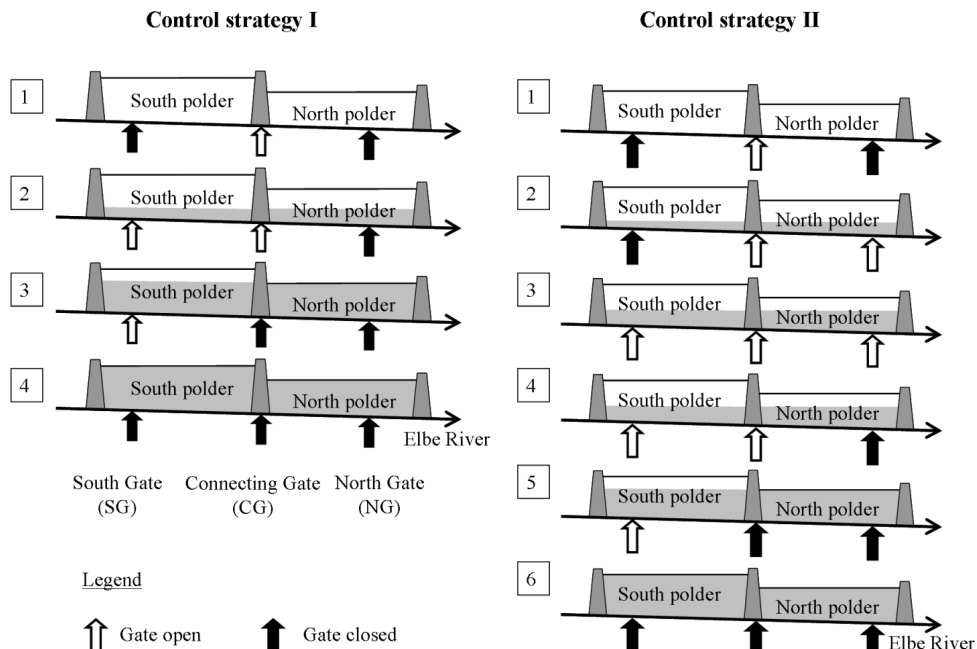


Fig. 7: Schematic cross-sectional view of the polder basins with gate operations for filling process according to control strategy I (left) and II (right)

5 RESULTS

Figures 8-11 show selected results obtained from simulation runs with varying hydrograph shape, return period and control strategy, whereas Table 2 summarises the peak attenuation for each case. The resulting water level lowering in the river given in Table 2 corresponds to the maximum difference between the peaks of the unaffected hydrograph and simulated attenuated hydrograph, while the highest water levels do not necessarily occur at the same time. The maximum possible water level reduction refers to the ideal case of a horizontal flood peak capping when using the full capacity of the storage area.

Scenario results are discussed for the case of the steep hydrograph with a return period of 200 years when control strategy I is applied with the gates opening sequentially (Figure 8). The other simulations are analogous. When a threshold discharge of $4200 \text{ m}^3/\text{s}$ is reached, the first south gate part is opened. Consequently flow through the south and the connecting gate starts and the discharge in the Elbe River drops and subsequently increases again with the rising limb of the flood wave. A volume of approximately 0.1 million m^3 flows through the south gate in the first 30 minutes until the first gate part is fully open. The other south gate parts are sequentially opened every time the threshold discharge is reached. After the south gate is completely open the discharge through the gate amounts to approximately $450 \text{ m}^3/\text{s}$, whereas the discharge through the connecting gate is approximately $220 \text{ m}^3/\text{s}$. The filling process continues for about 1.5 days until the design water levels in the polder basins are reached and consequently the gates are closed. Subsequently the water levels in the polder basin remain constant for about 8 days until the emptying process through south and north gates starts. When the flow direction at the south gate reverses, the gate is closed and subsequently the polder is drained through the north gate. A water level reduction of 21 cm just downstream of the storage area (at Elbe River 189.6 km) corresponding to a discharge of approximately $450 \text{ m}^3/\text{s}$ was simulated for the described scenario. This equals a relative discharge attenuation of 9.5%. In a similar study on a system of two polders at the Danube River in southern Germany a relative peak reduction of 11% was simulated (Fischer et al., 2005).

The results show that the water level attenuation in the Elbe River highly depends on the steepness of the flood hydrograph. Water level reductions for both flood scenarios differ by more than 10 cm. The filling time amounts to about 3 days in case of the wide hydrograph (Figure 9). The magnitude of the flood, however, does not influence the peak attenuation amount provided that they have the same hydrograph shape (Table 2).

A comparison of the two control strategies shows only slightly higher water level attenuation for control strategy II in case of the steep hydrograph (Figure 10). For the complete filling of the polder basins during very steep flood events it is advisable to increase the inlet discharge by additional utilisation of the northern control structure as done in strategy II. A volume of 2.4 million m^3 flows through the north gate before the filling is completed through the southern gate. Due to the lower elevation heights of the northern basin this strategy results in a pre-filling of this basin. Strategy II may therefore also be advantageous in view of erosion mitigation. However, a detailed study of the flow velocities is required to confirm this aspect and is a subject of future work. In view of the operational use, control strategy I may be easier to adopt because the number of gate operations is less.

A complete opening of the inlet south gate at once rather than opening the gate parts sequentially causes a sharp drop in the Elbe discharge, which is not desirable (Figure 11). The water level reduction obtained here is lower (18 cm) compared to the strategy of sequential opening of the gate parts (21 cm) for the case of the steep hydrograph when control strategy I is applied. Hence, the simulation runs for all scenarios were done applying the favourable sequential opening of gate parts. There are also real operation examples for the sequential inlet of flood water (see emergency storage area at the River Rhine in Bettmann and Bauer, 2005).

As mentioned above the investigated storage area is not yet constructed and hence only calibration data for the river is available. Due to the lack of observation data for the storage area the simulation results are compared with a similar study. In IWK (2003) the peak attenuation effect for several proposed flood storage areas along the Middle Elbe River was simulated considering floods with peak discharges ranging between $4000 \text{ m}^3/\text{s}$ and $5000 \text{ m}^3/\text{s}$. For the same storage area as investigated in the present study a peak

reduction between 262 m³/s (14 cm) and 497 m³/s (23 cm) at the gauge Wittenberg was simulated. These results are very similar to the range of water level reduction obtained in the present study.

In both studies the calculated peak attenuation seems rather low. However, a water level decrease in the range of 10 to 20 cm may reduce the

risk of dike failures due to overtopping, piping or saturation downstream along the river and hence decrease the risk of extensive inundations. The investigated storage area is part of a series of detention areas that is currently planned at the Middle Elbe River. Once they are in operation each of the areas will contribute to a larger overall water level reduction.

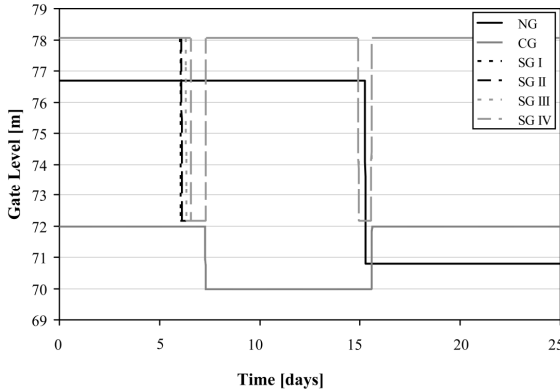


Fig. 8a: Gate levels: steep hydrograph, HQ200, control strategy I, gate opening in parts (NG north gate, CG connecting gate, SG I, II, III, IV south gate parts)

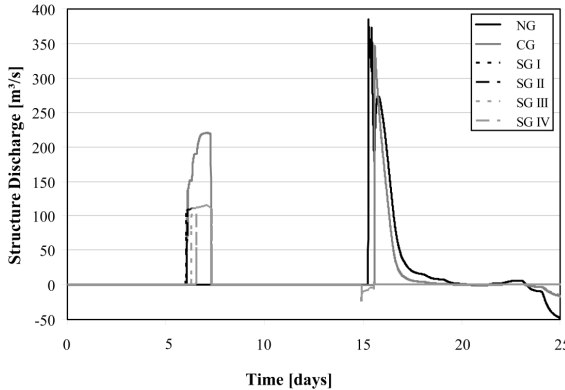


Fig. 8b: Gate discharge: steep hydrograph, HQ200, control strategy I, gate opening in parts

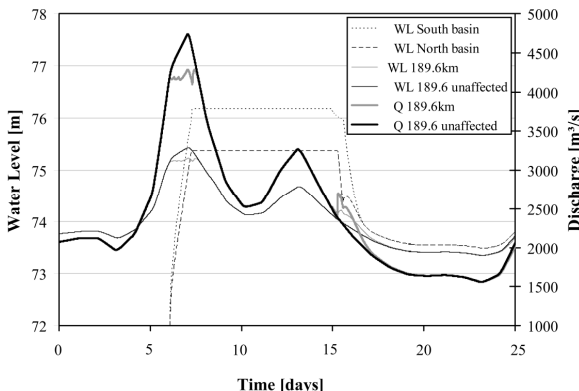


Fig. 8c: Simulated discharge and water levels: steep hydrograph, HQ200, control strategy I, gate opening in parts

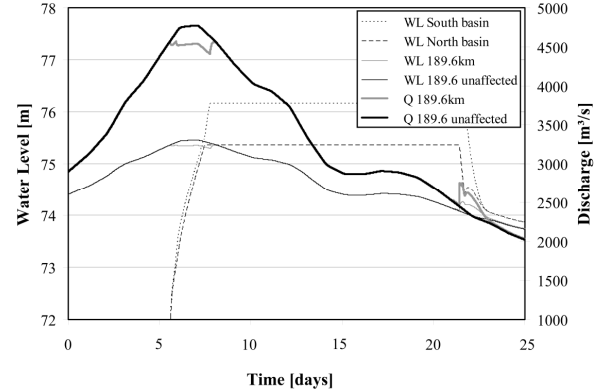


Fig. 9: Simulated discharge and water levels: wide hydrograph, HQ200, control strategy I, gate opening in parts

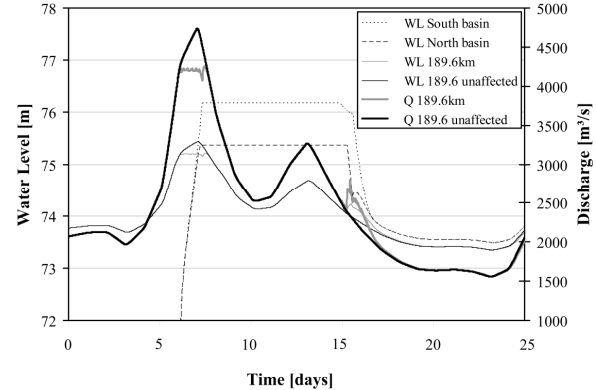


Fig. 10: Simulated discharge and water levels: steep hydrograph, HQ200, control strategy II, gate opening in parts

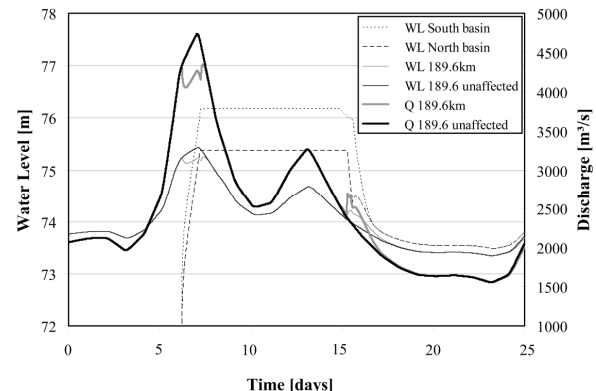


Fig. 11: Simulated discharge and water levels: steep hydrograph, HQ200, control strategy I, gate opening in one part, that is the entire 25m gate width opens together

Tab. 2: Maximum possible water level reduction, applied Elbe threshold discharge, simulated Elbe water level reductions and number of gate parts used during filling process for the investigated flood scenarios and control strategies

	Steep hydrograph, HQ200	Wide hydrograph, HQ200	Steep hydrograph, HQ100	Wide hydrograph, HQ100
Peak discharge (m^3/s)	4775	4775	4022	4022
Maximum possible water level reduction (cm)	24	11	23	11
Control Strategy I (Only South Gates)				
Threshold discharge (m^3/s)	4200	4575	3525	3825
Water level reduction (cm)	21	9	19	9
Number of gate parts used	4 SG	2 SG	4 SG	2 SG
Control Strategy II (Combination of North & South Gates)				
Threshold discharge (m^3/s)	4225	4575	3550	3825
Water level reduction (cm)	22	9	21	9
Number of gate parts used	2 NG + 4 SG	2 NG + 1SG	2 NG + 4 SG	2 NG + 2 SG

6 CONCLUSIONS AND DISCUSSION

The present study shows that from a hydraulic point of view the proposed detention site seems suitable for an effective peak reduction. This is mainly due to the large volume and the good drainage conditions of the investigated storage area. A local water level attenuation between 9 and 22 cm was simulated.

The study also shows that the peak reduction strongly depends on the steepness of the flood hydrograph. Hence, the river threshold discharge at which to open the control gate should be chosen depending on the forecasted hydrograph shape. Unless there are large dike failures or gauge malfunctions upstream of the storage area, the forecast information provided by the national flood forecasting system should be accurate and early enough to determine the required threshold discharge in advance and hence enable an optimised operation of the studied polder system.

A specific characteristic of the investigated storage area is the existence of two polder basins, each equipped with control structures. This facilitates an event-adapted management with different control strategies. It was seen that the peak reduction effect for steep hydrographs is significantly larger than for relatively wide flood hydrographs. In order to completely fill the storage

area in the short time a steep hydrograph passes by, it is advisable to increase the inflow capacity by utilising both control structures during the filling process. However, differences in peak capping between both control strategies are very small.

For the operational use of this specific emergency storage area further detailed investigations need to be carried out, in particular for the design of the hydraulic structures and their optimised operation.

Based on the experience gained in the present study general conclusions about the management of controlled storage areas can be drawn.

Flood storage in detention basins is most effective if it is controlled by adjustable gates. Dividing the inlet gate into separately operable parts has proved to be a promising strategy for a controlled water inflow. It also allows for the utilisation of the storage area in case of a gate malfunction. The existence of two or more separate polder basins can contribute to the flexibility of the polder operation because it enables the application of different control strategies according to the forecasted flood wave.

When planning further detention sites as currently done at the middle Elbe River it is important to study the effect of different hydrograph shapes on the peak attenuation as this affects the damage to be expected and hence the overall cost-benefit analysis for a certain detention site.

ACKNOWLEDGEMENTS

The research was jointly funded by the Alexander-von-Humboldt Foundation Fellowship Program and the Sixth Framework Program of the European Commission (FLOODsite project, EC Contract number: GOCE-CT-2004-505420). This paper reflects the authors' views and not those of the European Community. Neither the European Community nor any member of the

FLOODsite Consortium is liable for any use of the information in this paper.

Data were kindly provided by the following authorities: Landesbetrieb für Hochwasserschutz und Wasserwirtschaft Sachsen-Anhalt, Wasser- und Schifffahrtsamt Dresden and Landesvermessungsamt Sachsen-Anhalt. The authors are also grateful to the Danish Hydraulic Institute (DHI), Denmark for providing an evaluation copy of the MIKE 11 software.

Chapter IV

Comparison of hydrodynamic models of different complexities to model floods with emergency storage areas

ABSTRACT:

A flood emergency storage area (polder) is used to reduce the flood peak in the main river and hence, protect the downstream areas from getting inundated. In this study, the effectiveness of a proposed flood emergency storage area at the middle Elbe River, Germany in reducing the flood peaks is investigated using hydrodynamic modeling. The flow to the polders is controlled by adjustable gates. The extreme flood event of August 2002 is used for the study. A fully hydrodynamic 1D model and a coupled 1D-2D model are applied to simulate the flooding and emptying processes in the polders and flow in the Elbe River. The results obtained from the 1D and 1D-2D models are compared with respect to the peak water level reductions in the Elbe River and flow processes in the polders during their filling and emptying. The computational time, storage space requirements and modeling effort for the two models are also compared. It is concluded that a 1D model may be used to study the water level and discharge reductions in the main river while a 1D-2D model may be used when the study of flow dynamics in the polder is of particular interest. Further, a detailed sensitivity analysis of the 1D and 1D-2D models is carried out with respect to Manning's n values, DEMs of different resolutions, number of cross-sections used and the gate opening time as well as gate opening/closing duration.

Published as: Chatterjee C, Förster S and Bronstert A. 2008. Comparison of Hydrodynamic Models of Different Complexities to Model Floods with Emergency Storage Areas. Hydrological Processes. Published online, DOI: 10.1002/hyp.7079.

1 INTRODUCTION

Flood storage areas form part of the flood management strategy at many lowland rivers. They are used to temporarily store excess floodwater in order to reduce peak flood flows downstream. In the last few years various studies have been conducted to predict the flood peak reduction in the main river and to simulate the inundation process in the flood storage areas. These studies represent a special case of hydrodynamic floodplain modeling because of the controlled manner of detention and release of flood water. Flow may be controlled by spillways, adjustable inlet and outlet structures or engineered dike breaches.

Various researchers have used the hydrodynamic modeling approach to simulate flood inundation in the floodplains (Werner, 2004; Bates et al., 2005). The hydrodynamic modeling approach of flood inundation simulation essentially involves the solution of one dimensional and two dimensional Saint Venant equations using numerical methods. Various numerical models have been developed for flood plain delineation/flood inundation and flow simulation. These numerical models essentially involve solving the governing equations for flow in rivers and floodplains using certain computational algorithms. Based on the approximations used, the numerical models are categorised into (a) one-dimensional (1D) models, (b) two-dimensional (2D) models, and (c) one-dimensional river flow models coupled with two-dimensional floodplain flow (1D-2D) models.

Various software like HEC-RAS (HEC River Analysis System) from the U.S. Army Corps of Engineer's Hydrologic Engineering Center (HEC, 2002), U.S. National Weather Service's (NWS) DWOPER and FLDWAV (Fread et al., 1998), MIKE11 developed at the Danish Hydraulic Institute, Denmark (DHI, 1997), SOBEK-1D developed at the Delft Hydraulics, Delft (Werner, 2001) etc. have been used extensively for dynamic 1D flow simulation in rivers. The 1D models though simple to use and provide information on bulk flow characteristics, fail to provide detailed information regarding the flow field. Hence, attempts have been made to model the 2D nature of floodplain flow. Some of the most widely used soft-

ware for 2D modeling are FLO 2D (O'Brien, 2006), RMA2 (King et al., 2001), MIKE-21 (DHI, 2000), DELFT-FLS (Hesselink et al., 2003), DELFT-3D (Stelling and Duinmeijer, 2003) and TELEMAC-2D (Horritt and Bates, 2001).

The 1D models fail to provide information on the flow field while the 2D models require substantial computer time; hence, attempts have been made to couple 1D river flow models with 2D floodplain flow models. In the coupled 1D-2D models, the flow in the main river channel is simulated using the 1D equations, while the 2D equations are solved for the water spilling over the banks to the floodplains. The link between the two kinds of flow is usually done by a mass conservation equation. Dhondia and Stelling (2002) describe the 1D-2D model SOBEK (Rural/Urban) developed by the laboratory at Delft Hydraulics. The MIKE-21 model has been dynamically linked to the MIKE-11 model, into a single package called MIKE FLOOD developed at the Danish Hydraulic Institute (Rungo and Olesen, 2003).

Hydrodynamic models of different complexity have been used to simulate flow situations with flood storage areas. 1D models for the river coupled with storage cells that represent the polders have been used to simulate the peak capping effect. The storage cells are usually characterised by the relationship between volume or area as a function of elevation or by a series of cross sections (Minh Thu, 2002; Kúzniar et al., 2002; Faganello and Attewill, 2005). Also, there are a few studies applying combined 1D-2D model, where the flow in the river is solved in 1D whereas the flow in the storage area is simulated using a 2D approach (Baptist et al., 2006). Further, since full 2D or combined 1D-2D models are generally computationally very extensive, quasi 2D model approaches have been applied in order to give a simplified 2D representation of the storage area combined with a fast computation process (Aureli et al., 2005; Huang et al., 2007).

As far as floodplain inundation is concerned, several studies have been carried out to compare the predictive performances of hydrodynamic models of different complexities (Horritt and Bates, 2002; Tayefi et al., 2007). However, there has been no such detailed comparative study for simulating floods with emergency storage areas. In this study, a comparison of 1D MIKE11 and 1D-2D MIKEFLOOD models

to simulate flows for a proposed flood emergency storage area at the middle Elbe River, Germany is carried out.

2 STUDY AREA AND DATA USED

The proposed emergency storage area is located in the lowland area at the Middle Elbe River, Germany (Figure 1). It extends 7 km along the right bank of the Elbe River. The overall area amounts to 17 km² with a maximum storage capacity of approximately 40 million m³.

The storage area is divided into a northern and a southern polder basin by an already existing dike road running through the area. Both basins are connected by a sluice gate of 50 m width and 2 m depth. This gate is termed as the connecting gate. The filling and emptying process of the storage area is to be controlled by two adjustable overflow weirs of 25 m width each. The gate for the north polder is termed as the north gate while the gate for the south polder is termed as the south gate. The emergency

storage area is designed for reducing flood peaks of not less than 100 years return period. It has to be emphasised that the emergency storage area is a potential retention site and hence, at present neither the dikes surrounding the polder basins nor any control structures exist. Topographic data, river flow data and information on control structures and polder dikes were provided by the local water authorities according to the current planning stage.

In this study, the flood event of the period 5th Aug. to 17th Sep., 2002, i.e. a duration of 44 days is considered to study the effectiveness of the proposed polder. For this flood event, the peak discharge is 4420 m³/s which occurred on 18th Aug, 2002 at the gauge of Torgau. Besides, four other flood events are used for model calibration and validation as described later.

Currently about 90 % of the area is under intensive agricultural use. The rest is taken up by watercourses and forests, most of which are under nature protection. It is expected that the land will retain its original purpose after designation as emergency storage area.

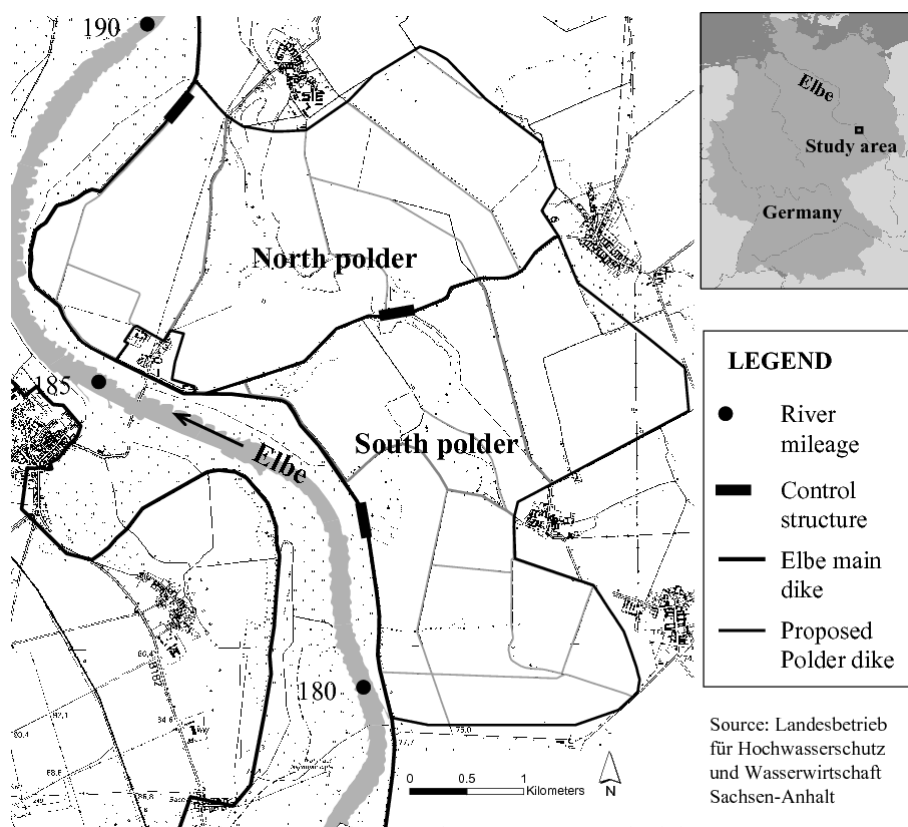


Fig. 1: Map of the proposed flood emergency storage area at the Middle Elbe River, Germany

3 METHODOLOGY

The one-dimensional model MIKE 11 and the coupled one-/two-dimensional model MIKEFLOOD are applied to simulate the flooding and emptying processes in the polders and flow in the Elbe River. The governing flow equations of MIKE 11 are one dimensional and are of shallow water types which are the modifications of Saint Venant equations (DHI, 1997; DHI, 2000). MIKEFLOOD integrates topographic data of the one-dimensional MIKE 11 river network with the two dimensional MIKE 21 floodplain (bathymetry data) through four different linkages i.e. (i) standard link where one or more MIKE21 cells are linked to the end of a MIKE11 branch, (ii) lateral link where a string of MIKE21 cells are laterally linked to a specified reach of MIKE11, (iii) structure link con-

sisting of a three point (upstream cross-section, structure and downstream cross-section) MIKE11 branch whose ends are linked to MIKE21 cells, and (iv) zero flow link specified to a MIKE21 cell will have zero flow passing across the cell (DHI, 2004). For this study, the standard link is the only relevant link that can be used and hence, it is selected.

3.1 One-dimensional model setup

The 1D model MIKE 11 is set up to represent a 18.6 km reach of the Elbe River (Figure 2), which is described by a series of 34 cross sections. These cross-section data are provided by the local water authority. The cross-section data available downstream of Elbe 187 km are not only very sparse but these are available for the main channel only. Hence, these cross-sections were extended to the dikes using elevation data from airborne laser altimetry.

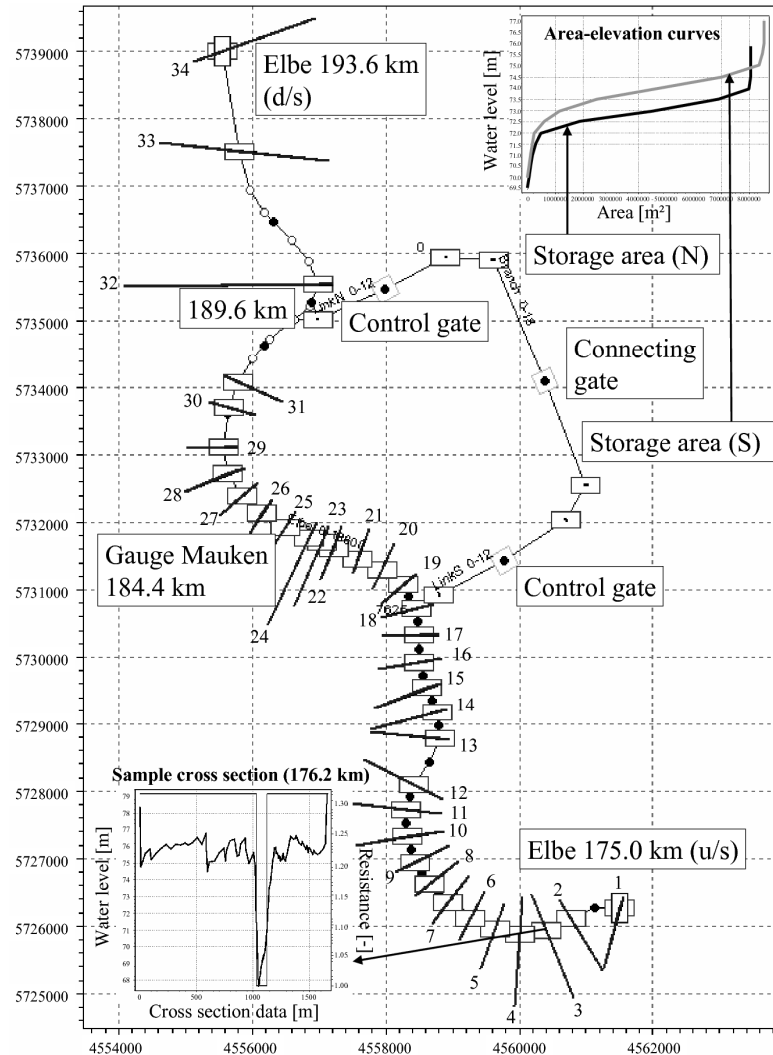


Fig. 2: MIKE 11 model layout for the proposed flood emergency storage area

The boundary condition at the upstream end of the reach at 175.0 Elbe-km is a discharge hydrograph of the Torgau gauging station. Although this gauge is located approximately 20 km upstream of the upper model boundary, utilisation of these discharge data is justified as there are only minor tributaries to the Elbe River between Torgau and the modelled river stretch. The downstream boundary condition at 193.6 Elbe-km is provided as a rating curve.

The emergency storage area is schematised in the model by two storage cells each representing one polder basin. The storage cells are described by their area-elevation curves (Figure 2). The curves are derived from a high-resolution Digital Elevation Model that was obtained from airborne LiDAR survey. The gates are implemented as control structures that operate due to certain pre-set conditions as mentioned later.

3.1.1 Calibration and validation of model

Calibration of the hydrodynamic models for emergency flood storage areas is difficult as emergency storage areas are usually designed to be used for flood peak capping during rare flood events. The storage area may have never been in operation before and hence, observation data for calibration purpose may not be available. The same is true for the present study which investigates a proposed flood storage area that is not yet constructed. However, the MIKE11 model is calibrated and validated for the flow in the Elbe River and its floodplain within the embankments.

The MIKE11 model is calibrated and validated against water levels recorded at the Mauken gauging station at 184.4 Elbe-km. Because of the different nature of bed materials two hydraulic roughness classes are distinguished, one for the main channel and one for the adjacent floodplain. In order to identify the two roughness coefficients, a two stage calibration and validation procedure is adopted. In the first stage, the roughness coefficient for the main channel is identified and in the second stage the roughness coefficient for the floodplain is identified. Four flood events during the period 1st October to 30th Nov 1999, 1st January to 31st March 2002, 1st August to 27th September 2004 and 1st March to 30th June, 2005 are selected for the process of calibration and validation. Of these, water does not spill over to the floodplains for the first and third events and hence,

these are used for calibration and validation for the main channel. Initially, the roughness information in the form of Manning's n values is taken from the literature (Chow 1959) and similar studies (Horritt and Bates 2002) which are then modified during the calibration process.

Two goodness of fit criteria are used to compare the simulated water levels with the observed values. These are (i) the Nash-Sutcliffe coefficient (E_{ns}) and (ii) the index of agreement (d), which are as follows:

$$E_{ns} = 1 - \frac{\sum(Q_o - Q_s)^2}{\sum(Q_o - Q_{av})^2} \quad (1)$$

$$d = 1 - \frac{\sum(Q_o - Q_s)^2}{\sum(|Q_o - Q_{av}| + |Q_s - Q_{av}|)^2} \quad (2)$$

Where, E_{ns} =Modeling efficiency, Q_o = Observed discharge (m^3/s), Q_s = Simulated discharge (m^3/s), Q_{av} = Mean of the observed discharge (m^3/s) and d = Index of agreement.

3.2 One-/ two-dimensional model setup

In the MIKEFLOOD model layout, the Elbe River and the three gates (inlet or south gate, connecting gate and outlet gate) are represented in the 1D model MIKE11. The polders are represented in the form of a DEM in the 2D model MIKE21. Both the 1D MIKE11 and 2D MIKE21 models are dynamically coupled by standard links. This coupled model is run with the same boundary conditions, flood scenario (i.e. for the August 2002 flood event) and gate operation as the 1D model. Thus, the essential difference between the 1D MIKE11 setup and MIKEFLOOD setup is in the representation of the polders.

In this study, three different DEMs are used which are obtained by resampling the LIDAR DEM to grid sizes of 8 m, 25 m and 50 m. Initially, the LIDAR DEM is processed to remove non-permanent objects, such as dung hills or vehicles, and to correctly represent line structures, such as dikes and ditches. While generating a DEM by interpolation of point data obtained by laser scanning, there is a risk that line structures are not continuous in the DEM. Thus, the following procedure is used for correct representation of line structures: (i) line structures are digitised as line objects using to-

pographic maps, (ii) height information is attached to the digitised line objects, (iii) a large number of points are generated along the line objects and (iv) the DEM is generated by interpolating point data that were collected by the laser scanner and generated from the line objects using GIS. As the laser scanner only collects water surface elevation, bottom height of ditches was obtained by terrestrial measurements and included in the DEM generation procedure. While aggregating LIDAR data to other grid sizes, the DEM gets “smoother”, i.e. dikes have lower elevation and ditches become shallower. In order to preserve the flooding characteristics, post-processing is done in the aggregated DEM by converting the line objects (with correct height information) to grid objects of the same grid size as the aggregated DEM. Subsequently, the corresponding grid cells in the aggregated DEM are replaced by grid cells of the line object. While aggregating the DEM to grid sizes of 8m, 25m and 50m, it is ensured that water does not spill over the dikes (Elbe dike and polder dikes) by setting the dike cells to their true elevations. However, the correct depths of the ditches inside the polders are not included in the aggregated DEMs as these ditches are very narrow (about 3 to 5 m wide) and hence, would be overrepresented when converting them into grid sizes of 8 m, 25 m and 50 m.

3.3 Sensitivity analysis

A detailed sensitivity analysis is carried out for the different hydrodynamic models with respect to a number of input parameters like (i) Manning's n values, (ii) DEM's of different resolutions, (iii) number of cross-sections used and (iv) gate opening time and opening/closing duration. The conditions under which the sensitivity analyses are carried out for each of these input parameters is presented below.

3.3.1 Manning's n

First the sensitivity analysis of the MIKE11 model setup for only the Elbe River (i.e. without the polders) is carried out with respect to Manning's n values. For this purpose, two cases of Manning's n values are considered. In the first case, the n values are decreased by 5% from the mean/calibrated values while in the second case, the n values are increased by 5% (Table 1). Subsequently, the sensitivity analysis

of the MIKE11 model setup to the Manning's n values is carried out by including the polders. Again, the same two cases of n values stated above are considered (Table 1).

The sensitivity analysis of the MIKEFLOOD setup to the Manning's n values is also carried out. In this case the n values for the river as well as the river floodplain are kept at their calibrated values while the n values for the polders are varied i.e. increased and decreased by 5% (Table 1).

Table 1: Range of Manning's n values for different land-use class considered in sensitivity analysis

Class	Manning's n*
River channel	0.0361 – 0.0399 (0.038)
River floodplain	0.0475 – 0.0525 (0.050)
Polder	0.0475 – 0.0525 (0.050)

*Calibrated values are indicated in brackets

3.3.2 DEM's of different resolutions

The sensitivity of the 1D MIKE11 model to the use of different DEM resolutions is studied. Two DEMs of horizontal resolution 8 m and 50 m are used to derive the area-elevation curves. The MIKE11 model is simulated for the August 2002 flood event with the area-elevation curves derived from the two different DEMs.

The sensitivity of the MIKEFLOOD model to the use of different DEM resolutions is also studied. The sensitivity analysis is carried out considering three DEM's of different horizontal resolutions for the polders viz. 8 m, 25 m and 50 m. The sensitivity of the use of these different DEM's to the water level and discharge reduction in the Elbe River as well as the flow dynamics in the polders is studied. The flood inundation extent and depth in the polders at a particular instant of time for the different DEM's is also studied.

3.3.3 Number of cross-sections used

The sensitivity of the 1D MIKE11 model to different number of cross-sections used is also studied. In this case also, only the Elbe River is modeled and the polders are not considered. As stated earlier, a total of 34 cross-sections are used to define the Elbe River in the MIKE11 model (Figure 2). These cross-sections are in general 400 m to 800 m apart but the cross-section spacing is more in the downstream side

with a maximum spacing of 2.4 km between Elbe River 189.6 km and 192 km. In order to study the sensitivity of the results to the number of cross-sections used, two different cases are considered in which different number of cross-sections are used:

Case-I: Only 20 out of 34 cross-sections are used, i.e. 14 cross-sections (nos. 3, 5, 7, 9, 11, 13, 15, 17, 19, 21, 23, 25, 27 and 29 (Figure 2)) are removed. Here, the 14 cross-sections which are removed are in the stretch of the Elbe River 175 km to 187.6 km. In this stretch of the river, the cross-section spacing varies from 400 to 800 m, i.e. they are closely spaced. Thus, the results obtained from the removal of these cross-sections would indicate the closeness at which the cross-sections are to be provided.

Case-II: Again another set of 20 cross-sections are used, i.e. a different set of 14 cross-sections are removed (nos. 2, 4, 6, 8, 10, 12, 14, 16, 18, 20, 22, 24, 26 and 28 (Figure 2)) in the same stretch of the Elbe River 175 km to 187.6 km.

3.3.4 Gate opening time and opening/closing duration

The sensitivity of the 1D MIKE11 model to the time of opening of the south gate during the polder filling process is studied. For this the following two gate opening times are considered for the south gate:

Case-I. 6 hour ahead of the actual opening time.

Case-II. 6 hour after the actual opening time.

The sensitivity of the 1D MIKE11 model to different gate opening and closing duration during the polder filling process is also studied. In this study all the gates (i.e. the south and north as well as the connecting gates) open or close in a span of 30 min (based on information from local water authority). In order to study the sensitivity of the gate opening and closing duration to the water level and discharge reduction in the Elbe River, two different gate opening and closing durations are considered:

Case-I: All the gates take 5 min to open or close.

Case-II: All the gates take 60 min to open or close.

4 RESULTS AND DISCUSSIONS

4.1 Calibration and validation of the one-dimensional model

Table 2 shows the performance indices for different trial values of Manning's n for MIKE11 simulated water levels at the Mauken gauging site during calibration and validation for the main channel only. The E_{ns} and d values are found to be the highest for n equal to 0.038 during calibration. Using this n the E_{ns} and d values are also found to be very high during validation. Hence, the Manning's n value of 0.038 is chosen for the main channel.

Table 2: Performance indices for MIKE11 simulated water levels at the Mauken gauging site during calibration and validation (for the main channel only)

Events →	Calibration		Validation		
	Manning's n	E_{ns}	d	E_{ns}	d
0.037	0.662	0.931	-	-	-
0.038	0.925	0.984	0.92	0.983	
0.039	0.844	0.967	-	-	

Table 3: Performance indices for MIKE11 simulated water levels at the Mauken gauging site during calibration and validation (for the floodplains)

Events →	Calibration		Validation		
	Manning's n	E_{ns}	d	E_{ns}	d
For river	For floodplain				
0.038	0.035	0.976	0.724	-	-
	0.04	0.98	0.728	-	-
	0.045	0.981	0.732	0.979	0.584
	0.05	0.979	0.736	0.982	0.594

Different trial values of Manning's n for the floodplain are chosen keeping the main channel n value equal to 0.038. Table 3 shows the performance indices for the MIKE11 simulated water levels at the Mauken gauging site during calibration and validation for the floodplain. For the Jan-Mar, 2002 event, the E_{ns} value is found to be the highest for floodplain n value equal to 0.045 while the d value is found to be the highest for floodplain n value equal to 0.050. But during validation with the Mar-Jun, 2005 event, both the E_{ns} and d values are found to be the highest for floodplain n value equal to

0.050. Hence, the Manning's n value of 0.050 is chosen for the floodplains. Figure 3 shows a comparison of the observed and simulated water levels at the Mauken gauging site during calibration and validation for the floodplains.

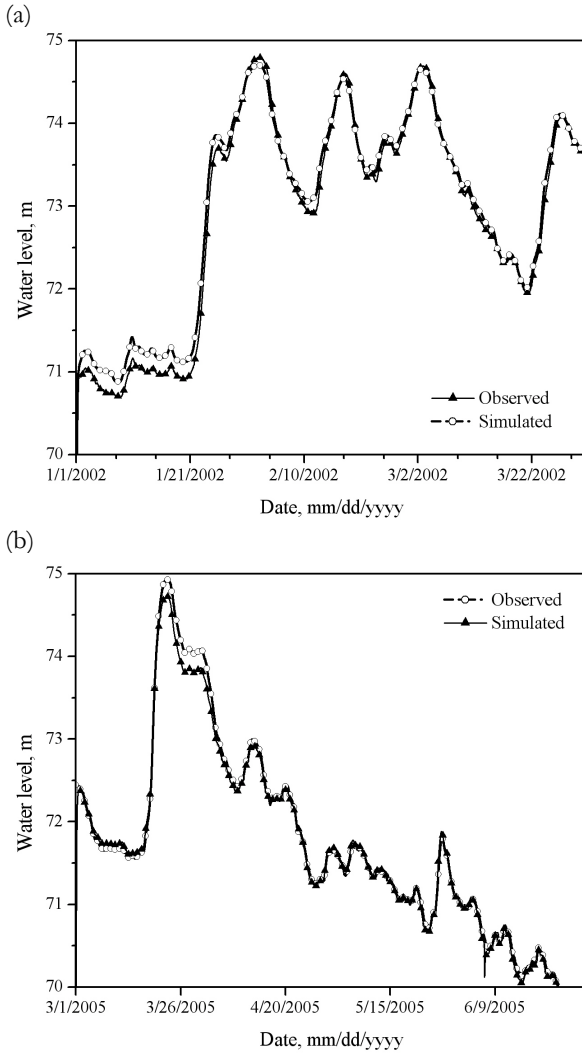


Fig. 3: Comparison of observed and simulated water levels at the Mauken gauging site during (a) Calibration for the flood event of 1st January to 31st March 2002 and (b) Validation for the flood event of 1st March to 30th June, 2005

4.2 One-dimensional model results for flooding and emptying processes in the polder

Figures 4a to c show the results obtained from MIKE11 simulation for the flooding and emptying processes in the polders and flow in the Elbe River for the August 2002 flood event. The peak discharge for this flood event is 4420 m^3/s . Here, the area-elevation curves for the storage areas are derived from a 50 m grid DEM. It is observed from these figures that the

south gate opens when the water level in the Elbe River reaches a threshold value of 76.94 m corresponding to a discharge of 4100 m^3/s (Figures 4a and b). At this instant of time a discharge of about 440 m^3/s enters through the south gate (Figure 4c) and this results in a sharp reduction in the Elbe discharge and water level (Figure 4a). Subsequently, the connecting gate and the south gates close when the water level reaches the design value in the north and south polders, respectively. The entire filling process takes about 30 hours. After the gates close, the discharge and water level in the Elbe River rise again. The water level reduction at the Elbe River 184.4 km (i.e. at the Mauken gauge) is 25 cm while the corresponding discharge reduction at this point is 310 m^3/s (Figure 4a).

In order to achieve the maximum water level reduction in the Elbe River for given polder volumes, the discharge in the Elbe River should be as close as possible to a straight line after the filling process starts in the polder. The factors affecting the magnitude of water level reduction in the Elbe River for given polder volumes are (i) time of opening of the gates during the polder filling process, (ii) gate opening/closing duration (iii) gate width or partitioning of the gates and (iv) shape of the flood hydrograph. A detailed investigation on the effect of (i) sequential operation of the north and south gates during the filling process (ii) partitioning of the gates and (iii) shape of the flood hydrograph, on the magnitude of water level reduction in the Elbe River is reported in Förster et al. (2008). In this study, only the south and the connecting gates (and not the north gate) operate during the polder filling process. The gate opening/closing durations are 30 min and the gate widths are 25 m (based on information collected from local water authority). Further, as stated earlier, the August 2002 flood hydrograph is considered here. Thus, in this study, the time of opening of the south gate during the start of the filling process of the polders is the only crucial factor for obtaining the maximum possible water level reduction in the Elbe River. The time of opening of the south gate during the filling process of the polder is decided manually based on a trial and error process so as to maximise the water level reduction in the Elbe River. Several trial runs are carried out with different opening times for the south gate (specified in MIKE11 for each trial run) while the connecting and south gates close

when the design water level is reached in the north and south polders, respectively. For each run the water level reduction in the Elbe River is noted. It is observed that when the south gate is opened corresponding to a water level of 76.94 m at Elbe River chainage 184.4 km (i.e. on 17th Aug, 2002 at 15.40 hrs for the August 2002 flood event), a maximum water level reduction of 25 cm occurs in the Elbe River.

The gate operation during the polder emptying process is also decided manually. The objective is to empty the polders as soon as possible. Thus, it is decided to release the water from the polders into the Elbe River as soon as the water level in the river falls below the water level in the polders. Accordingly, it is decided that the emptying process start when the water level in the Elbe River near the south gate falls to 75.64 m (Figure 4a) i.e. 2 days after the filling process ends which allows for a safe release of the flood water. The south gate is opened first followed by the north gate 8 hours later. The connecting gate is opened 7 hours after the north gate is opened (Figure 4b). Immediately after the connecting gate is opened, the south gate is closed as the flow direction reverses and water starts entering the polders again. As per the MIKE11 simulation, the entire emptying process takes about 24 days. The long duration of the emptying process is because after a certain time the water level of the polders become same as the water level in the Elbe and hence, the water levels in the polder fall along with the river water level. It is to be mentioned here that all gate operations are automatically executed in the MIKE11 model simulations based on the selected decision criteria.

As mentioned earlier the storage area under investigation is yet to be constructed and hence, only calibration data for the river is available. Due to lack of calibration/validation data sets for the storage area the simulation results obtained herein are compared with a similar study. In IWK (2003) the peak attenuation effect for several proposed flood storage areas along the Middle Elbe River was simulated considering floods with peak discharges ranging between $4000 \text{ m}^3/\text{s}$ and $5000 \text{ m}^3/\text{s}$. For the same storage area as investigated in the present study a peak reduction between $262 \text{ m}^3/\text{s}$ (14 cm) and $497 \text{ m}^3/\text{s}$ (23 cm) at the gauge Wittenberg was simulated. These results are very similar to the range of water level reduction obtained in the present study.

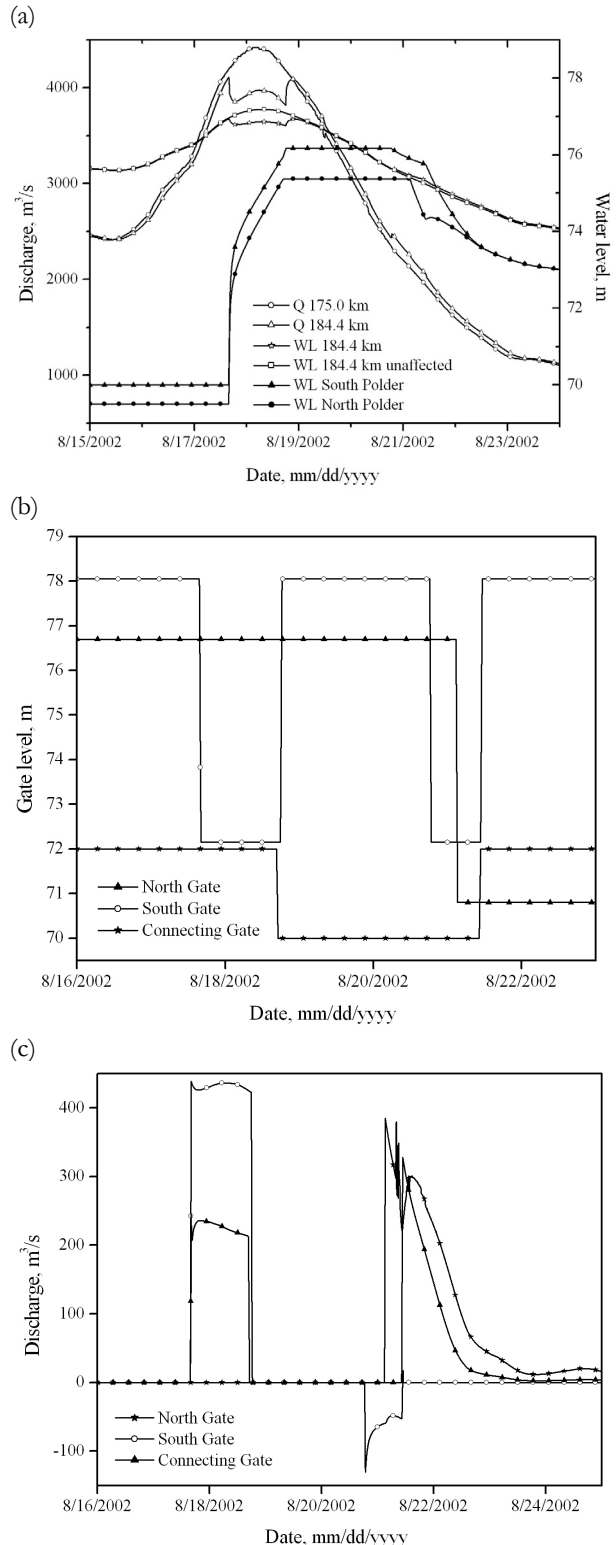


Fig. 4: MIKE11 simulation results for the proposed emergency storage area for the August 2002 flood event (positive discharge in flow direction from South to North): (a) Simulated discharge and water levels, (b) Gate levels, (c) Gate discharge

4.3 Comparison of one- and one-/ two-dimensional model results

The DEM grid size used for MIKEFLOOD is 50 m and the area-elevation curves for MIKE11 are also extracted from 50 m grid DEM. A comparison of the results obtained from MIKE11 and MIKEFLOOD simulation runs show that there is absolutely no difference in the water level and discharge reduction in the Elbe River. This is because the discharge through the south gate is the same for both models. The identical discharge is because it is a case of free flow discharge controlled by the upstream water level and the upstream water level for the south gate for both the models is same even though the downstream water level differs.

The differences between MIKE11 and MIKEFLOOD results are that for MIKE11 the water front reaches the connecting gate at the same instant at which the south gate is opened while for MIKEFLOOD the water front takes about an hour to reach the connecting gate. Further, due to the different treatment of the polder filling in the models, the water levels upstream and downstream of the connecting gate differ for the two models. As a result there is a slight difference in the discharge through the connecting gate for the two models.

In the emptying process of the polders there is significant difference between MIKE11 and MIKEFLOOD results. For the MIKEFLOOD model, the emptying process continues till the water level in the polders lowers down to about 73.25 m. The emptying process takes about 4 days with most of the emptying taking place in the first one and a half days. The emptying process stops after the water level reaches 73.25 m because the ground elevations near the north gate are higher than its sill elevation (70.8 m) and this does not permit further draining of the water to take place. However, for the MIKE11 model, the emptying process continues till the water level in the polders lowers to the sill elevation of the north gate (70.8 m) along with the river water level. The emptying process takes about 24 days. This emptying result of MIKE11 is in fact incorrect since practically the draining process cannot continue below the water level of 73.5 m because of the ground elevation conditions near the north gate as mentioned above. Such an error is expected to occur in MIKE11 because the area-elevation curves which describe the polders do not take care of the spatial

variations of ground elevations. However, a work around is possible in MIKE11 by raising the sill level of the north gate to 73.5 m when the water level in the north polder lowers to 73.5 m during the emptying process. However, this would require the use of MIKEFLOOD model to ascertain the required water level (73.5 m in this study) prior to using MIKE11. Such an approach was not adopted herein as this paper aims at an independent comparison of the 1D and 1D-2D models to model floods with emergency storage areas.

MIKEFLOOD results for the polders show large tracts of agricultural land, particularly in the northern side of the north polder (with depths of water as high as 1.5 to 2 m in some places) remain inundated after the emptying process through the north and south gates. Because of the topography, this water cannot be drained using the gravity process through the gates. Hence, some of the water may be drained using a small gate in a stream on the northern boundary (not considered here in the modeling process) and the rest of it has to be pumped out or gradually evaporate or seep away.

An additional information which is obtained from MIKEFLOOD is the water velocities in the polders. It is observed that at some places in the polder near the south gate, the velocity is higher than the mean velocity of 1.5 m/s (for 50 m grid size DEM). This type of information will be of particular help in studying the erosion and sedimentation problems in the polder as well as in the subsequent risk analysis.

4.4 Computation time, storage space requirements and modelling effort

A comparison of the computational time requirements for the two models was carried out. For this the models were run in a personal computer having AMD Athlon(tm) 64 3500+ processor with 2.2 GHz speed and 2GB RAM. Also, the models were run for the filling and emptying processes in the polders as well as flow in the Elbe River for the same August 2002 flood event. The MIKEFLOOD (with 8 m grid DEM for the polders) model was run for shorter durations because of very high computational time and storage space requirements. The simulation time step interval and result storing frequency for the different runs are shown in Table 4. The computational time as well as storage space requirements for the

model runs is shown in Table 5. It is observed that the computation time as well as the storage space requirements for MIKE11 model is very low while these are very high for the MIKEFLOOD model. As expected, for MIKEFLOOD the computation time and storage space requirements increase drastically when finer resolution DEMs are used.

Tab. 4: Model run details for the August 2002 flood event

Model	Simulation time step interval (s)	Result storing frequency (min)
MIKE11	5 s	5
MIKEFLOOD	MIKE11 – 2 s	2
	MIKE21 – 2 s	15

As far as the modelling effort is concerned, considerable effort is required in setting up of the MIKEFLOOD model. For MIKEFLOOD, quite a few adjustments had to be made in the

DEM near its links with the structures of MIKE11 to bring about model stability. The DEM is cut and levelled near the structures and provided with an initial water level. In comparison, considerably less effort is required in setting up the MIKE11 model.

Tab. 5: Computation time and storage space requirement for different model runs

Model	DEM grid size	Computation time (h:min)	Storage space
MIKE11		2 min	22 MB
MIKEFLOOD	50 m DEM	3 h 43 min	1.1 GB
	25 m DEM	14 h 23 min	3.1 GB
	8 m DEM*	12 h 40 min	1.3 GB

* The MIKEFLOOD model with 8 m grid DEM is simulated only for the polder filling process i.e. from 5th Aug. to 21st Aug., 2002.

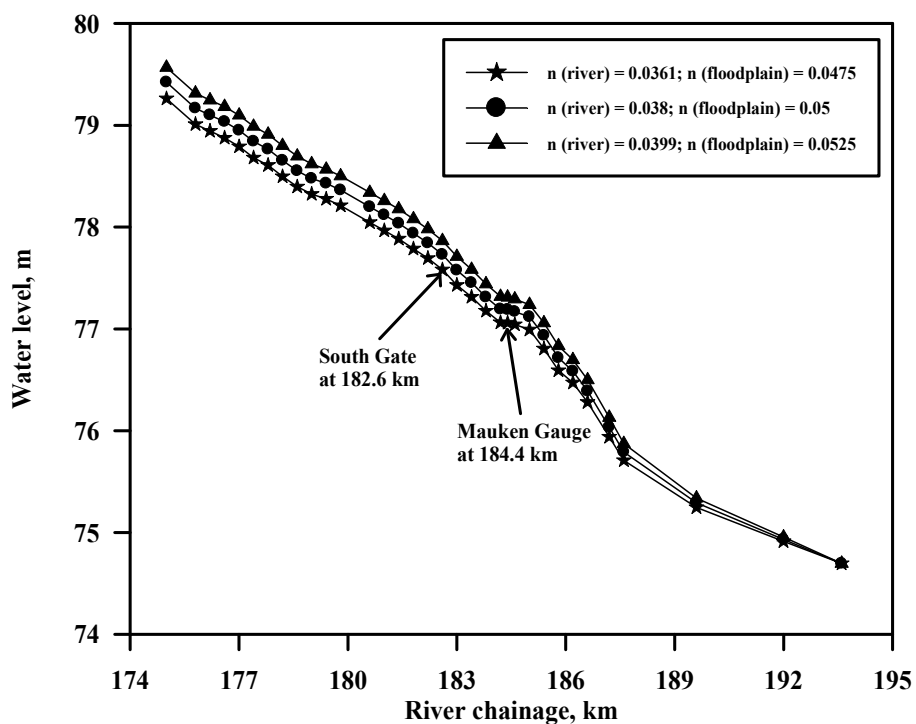


Fig. 5: Maximum water levels along longitudinal section of Elbe River as obtained from M11 (polders are not considered) for different 'n' values for the August 2002 flood event

4.5 Sensitivity analysis

4.5.1 Manning's n

Figure 5 shows the maximum water levels along the longitudinal section of Elbe River as obtained from MIKE11 (when only the Elbe River is modeled and the polders are not considered) for different ' n ' values for the August 2002 flood event. It is seen that as the n values are decreased the water level decreases and vice-versa. When the n values are decreased by 5%, the maximum water level difference occurs at the upstream end which is 16 cm while the water level differences at the points of interest i.e. at the south gate is 15 cm and at the Mauken gauging site is 13cm. Similarly, when the n values are increased by 5%, the maximum water level difference also occurs at the upstream end which is 15 cm while the water level differences at the points of interest i.e. at the south gate is 14 cm and at the Mauken gauging site is 12 cm.

Considering the fact, that the maximum water level reduction at the Mauken gauging site is 25 cm (as stated earlier), these water level differences of 12-15 cm due to change of n values seem to be significant.

Figures 6a and b show the results of sensitivity analysis of the MIKE11 model to the Manning's n values when the polders are included. It is observed that when the n values are decreased by 5%, the water level reduction is only 12.3 cm and discharge reduction is 137 m^3/s (Figure 6a). While the water level reduction is only 17.0 cm and discharge reduction is 218 m^3/s when the n values are increased by 5% (Figure 6b). This happens because though the south gate is still opened at the same water level value of 76.94 m, the river discharge corresponding to this water level is different for the two cases due to different n values. As stated earlier, the water level reduction is 25 cm and discharge reduction is 310 m^3/s when the calibrated values of n are used. Thus, the model is quite sensitive to changes in n value.

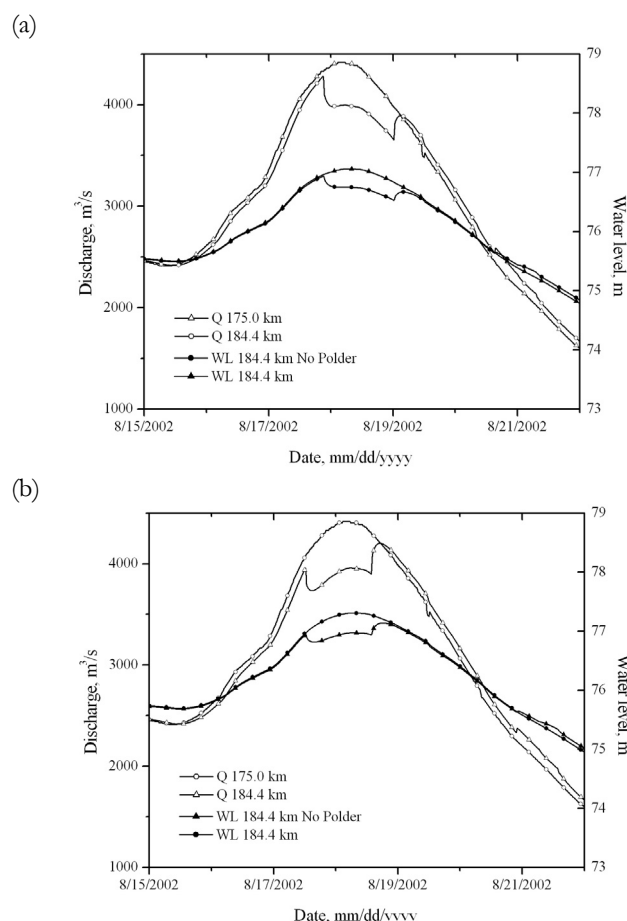


Fig. 6: Sensitivity of MIKE11 model to Manning's n values when polders are considered: (a) $n = 0.0361$ for river and 0.0475 for floodplain, (b) $n = 0.0399$ for river and 0.0525 for floodplain

In this study, as mentioned earlier, the Manning's n values obtained during the calibration and validation process are 0.038 and 0.05 for the main channel and adjacent floodplain, respectively. The corresponding normal values of Manning's n for the prevailing land-use mentioned in literature (Chow, 1959) are 0.035 (for natural streams – major rivers) and 0.05 (for floodplains – light brush). As the calibrated values are very close to those mentioned in the literature and the land-use in the study area is quite uniform, a lower range ($\pm 5\%$) of Manning's n is used in the sensitivity analysis. The uncertainty associated with the roughness values in modelling floods has been a subject of continuous research (Werner et al., 2005). Horritt (2005) states the difficulty in specifying the hydraulic roughness values in spite of having a reasonable idea of the land-use. The author further suggests the use of calibration approach to remove this difficulty. Hence, it is proposed that a more detailed calibration and validation procedure be adopted considering a large number of flood events in order to reduce the uncertainties associated with the Manning's n values. However, it is also expected that the sensitivity to n values would decrease when more than one polder is used and the consequent peak water level reduction in the Elbe River is much higher.

The results of sensitivity analysis of the MIKEFLOOD model show that they are insensitive to the variation of n values in the polders. This is quite expected because (i) the inflow to the polder remains the same as it is not influenced by the polder water level and (ii) n is proportional to the velocity which in bulk characteristic is low. This finding justifies using only one roughness value for the polders rather than differentiating into several roughness classes. Similar results are also reported by Werner et al. (2005).

4.5.2 DEM's of different resolutions

The results of sensitivity analysis of MIKE11 model to area-elevation curves derived from different grid size DEMs show that the water level and discharge reduction in the Elbe River remains unchanged. However, when the south gate is closed after the filling process, the discharge in the Elbe River for the 8 m DEM case increases to a lesser extent than that of the 50 m DEM case. For both the DEM

cases the polders are filled to their design levels i.e., 76.14 m for south polder and 75.35 m for the north polder. Though the discharge through the south and connecting gates are same for both cases, the gates close a little earlier for 50 m DEM case than 8 m DEM case. This minor difference in the result is due to the slightly different volume-elevation curves derived from the two DEMs. Because of averaging, the 50 m DEM has a slightly lesser volume for the design water level as compared to the 8 m DEM. For the 50 m DEM, the volume of water corresponding to the design water levels are 20.24 Mm³ in the north polder and 20.32 Mm³ in the south polder (i.e. a total volume of 40.56 Mm³). Whereas for the 8 m DEM, the volume of water corresponding to the design water levels are 20.44 Mm³ in the north polder and 20.54 Mm³ in the south polder (i.e. a total volume of 40.98 Mm³). Thus, the total difference in volume of polders for both cases is 0.42 Mm³. But this does not produce significantly different results. Hence, a 50 m DEM can very well be used to derive the area-elevation curves for the 1D MIKE11 model and yet get accurate results.

The results of sensitivity analysis of MIKEFLOOD model to the use of different DEM resolutions for the polders also show that the water level and discharge reduction in the Elbe River remain the same. However, when the south gate is closed after the filling process, the discharge in the Elbe River for the 8 m DEM case increases to a lesser extent than that of the 25 m DEM case which in turn increases to a lesser extent than that of the 50 m DEM case. This is because for the design water level, the volume of 8 m grid DEM is slightly higher than that of the 25 m grid DEM which in turn is higher than that of the 50 m grid DEM. As a result, for the 50 m DEM case the south gate closes ahead of the 25 m DEM case which in turn closes ahead of the 8 m DEM case. The south gate discharge is same in all cases because of same upstream water level. So, even though the downstream water levels differ, the discharge remains the same as it is a case of free flow discharge governed by upstream water level. The water front takes about an hour to reach the connecting gate for all cases. However, the discharge through the connecting gate is slightly different for the three grid size DEMs because of varying upstream and downstream

water levels for the three cases. The upstream water level for the 8 m case remains lower than for the other two since the 8 m DEM has the same volume of water at a lower elevation compared to that of 25 m and 50 m DEM.

Figures 7a to c shows the flood inundation extent and depth in the south polder for the three DEM cases (8 m, 25 m and 50 m) on 17th August 2002 at 16.30 hours, i.e. 40 min after the filling process starts through the south gate. At this instant of time, the volume of water that enters the south polder is the same for all the three cases as the discharge through the south gate is the same for all cases. For the 50 m DEM, the inundation extent is 1.35 km² and the maximum water depth is 3.01 m (Figure 7c). For the 25 m DEM, the inundation extent is 1.23 km² and the maximum water depth is

3.36 m (Figure 7b). For the 8 m DEM, the inundation extent is 1.23 km² and the maximum water depth is 3.64 m (Figure 7a). For the 50 m DEM, the surface elevations are higher than the 25 m and 8 m DEM. Hence, the maximum water depth is the lowest for 50 m DEM and the resulting inundation extent is the highest. Further, though the total inundation extent for the 8 m and 25 m DEM are same, their spatial variation is different, particularly at the fringes (Figure 7a and b). Unlike floodplain inundation studies, for polder studies, the analysis of the inundation extent and depth for different DEMs is not of much significance since after the initial phase where the water front progresses, the polders begin to fill up and the DEM resolution does not play a major role.

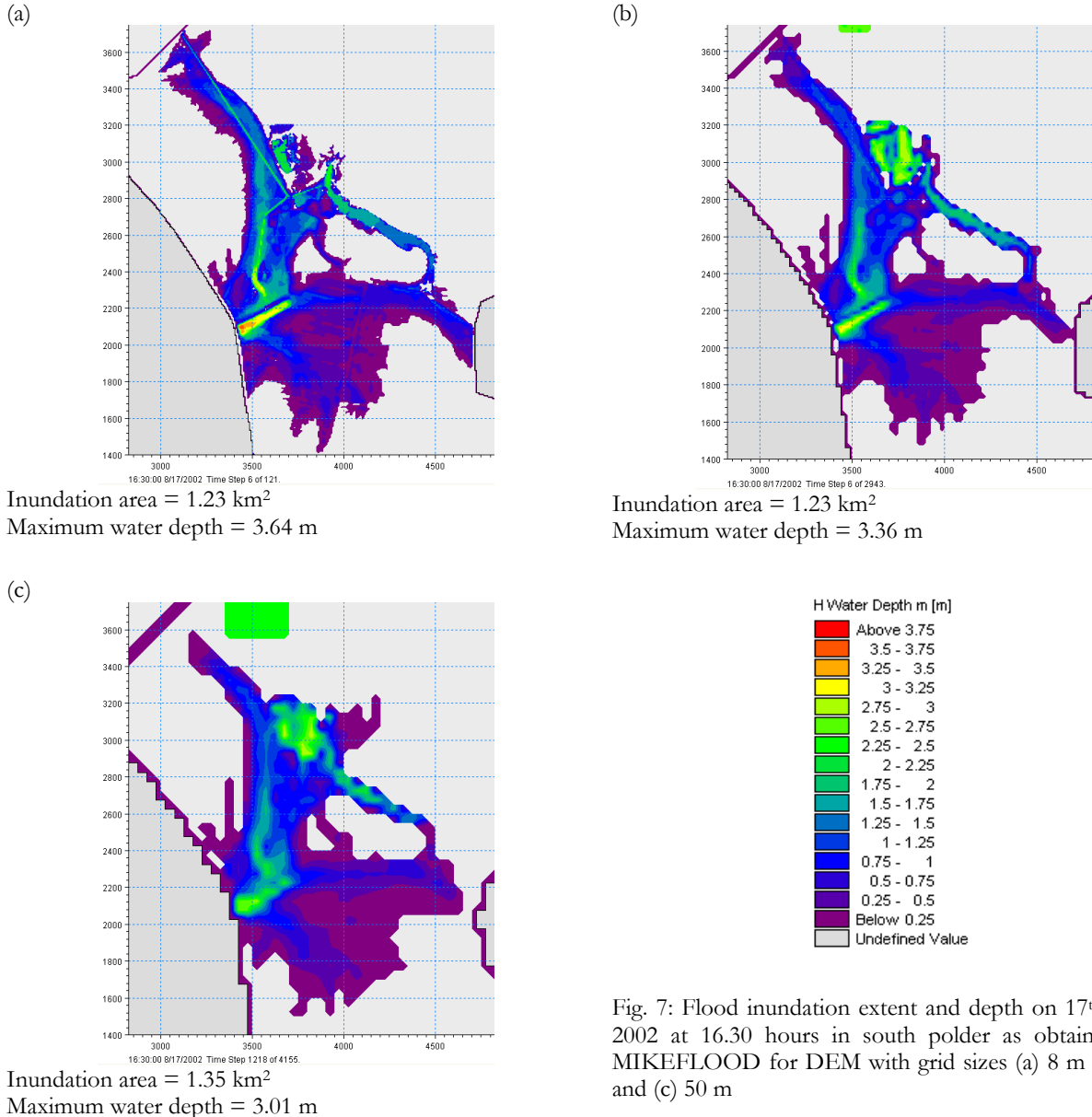


Fig. 7: Flood inundation extent and depth on 17th August 2002 at 16.30 hours in south polder as obtained from MIKEFLOOD for DEM with grid sizes (a) 8 m (b) 25 m and (c) 50 m

4.5.3 Number of cross-sections used

Figure 8 shows the maximum water levels along the longitudinal section of the river as obtained from MIKE11 for the case when all the 34 cross-sections are used and for the two different cases of cross-sections used for the August 2002 flood event. It is observed that for case I, the water levels are sometimes a little

higher and sometimes a little lower than the case when all 34 cross-sections are used. Whereas, the water levels for case-II are in general a little lower than the case when all 34 cross-sections are used. However, for the lower reaches of the river, the water levels for both cases I and II almost coincide with the water level for the case when all 34 cross-sections are used.

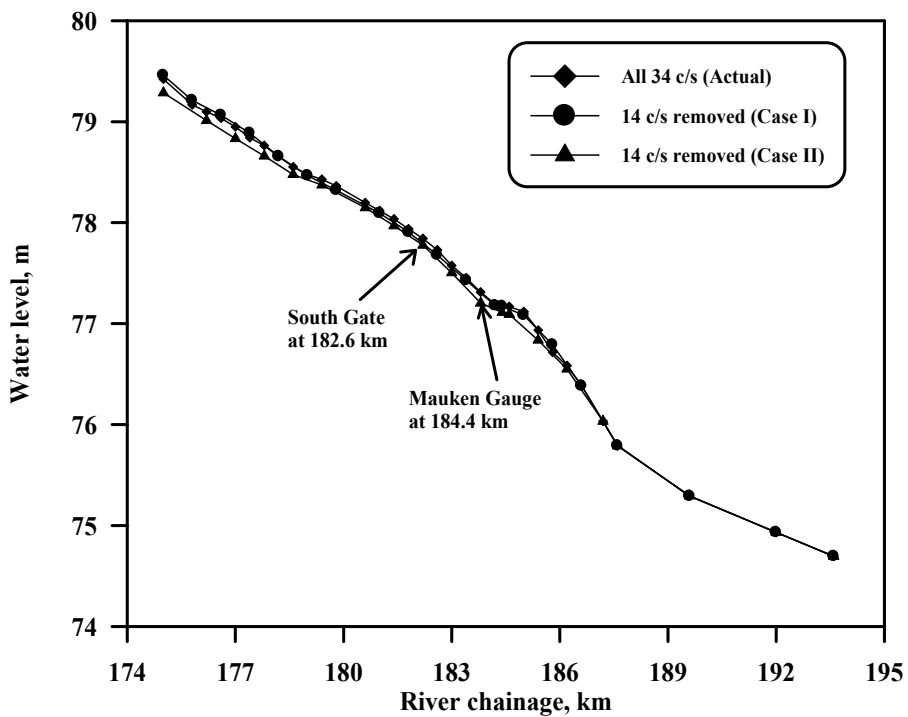


Fig. 8: Maximum water levels along longitudinal section of Elbe River as obtained from M11 for different sets of cross-sections for the August 2002 flood event

The water level differences at the points of interest i.e. south gate and Mauken gauging site for the different cases are shown in Table 6. It is seen that the water level differences are not that significant considering that 14 cross-sections are removed.

Table 6: Water level differences (in m) in the Elbe River due to use of different sets of cross-section data

Case	No. of Cross-sections removed	Water level difference (m) at river chainage	
		182.6km	184.4km
I	14	-0.05	-0.02
II	14	-0.09	-0.08

These results indicate that for the two cases when 14 cross-sections are removed, the shape of the river including its depth and width are

very well represented by the remaining 20 cross-sections. Thus, in general it can be seen that the number of cross-sections used in this study to model the Elbe water level is reasonably sufficient.

4.5.4 Gate opening time and opening/closing duration

As mentioned earlier, during the filling process of the polder, the south gate is opened at 15.40 hrs on 17th Aug, 2002 in order to obtain a maximum water level reduction of 25 cm in the Elbe River. When the south gate opens 6 h ahead of this opening time at 9.40 hrs on 17th Aug, 2002 (corresponding to the Elbe water level of 76.71 m at the Mauken gauge instead of 76.94 m), the water level reduction decreases to 14.8 cm (from 25.0 cm) which corresponds to a discharge reduction of 182 m³/s. Similarly,

when the south gate opens 6 h after the actual opening time at 21.40 hrs on 17th Aug, 2002 (corresponding to the Elbe water level of 77.10 m at the Mauken gauge instead of 76.94 m), the water level reduction decreases to 8.6 cm (25.0 cm) which corresponds to a discharge reduction of 93 m³/s. This shows the importance of a very good forecast for an effective reduction of water levels in the main river.

The results of sensitivity analysis of MIKE11 model to different gate opening/closing durations during the polder filling process show that for case-I, there is a sudden fall in the Elbe River discharge (as compared to the 30 min duration case) when the south gate opens. This is because the south gate opens faster and hence, the initial discharge through the south gate is higher. Also, the south gate closes earlier (than for the 30 min duration case). This is because both the south and connecting gates are closed when the respective design water levels are reached in the polders. As the gates close very fast for case-I, the water level (and hence, the volume) in both the polders after the gates are fully closed are lower as compared to the 30 min case. The final volume of water in the north and south polders for case-I are 20.10 Mm³ and 20.08 Mm³, respectively; while the final volume of water in the north and south polders for the 30 min case are 20.32 Mm³ and 20.24 Mm³, respectively. Thus, as the storage volume in the polders is a little less for case-I, the discharge and water level at Elbe River 184.4 km rises a little higher than the 30 min case. However, the total discharge and water level reduction in the Elbe River for case-I is the same as that for the 30 min case, because the total discharge and water level reductions are still governed by the threshold discharge and water levels at which the south gate opens, and this threshold discharge and water level are the same for both the cases. Similarly, for case-II, as the gates open and close slowly the final volume of water in the north and south polders are 20.58 Mm³ and 20.43 Mm³, respectively. Thus, as the storage volume in the polders is a little more, the discharge and water levels at Elbe River 184.4 km rises a little lower than the 30 min case. However, in this case also, the discharge and water level reductions are the same as that for the 30 min case.

5 CONCLUSIONS

For the August 2002 flood event, the potential polder with the proposed gate dimensions and gate control strategy is capable of reducing the peak water levels near the Mauken gauging site in the Elbe River by about 25 cm while the corresponding discharge reduction is about 310 m³/s. The time of opening of the south gate during the polder filling process is decided using a trial and error process so as to maximise the water level reduction in the Elbe River. The water level reduction can be further improved through different gate control strategies. This aspect as well as the effectiveness of the polders in reducing the water levels in the Elbe River for floods of different magnitudes and duration is discussed in a separate paper by the same authors (Förster et al., 2008). As far as the emptying of the polders are concerned, there are not much intricacies involved. The emptying process starts when the discharge in the main river falls to a low threshold value.

Both the 1D and coupled 1D-2D model simulations for the potential polder yield the same water level and discharge reductions in the Elbe River. However, due to difference in treatment of the polders in both the models, the results for the flow processes in the polders are slightly different. For example, there are differences in the time for the water front to reach the connecting gate as well as the discharge through the connecting gate. Also, the emptying process of the polders differs significantly for the two models. While the 1D model drains the polders completely in 24 days, the 1D-2D model drains it only partially in 4 days. The 1D-2D model result is practically correct as the polders cannot be drained below a certain water level because of ground elevation conditions near the gates. The 1D-2D model provides additional information in terms of the areal extent as well as depth of water in the polders after the emptying process as well as the water velocities in the polders. The information on velocities will be particularly useful in studying the erosion and sedimentation problems and subsequent risk analysis in the polders. The computational time as well as the storage requirements for the 1D model is very less while this is significantly higher for the 1D-2D model and more so when finer resolution DEMs are used. Further, unlike the 1D model, considerable effort is required in setting up and simulating the

1D-2D model. In view of all these, it is recommended to use a 1D model for studying the flooding processes of polders, particularly the water level and discharge reductions in the main river. The computational time requirement suggests that a 1D model may be used in a near real time mode as well. However, a 1D-2D approach may be used when the study of flow dynamics in the polder is of particular interest.

The 1D model is quite sensitive to changes in the values of Manning's n for the river and its floodplain within the embankments. Thus, there is a need for a rigorous calibration and validation of the model before it is put to use. The 1D-2D model is not very sensitive to change in the Manning's n values for the polders. This is because the ' n ' values do not have a role to play once the water front reaches the boundary of the polders and the water level in the polders starts rising.

A coarse resolution DEM can very well be used to derive the area-elevation relationship for the polders for use in the 1D model and yet obtain accurate results. The same holds true for a coupled 1D-2D model wherein a coarse resolution DEM for the polders can be effectively used. This would result in significant reduction of the computational time and storage space requirements. In this study, the use of a 50 m grid DEM was found to yield good results.

The number of cross-sections should be chosen such that the shape of the river including its depth and width are very well represented by them. In this study, it is seen that the 34 cross-sections used to model the Elbe water levels is quite sufficient.

A different gate opening time for the south gate causes the water level reduction to decrease drastically. This indicates that it is very essential to have a good flood forecast in order to effectively reduce the water levels in the main river. The change in gate opening and closing durations from 5 min to 60 min does not have an effect on the water level reductions in the Elbe River. In this study, the gate opening and closing duration of 30 min is selected based on information provided by the local water authorities.

ACKNOWLEDGEMENTS

The research was jointly funded by the Alexander-von-Humboldt Foundation Fellowship Program and the Sixth Framework Program of the European Commission (FLOODsite project, EC Contract number: GOCE-CT-2004-505420). This paper reflects the authors' views and not those of the European Community. Neither the European Community nor any member of the FLOODsite Consortium is liable for any use of the information in this paper.

Data were kindly provided by the following authorities: Landesbetrieb für Hochwasserschutz und Wasserwirtschaft Sachsen-Anhalt, Wasser- und Schifffahrtsamt Dresden and Landesvermessungsamt Sachsen-Anhalt. The authors are also grateful to the Danish Hydraulic Institute (DHI), Denmark for providing an evaluation copy of the MIKE software.

Chapter V

Simulation of water quality in a flood detention area using models of different spatial discretisation

ABSTRACT:

Detention areas are used to lower peak discharges during extreme flood events by temporary storage of excess water. Hence, the risk of dike failures and extensive inundations in adjacent and downstream river reaches is reduced. However, ecological side effects such as a deterioration of water quality during water retention may occur. This is mainly due to the large amount of organic matter in the flood water and the inundation of terrestrial vegetation in the detention area. Decay processes can cause a severe depletion of dissolved oxygen (DO) in the temporary water body.

The impact of water retention on the DO dynamics in a planned detention area at the Elbe River (Germany) is studied by means of water quality modeling. Models of different spatial discretisation, a zero-dimensional (0D) and a two-dimensional (2D) approach, were applied to assess their suitability in terms of performance and modeling effort. Both model approaches solely differ in their spatial discretisation, while conversion processes, parameters, and boundary conditions were kept identical.

The dynamics of DO simulated by the two models are similar in the initial flooding period but diverge when the system starts to drain. The deviation can be attributed to the different spatial discretisation of the two models, and hence the different approach of determining flow velocities and water depths. The 2D model requires significantly higher efforts for pre- and post-processing and longer computing times. It is therefore not suitable for investigating various flood scenarios and for testing the model's reliability with an extensive sensitivity analysis. However, studying the impact of the spatial variability on the evolution of the state variables necessitates a spatially distributed model approach.

For practical applications, it is recommended to firstly set up a fast-running model of reduced spatial discretisation, e.g. a 0D model. Using this tool, the reliability of the simulation results should be checked by analyzing the impact of uncertain parameters of the water quality model with a particular focus on those parameters that are spatially variable and, therefore, assumed to be better represented in a 2D model. The benefit from the application of the more costly 2D model should be assessed, based on the analyses carried out with the 0D model. A 2D model appears to be preferable if the simulated detention area has a complex topography, flow velocities are highly variable in space, and the parameters of the water quality model are well known.

1 INTRODUCTION

Detention areas form part of the flood management strategy for many lowland rivers such as the Elbe River (Germany). They are used to lower peak discharges in the river during large flood events. Excess water is temporarily stored, hereby reducing the flood hazard at adjacent downstream reaches. The utilisation of flood detention areas has been proved to successfully reduce the peak discharge during the Elbe flood in 2002 (Förster et al., 2005). However, such areas are often used for agriculture and, apart from economic losses due to the inundation of crops, water quality problems may occur. The decay of submerged biomass causes high oxygen consumption rates and may lead to a severe depletion of dissolved oxygen (DO) levels. Large amounts of organic matter contained in the river water during extreme floods (IKSE, 2004) also contribute to oxygen consumption. When a large detention area at the Elbe River was flooded in 2002, fish extinction due to DO depletion was nearly 100% (Böhme et al., 2005).

Water quality modeling provides a means to study the impact of flooding on ecologically relevant parameters, such as dissolved oxygen. For example, different hydrological scenarios can be simulated to examine the effect of flooding depth, water residence time, and initial vegetation cover. To produce meaningful predictions, the water quality model must provide both a reasonable description of the turnover processes (ecological submodel) as well as an appropriate representation of heterogeneity, i.e. spatial discretisation. What kind of discretisation is appropriate, is determined by the hydrodynamic situation (geometry and boundary conditions) as well as the relevant turnover processes. In practice, however, the actual choice is often dictated by the cost of setting up a multi-dimensional and/or high-resolution simulation model and - more often - by data availability.

In this study, we explicitly investigated the impact of model discretisation. For that purpose, we simulated the oxygen dynamics in a planned flood detention area using two models in parallel: a zero-dimensional approach (0D model) and a two-dimensional one (2D model).

The ecological submodel, covering the state variables and interactions shown in Figure 1 is, however, identical. The objective is to point out pros and cons of the two levels of discretisation and to assess the suitability of either approach to predict DO concentrations in a flooded detention area.

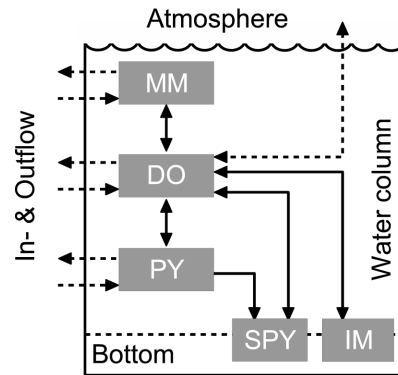


Fig. 1: State variables of the water quality model. *DO* represents the concentration of dissolved oxygen, *MM* is the concentration of 'mobile' organic matter in the water column and *PY* is the symbol for phytoplankton (all in g m^{-3}). *IM* represents the areal concentration of 'immobile degradable matter' at the reservoir's bottom and *SPY* is the concentration of settled phytoplankton (both in units of g m^{-2}). *DO*, *MM*, and *PY* are controlled by external forcings (dashed arrows). Interactions between the state variables, including negative feedbacks, appear as solid lines. Details on the modeled processes are given in Section 3.2.

2 STUDY SITE

The test site for model comparison is a flood detention area to be built at the Middle Elbe River (Germany; $51^{\circ}43' \text{N}, 12^{\circ}54' \text{E}$). The area with a total extent of 17 km^2 is separated from the River by the main dike. It consists of two linked reservoirs with a total storage capacity of 40 million m^3 (Figure 2). The shallow reservoirs are designed to temporarily store part of the discharge of the Elbe River in the case of flood events with a return period > 100 years. Filling of the reservoirs and post-event drainage are regulated by means of the three control structures shown in Figure 2.

Currently about 90% of the area is under intensive agricultural use with main crop types being grain crops, corn, canola, and intensive grassland. The remaining 10% are taken up by a small watercourse and adjacent wetland forests, most of which are under protection according

to national and European environmental legislation. It is expected that the land will retain its original purpose after designation as a detention area.

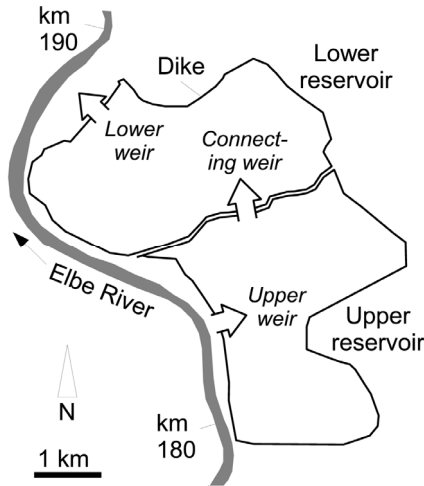


Fig. 2: Map of the flood detention area at the Middle Elbe River. The arrows used for labeling the locations of weirs indicate the normal flow direction.

Tab. 1: Comparison of basic features of the 0D and 2D model.

	0D model	2D model
Hydrodynamics and transport		
Spatial discretisation	2 stirred tank reactors	50 x 50 m grid model
Flow model	Continuity eqn.	2D St. Venant eqn.
Geometry input	Storage functions	DEM as grid
Transport model	Mass balance	2D Advect.-Disp. eqn.
Time step	variable, 2 min	variable, 2 sec ^a
Boundary conditions	In- & Outflow rates; see Section 3.4	
Water quality model		
Components & processes	User-defined; see Section 3.2	
Numerical solver	LSODA ^b	5th order Runge-Kutta
Time step	variable, 2 min	variable, 2 min
Boundary conditions	In-river concentrations, meteorology; see Section 3.4	
Computational aspects		
Software environment	R-Script ^c	MIKE, Ecolab ^d
Computation time ^e	~ 2.5 min	~ 5 hours
Size of output files ^f	~ 0.8 MB	~ 1.7 GB

a Required to ensure Courant numbers < 1

b From R-package ‘odesolve’; Originally by Hindmarsh (1983) and Petzold (1983)

c Implemented by D. Kneis using R version 2.6 (R Development Core Team, 2007)

d Developed by the Danish Hydraulic Institute (DHI, 2003)

e Includes simulation and post-processing on a PC with 2.2 GHz CPU and 2 GB RAM

f Uncompressed ASCII text; storage interval 15 min

The difference between the two model is solely due to a very different discretisation of the model domain as illustrated by Figure 3. The 2D model accounts for lateral heterogeneities in hydrodynamic variables and concentrations. It solves the advection-dispersion equation to simulate lateral transport but still

3 METHODS AND DATA

3.1 Comparison of the 0D and the 2D approach

All the basic features of the 0D and the 2D modeling approach are summarised in Table 1. Since we aimed at studying the impact of the models' spatial discretisation, we kept all features except discretisation identical. Consequently, the set of state variables and processes is the same in both the 0D and the 2D approach (Figure 1). The two models simulate the evolution of concentrations in a control volume by solving a common set of ordinary differential equations (Table 2, Eq.s 4-20) for a common set of boundary conditions (Section 3.4).

assumes vertical mixing of the water column (Figure 3, left). In the 2D model, each grid cell with the extent $\Delta x = \Delta y = 50\text{ m}$ has its individual depth D as determined from the water surface elevation h and the digital elevation model (DEM). Turnover computations are carried out for each cell.

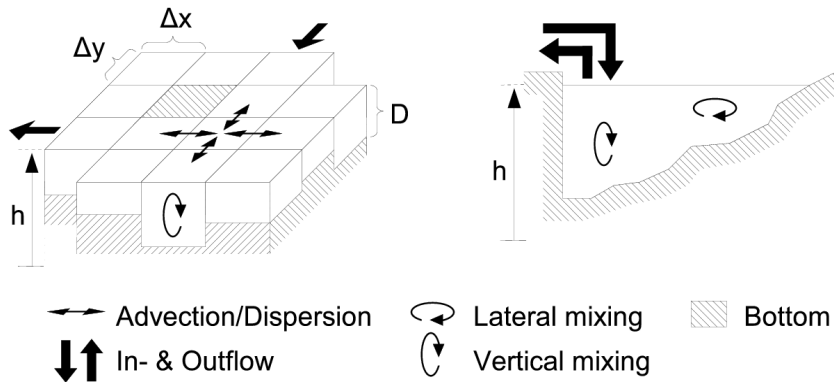


Fig. 3: Discretisation of a modeled reservoir in the vertically averaged 2D model (left) and the 0D stirred tank model (right). Symbol h represents the water surface elevation and D is the depth of a grid cell (2D model) or the average depth of the stirred tank (0D model). For this study we used $\Delta x = \Delta y = 50$ m.

In contrast, in the 0D model, each of the two reservoirs shown in Figure 2 is considered as a stirred tank reactor (short: STR; Chapra, 1997). A STR is assumed to be both laterally and vertically mixed (Figure 3, right). Therefore, it is characterised by homogeneity with respect to all state variables, e.g. concentrations. As opposed to the 2D model, the 0-dimensional stirred tank approach is built on aggregated information on the water body's geometry in the form of storage functions (Figure 4). The basic relation is the one between the water surface elevation h and the surface area A . $A(h)$ is easily computed from a DEM. The relation for the storage volume $V(h)$ as well as for the depth $D(h)$ derive from $A(h)$ according to Eq.s 1 and 2. Here, in contrast to the 2D approach, $D(h)$ is an average value that is assumed to be representative for the STR, i.e. the entire reservoir.

$$V(h) = \int_{z=0}^{z=h} A(z) dz \quad (1)$$

$$D(h) = \frac{V(h)}{A(h)} \quad (2)$$

Flooding and emptying of the proposed detention area were simulated with the MIKEFLOOD hydrodynamic modeling package (DHI, 2004). The model integrates a one-dimensional representation of the Elbe River (~ 20 km reach) and a two-dimensional model of the detention area itself. The 2D part of the model uses a rectangular grid with a resolution of 50 x 50 m for compatibility with

the 2D water quality model. The computation of flow rates and depths is based on a finite difference approximation of the Saint Venant Equations.

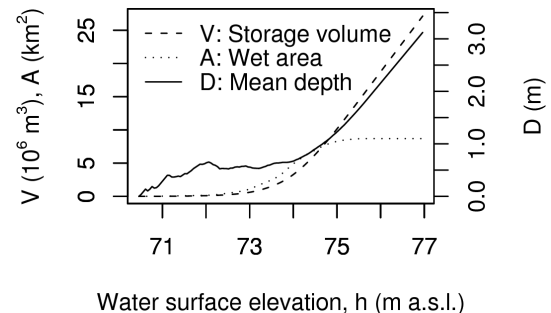


Fig. 4: Storage functions representing the upper reservoir's geometry in the 0-dimensional stirred tank approach.

The computed inflow rates to the upper reservoir, exchange flows at the connecting weir as well as outflow rates at the lower weir (see Figure 5 in Section 3.4) served as boundary conditions for the water quality simulations in both the 0D and the 2D model. However, only the latter approach uses the computation results for each grid cell (velocity components, depth) in the simulation of lateral transport as well as turnover.

3.2 Water quality processes

The control of the state variables (Figure 1) by conversion processes and boundary conditions is best illustrated by a Peterson matrix (Reichert et al., 2001) as shown in Table 2. The actual dynamics of the state

variables are determined by the process rates r according to Eq. 3, where γ_i is the i-th state variable, n is the total number of processes considered in the model and the vector of stoichiometry factors $q_{i,k=1\dots n}$ represents the i-th column of the stoichiometry matrix (see

Table 2). The rate expressions are presented in the subsequent paragraphs (Eq.s 4-20).

$$\frac{d Y_i}{d t} = \sum_{k=1}^n (q_{i,k} \cdot r_k) \quad (3)$$

Tab. 2: Process matrix of the water quality model showing the influence of processes on the simulated state variables. The columns 4-10 represent the stoichiometry matrix. It contains the factors $q_{i,k}$ appearing in Eq. 3. If $q_{i,k} > 0$, the k-th process is responsible for an increase in the value of the i-th state variable whereas $q_{i,k} < 0$ indicates a decrease according to Eq. 3. For clarity, a period is displayed in those positions where a state variable is not affected by a process, i.e. $q_{i,k} = 0$. The rate expressions for all processes are presented separately in Eq.s 4-20. See Tables 3 , 4, and 5 for the definition of all symbols.

#	Process	Rate expression	MM (g m^{-3})	IM (g m^{-2})	PY (g m^{-3})	SPY (g m^{-2})	DO (g m^{-3})	TW ($^{\circ}\text{C}$)	V (m^3)
1	Inflow	Eq. 4	$\frac{MM_x - MM}{V}$.	$\frac{PY_x - PY}{V}$.	$\frac{DO_x - DO}{V}$	$\frac{TW_x - TW}{V}$	1
2	Outflow	Eq. 5	-1
3	Decay of MM	Eq. 6	-1	.	.	.	$-f_{MM}$.	.
4	Decay of IM	Eq. 7	.	-1	.	.	$-f_{IM}/D$.	.
5	Decay of SPY	Eq. 8	.	.	.	-1	$-f_{PY}/D$.	.
6	Growth of PY	Eq. 9	.	.	1	.	f_{PY}	.	.
7	Respiration of PY	Eq. 12	.	.	-1	.	$-f_{PY}$.	.
8	Settling of PY	Eq. 13	.	.	-1	D	.	.	.
9a	Aeration 1	Eq. 15	1	.	.
9b	Aeration 2	Eq. 17	1	.	.
10	Heatflux	Eq. 20	1	.

Process rates 1 and 2: In- and Outflow

The process rate r_1 accounting for the inflow of water to the reservoir (OD model) or a control volume (2D model) is nothing but the flow rate Q_{in} (Eq. 4). Likewise, the process of outflow r_2 is described by the corresponding flow rate Q_{out} (Eq. 5). The unit of the two rates is $\text{m}^3 \text{s}^{-1}$.

$$r_1 = Q_{in} \quad (4)$$

$$r_2 = Q_{out} \quad (5)$$

Process rate 3: Degradation of mobile organic matter

The rate r_3 describing the velocity of the degradation of MM is given by Eq. 6. Here, MM is the concentration of mobile organic matter in the water column (g m^{-3}), k_{MM} (s^{-1}) is the rate of aerobic decay, and t_{MM} (-) controls the process' dependence on water temperature TW ($^{\circ}\text{C}$) through an Arrhenius term. DO (g m^{-3}) is the oxygen concentration and h_{DO}

(g m^{-3}) is the half-saturation constant in the Monod term accounting for inhibition of the aerobic process at low oxygen levels. The unit of the process rate r_3 is $\text{g m}^{-3} \text{s}^{-1}$.

$$r_3 = MM \cdot k_{MM} \cdot t_{MM}^{(TW-20)} \cdot \frac{DO}{DO + h_{DO}} \quad (6)$$

Process rate 4: Degradation of immobile organic matter

The rate r_4 as defined by Eq. 7 controls the degradation of immobile organic matter that is attached to the reservoir's bottom. In Eq. 7, IM is the areal concentration of the degradable material (g m^{-2}), D (m) is the water depth and D_{min} is a threshold value of the depth at which die-off and decay of the vegetation sets in. The meaning of the constants k_{IM} and t_{IM} is equivalent to the corresponding parameters in Eq. 6. They were introduced to allow for different degradability of IM as compared to MM . The remaining symbols TW , DO , and h_{DO} are the same as in r_3 (Eq. 6). Since IM is defined in g m^{-2} the unit of rate r_4 is $\text{g m}^{-2} \text{s}^{-1}$.

$$r_4 = \begin{cases} IM \cdot k_{IM} \cdot t_{IM}^{(TW-20)} \cdot \frac{DO}{DO + h_{DO}} & \text{for } D > D_{min} \\ 0 & \text{for } D \leq D_{min} \end{cases} \quad (7)$$

Process rate 5: Degradation of settled phytoplankton

The degradation of settled phytoplankton SPY (r_5 , Eq. 8) is computed in a similar way as the decay of IM (see Eq. 7) and the rate unit is $\text{g m}^{-2} \text{ s}^{-1}$ as well, because, like IM , SPY is an areal concentration (g m^{-2}). To allow for different degradability, a separate rate constant (k_{SPY}) and temperature correction factor (t_{SPY}) were introduced.

$$r_5 = SPY \cdot k_{SPY} \cdot t_{SPY}^{(TW-20)} \cdot \frac{DO}{DO + h_{DO}} \quad (8)$$

Process rate 6: Growth of phytoplankton

Phytoplankton growth is considered in the model as it compensates for oxygen consumption by aerobic decay at daytime. The growth rate r_6 is computed as a function of the current phytoplankton concentration PY (g m^{-3}) using a potential growth rate k_{grow} (s^{-1}) which defines the rate of cell division under optimum conditions (Eq. 9). The model accounts for the effects of light limitation by the function $ilim$ (see Eq. 10) representing the depth-integrated Steele equation (Ambrose et al., 2001). The impact of temperature is described by an Arrhenius term (dimensionless parameter t_{grow}) similarly to Eqs. 6-8. For this study, we assume that phytoplankton growth is not limited by nutrients because the concentrations of nitrogen and phosphorus in the river are high during flood and additional nutrients are remobilised from the inundated soil and the mineralisation of vegetation.

$$r_6 = PY \cdot k_{grow} \cdot t_{grow}^{(TW-20)} \cdot ilim(I_{srf}, I_{opt}, D, e_{back}, f_{chl}, PY) \quad (9)$$

Arguments to the function $ilim$ are the intensity of photosynthetic active radiation just below the water surface I_{srf} (W m^{-2} , boundary condition) as well as the optimum intensity I_{opt} at which gross growth reaches a maximum. Further arguments to $ilim$ are the current phytoplankton concentration PY (g m^{-3}), the water depth D (m), a background extinction coeffi-

cient e_{back} (m^{-1}), and the chlorophyll-a content of the phytoplankton f_{chl} (g g^{-1}). The latter two parameters are used for computing the total extinction coefficient e_{tot} (m^{-1}) according to Eq. 11 (adapted from Ambrose et al., 2001). Light adaption is not taken into account, i.e. $f_{chl} = const$.

$$ilim = \frac{2.718}{e_{tot} \cdot D} \left(\exp\left(-\frac{I_{srf}}{I_{opt}} \cdot \exp(-e_{tot} \cdot D)\right) - \exp\left(-\frac{I_{srf}}{I_{opt}}\right) \right) \quad (10)$$

$$e_{tot} = e_{back} + 8.8 \cdot PY \cdot f_{chl} + 5.4 \cdot (PY \cdot f_{chl})^{(2/3)} \quad (11)$$

Process rate 7: Respiration of phytoplankton

This process accounts for the loss of phytoplankton biomass by respiration and mineralisation of dead algae. The rate r_7 with the unit $\text{g m}^{-3} \text{ s}^{-1}$ is computed according to Eq. 12. The rate constant k_{resp} (s^{-1}) and the parameter t_{resp} (-) are equivalent to the corresponding constants in Eqs 6-8 and the other symbols were explained in conjunction with Eq. 6.

$$r_7 = PY \cdot k_{resp} \cdot t_{resp}^{(TW-20)} \cdot \frac{DO}{DO + h_{DO}} \quad (12)$$

Process rate 8: Settling of phytoplankton

By the process of settling, phytoplankton (PY) is transferred from the water column to the reservoir's bottom. The rate of transfer r_8 has the unit $\text{g m}^{-3} \text{ s}^{-1}$. It is estimated by Eq. 13 using an effective settling velocity u_{sett} (m s^{-1}) and the water depth D (m).

$$r_8 = PY \cdot \frac{u_{sett}}{D} \quad (13)$$

Process rate 9: Oxygen flux between water column and atmosphere

The model computes the rate of oxygen exchange through the water surface as a linear function of the DO saturation deficit, i.e. the difference between the actual DO concentration and the temperature-dependent saturation level $dosat(TW)$ (g m^{-3} , Eq. 14).

$$dosat = 14.652 - 0.41022 \cdot TW + 0.007991 \cdot TW^2 - 0.000077774 \cdot TW^3 \quad (14)$$

Two separate approaches are used for estimating the transfer coefficients (proportionality factors). In the process rate r_{9a} ($\text{g m}^{-3} \text{ s}^{-1}$, Eq. 15) the transfer coefficient $k_{aer,wind}$ is computed as a function of wind speed WSP (m s^{-1}) and water depth D (m) using Eq. 16 that has been found by Banks and Herrera (1977).

$$r_{9a} = (dosat(TW) - DO) \cdot k_{aer,wind}(D, WSP) \quad (15)$$

$$k_{aer,wind} = \frac{0.728 \cdot \sqrt{WSP} - 0.317 \cdot WSP + 0.0372 \cdot WSP^2}{86400 \cdot D} \quad (16)$$

In the process rate r_{9b} ($\text{g m}^{-3} \text{ s}^{-1}$, Eq. 17), the transfer coefficient $k_{aer,flow}$ (s^{-1}) is estimated from the flow velocity U (m s^{-1}) and the flow depth D (m) according to the approach of O'Connor & Dobbins (McCutcheon, 1989) displayed as Eq. 18.

$$r_{9b} = (dosat(TW) - DO) \cdot k_{aer,flow}(D, U) \quad (17)$$

$$k_{aer,flow} = \frac{3.93 \cdot U^{1/2}}{86400 \cdot D^{3/2}} \quad (18)$$

The flow velocity U appearing in Eq. 18 is variable in space and time. In the 2D model, values of U are available for each grid cell from the hydrodynamic simulation. However, in the 0D model, a rough estimate of U can be derived only. For that purpose, we used Eq. 19 where the denominator represents the wet cross-section of a circular reservoir with depth D (m) and water surface area A (m^2).

$$U = \frac{\max(Q_{in}, Q_{out})}{D \cdot 2 \cdot \sqrt{A/\pi}} \quad (19)$$

Process rate 10: Change in water temperature

For this study, the water temperature TW was simulated by a simple equilibrium approach (Eq. 20). The process rate r_{10} with the unit ^oC s^{-1} is controlled by the parameter tw_{equi} , representing the ultimate water temperature under given meteorological conditions. The rate constant k_{heat} determines how fast TW approaches tw_{equi} . Symbol D (m) represents the water depth.

$$r_{10} = k_{heat} \cdot \frac{tw_{equi} - TW}{D} \quad (20)$$

3.3 Computational procedures

The system of ordinary differential equations to be solved by the 0D model consists of $2 \times n$ equations in the form of Eq. 3 where n is the number of state variables in a stirred tank (see Table 2). There are $2 \times n$ equations because the model is designed to also handle alternating flow directions at the connecting weir shown in Figure 2. Hence, upper and lower reservoir are simulated simultaneously. Numerical integration is performed by the stiffly stable LSODA method originally developed by Hindmarsh (1983) and Petzold (1983).

In the 2D model, the concentrations are computed for each grid cell at all time steps by (I) calculating the concentration gradients between the previous and the actual time step according to the advection-dispersion conditions, (II) calculating the concentration gradients for the actual time step according to the water quality process rates, and (III) calculating the resulting concentrations by numerical integration of the time step gradients from both the advection-dispersion and the water quality differential equations (DHI, 2003). The integration method used is a 5th order Runge-Kutta scheme.

3.4 Boundary conditions, parameters, and initial values

To examine the specific impact of spatial discretisation, we ran the 0D and the 2D model with exactly the same boundary conditions such as flow rates, external loads, and meteorological conditions. A summary of the common driving forces is given in Table 3.

As a hydrological boundary condition for this study we adopted the hydrograph of the Elbe River from the 2002 event (return period ~ 200 years). The gates were assumed to be operated in a way that minimises the peak flow in the river while using the detention area's full storage capacity. Details on hydrodynamic simulations carried out for this and other flood events can be found in Chatterjee et al. (2008) and Förster et al. (2008). The relevant flow rates at the three weirs (Figure 2) are presented in Figure 5.

Tab. 3: Boundary conditions of the water quality models.

Symbol	Units	Description
Q_{in}	$\text{m}^3 \text{s}^{-1}$	Inflow into the reservoir from the river or the adjacent reservoir (0D model) or inflow of a single grid cell (2D model).
O_{out}	$\text{m}^3 \text{s}^{-1}$	Outflow from the reservoir (0D model) or outflow of a single grid cell (2D model).
MM_x	g C m^{-3}	Concentration of degradable organic matter (MM) in the inflow. ^a
PY_x	g C m^{-3}	Concentration of phytoplankton (PY) in the inflow. ^b
DO_x	g DO m^{-3}	Concentration of DO in the inflow.
TW_x	$^\circ\text{C}$	Temperature of inflow.
I_{srf}	W m^{-2}	Photosynthetically active radiation just below the water surface. ^c
WSP	m s^{-1}	Wind speed at the nearest meteorological station.

a For inflow from the river, MM_x was estimated from observed concentrations of total organic carbon in the Elbe River.

b For inflow from the river, PY_x was derived from observed chlorophyll-a in the Elbe River using the value of f_{chl_a} from Table 4.

c I_{srf} was computed from shortwave radiation at the nearest meteorological station assuming that 45% of the energy is available for photosynthesis (Ambrose et al., 2001; Romero et al., 2004). An approximate albedo a was computed as $a = 0.08 + 0.02 \cdot \sin(N \cdot 2\pi/365 + \pi/2)$ where N is the day of the year (Antenucci and Imerito, 2002).

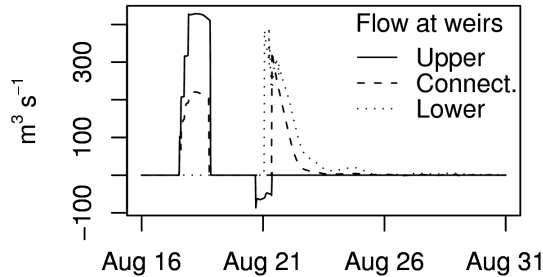


Fig. 5: Flow rates at the three gates shown in Fig. 2. Positive values indicate flows in the following direction: River → upper reservoir → lower reservoir → river.

The loads of mobile components entering the upper reservoir were computed from the inflow hydrograph at the upper weir (Figure 2) and observed concentrations in the Elbe River for the respective time period with daily resolution (Lindenschmidt et al., 2008). Time series of wind speed and solar radiation were adopted from the nearby meteorological station Bethau.

In addition to common boundary conditions, we used an identical set of parameters and initial conditions in the two models (Tables 4 and 5). One should note that most of the parameter values were taken from the literature. This was necessary, because the studied flood detention area is not yet built and,

therefore, observation data for model calibration do not exist. Since this study aims at comparing alternative models rather than at making precise predictions, the lack of calibration data is less severe. However, using the values from Tables 4 and 5, the obtained dynamics and the minimum DO concentration are in good agreement with observations from other detention areas that were flooded during the same event, i.e. the Elbe flood in 2002 (Knösche, 2003).

3.5 Analysis of uncertainty

Overall model uncertainty results from the combined effect of uncertain input data, model parameters, and structural deficits (Kneis, 2007; Radwan et al., 2004). To get more insight in the reliability of the simulation results, the 0D model was integrated in a Monte-Carlo environment. We simultaneously varied those parameters of the water quality model which we considered most uncertain, such as the various rate constants controlling the decay of organic matter. 250 parameter sets were created with the latin-hypercube method using the ranges given in Table 6 and assuming a uniform distribution for each varied item. Based on the

output of all model runs, we calculated quantiles of the predicted concentrations for every time step.

In addition to the Monte-Carlo simulation described above, we run the 0D model with the standard parameters from Table 4 but eight

different empirical formulas describing the dependence of re-aeration on wind speed and water depth. One of the tested relations is Eq. 16 and the remaining seven approaches were selected from a list provided by Bowie et al. (1985).

Tab. 4: Parameters of the water quality models and standard values used in the comparison of the 0D and 2D approach.

Symbol	Value	Units	Description
f_{MM}	2.76 ^b	g g^{-1}	Oxygen-to-carbon ratio for the decay of <i>MM</i> .
f_{IM}	2.8 ^c	g g^{-1}	Oxygen-to-carbon ratio for the decay of <i>IM</i> .
f_{PY}	2.76 ^b	g g^{-1}	Oxygen-to-carbon ratio for the decay of <i>PY</i> .
$f_{chl\alpha}$	0.028 ^b	g g^{-1}	Chlorophyll-a to carbon ratio in phytoplankton.
k_{MM}	0.032 ^d	d^{-1}	Rate constant for decay of <i>MM</i> at 20°C.
k_{IM}	0.018 ^e	d^{-1}	Rate constant for decay of <i>IM</i> at 20°C.
k_{SPY}	0.032 ^f	d^{-1}	Rate constant for decay of <i>SPY</i> at 20°C.
k_{resp}	0.125 ^g	d^{-1}	Rate constant of <i>PY</i> respiration at 20°C.
k_{grow}	1.8 ^{a,b}	d^{-1}	Maximum phytoplankton growth rate at 20°C.
u_{sett}	0.1 ^g	m s^{-1}	Effective settling velocity of phytoplankton.
h_{DO}	0.5 ^a	g m^{-3}	Half-saturation concentration of DO for aerobic degradation of organic matter.
D_{min}	0.03	m	Water depth at which vegetation die-off starts.
t_{MM}	1.045 ^a	-	Temperature coefficient for decay of <i>MM</i> .
t_{IM}	1.045 ^a	-	Temperature coefficient for decay of <i>IM</i> .
t_{SPY}	1.045 ^a	-	Temperature coefficient for decay of <i>SPY</i> .
t_{resp}	1.068 ^g	-	Temperature coefficient for <i>PY</i> respiration.
t_{grow}	1.045 ^g	-	Temperature coefficient for <i>PY</i> growth.
I_{opt}	145 ^h	W m^{-2}	Optimum light intensity for <i>PY</i> growth.
e_{back}	2 ⁱ	m^{-1}	Background light extinction coefficient.
tw_{equi}	20 ^j	°C	Equilibrium temperature.
k_{heat}	0.2 ^j	s^{-1}	Heat transfer rate.

a From Bowie et al. (1985)

b From Lindenschmidt (2006)

c Computed from C/N ratio of biomass.

d Estimated from *BOD*, and *TOC* data of the Elbe River making use of f_{MM} .

e Derived from experiments undertaken by Peukert (1970).

f Set to k_{MM} .

g Values recommended by Ambrose et al. (2001).

h Average of values presented by Bowie et al. (1985); $1 \text{ W m}^{-2} = 2.065 \text{ Ly d}^{-1}$.

i Calculated from Secchi depth D_s (m) and Chlorophyll-a data for the Elbe River using Eq. 11 and the approximation $e_{tot} = 1.7/D_s$.

j For this study, the temperature model was practically turned off by setting tw_{equi} equal to the water temperature of the river and choosing a large value for k_{heat} .

Tab. 5: State variables of the water quality models and initial values.

Symbol	Units	Description	Initial value
MM	g C m^{-3}	Concentration of, mainly dissolved, degradable organic matter (as carbon) in the 0 ^a water column.	
IM	g C m^{-2}	Areal concentration of degradable plant matter at the bottom.	175 ^b
PY	g C m^{-3}	Concentration of total phytoplankton.	0 ^a
SPY	g C m^{-2}	Areal concentration of settled phytoplankton.	0
DO	g m^{-3}	Dissolved oxygen concentration.	$f(TW)$ ^c
TW	$^{\circ}\text{C}$	Water temperature.	TW of river ^a
V	m^3	Storage volume of the reservoir (0D model) or grid cell (2D model).	1 ^a
A	m^2	Water surface area of the reservoir (0D) or grid cell (2D).	$f(V)$ ^d
D	m	Water depth; Reservoir-average in the 0D model.	$f(V)$ ^d

a The initial value has no effect on simulation results because the reservoir's initial volume is negligible compared to its storage volume after filling. A non-zero initial volume is required because water depth and storage volume appear in the denominator of many expressions (see e.g. Table 2).

b Calculated from a plant matter of 600 g DW m^{-2} with a carbon content of 0.46 g C (g DW) $^{-1}$ (MLUR, 2007). About 35% of the material was considered as non-degradable within the relevant time span (Peukert, 1970).

c The DO saturation level at the initial value of TW was used.

d In the 0D model, the values are computed from V based on the reservoir's geometry.

Tab. 6: Parameter ranges considered in the Monte-Carlo simulation carried out with the 0D model.

Item(s)	Range
Rate constants k_{mm} , k_{im} , k_{spy} , k_{resp}	Values from Table 4 \pm 50 %
Phytoplankton growth rate k_{grow}	Value from Table 4 \pm 25 %
Optimum light intensity I_{opt}	Value from Table 4 \pm 25 %
Phytoplankton settling velocity u_{sett}	Value from Table 4 \pm 50 %
Chlorophyll-carbon ratio f_{chl}	Value from Table 4 \pm 25 %
Background extinction coefficient e_{back}	1.5-2.5 m^{-1}
Equilibrium water temperature tw_{equi}	20-25 $^{\circ}\text{C}$
Initial value of IM	Value from Table 5 \pm 25%

4 RESULTS

4.1 Simulation results of the two models

Figures 6-9 depict the evolution of state variables and process rates as simulated by the two models. We only present figures for the upper reservoir shown in Figure 2 because the results for the lower one are very similar. To illustrate the spatial variability in the 2D model, the median is plotted as well as the 10- and 90-percentile of all cells that are wet at a time.

Figure 6 illustrates the change in the upper reservoir's flooding depth over the simulation period as a result of the in- and outflow rates (recall Figure 5). In general, the reservoir's average water depth as output by the 0D model is close to the median depth computed by the 2D approach. However, due to the reservoir's natural topography, the actual depth varies between 1.5 and 3.4 m at the time of maximum storage (10- and 90-percentile).

Using the same plot setup as in Figure 6, Figure 7 illustrates the simulated concentration of dissolved oxygen in the upper reservoir. Starting at an equilibrium value of $\sim 9 \text{ g m}^{-3}$ before flooding, the inflow of undersaturated

river water on August 17 causes a first significant drop to a DO level of about 6.5 g m^{-3} . After 4 days of declining concentrations, the DO concentration has almost reached its minimum at 1 g m^{-3} on August 21. This minimum occurs shortly after the time of maximum storage. Over the subsequent days, the oxygen concentration slowly rises and a pronounced diurnal variation develops.

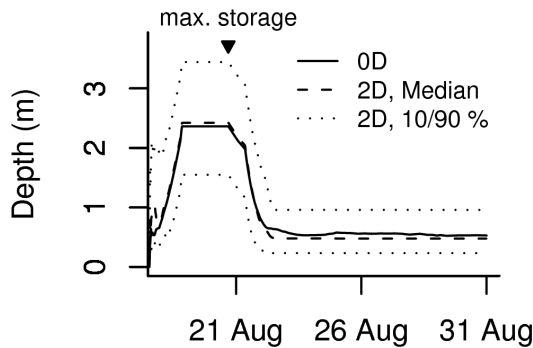


Fig. 6: Water depth in the upper reservoir as simulated by the 0D stirred tank approach and the 2D model (spatial median, 10- and 90-percentile). The abscissa's left limit corresponds to the time when the reservoir becomes flooded. The triangle marks the time of maximum storage when emptying of the reservoir begins.

During the period of falling DO levels, the results of the 0D model are close to the output of the 2D simulation. As indicated by the narrow range of the 10- and 90-percentile in Figure 7, the concentration does not show significant spatial variability. At the time of maximum storage, the output of the two models starts to diverge, with higher DO levels being predicted by the 0D approach.

As can be seen in Figure 8, the predicted concentration of phytoplankton continuously rises throughout the simulation period. During the simulated event, the corresponding concentration in the Elbe River amounts to $\approx 0.2 \text{ g m}^{-3}$. In the detention area, the value rises up to 5 g m^{-3} in the 2D model and 8 g m^{-3} in the 0D model. According to the stoichiometry factor f_{chl_a} from Table 4, this is equivalent to chlorophyll levels of 140 and $244 \mu\text{g L}^{-1}$, respectively. Beginning at the time of maximum storage, the predictions of the two approaches diverge. The reservoir-average phytoplankton level as output by the 0D model becomes similar to the spatial 90-percentile calculated from the 2D simulation results.

The simulated dynamics of dissolved oxygen (Figure 7) is also reflected by the process rates. For example, Figure 9 illustrates how the rate of degradation of organic matter at the reservoir's bottom develops. Due to the Monod term appearing in Eq. 7, this process rate is directly affected by the concentration of DO. Both the computed dynamics as well as the deviation between the results of the two models show similarities with Figure 7.

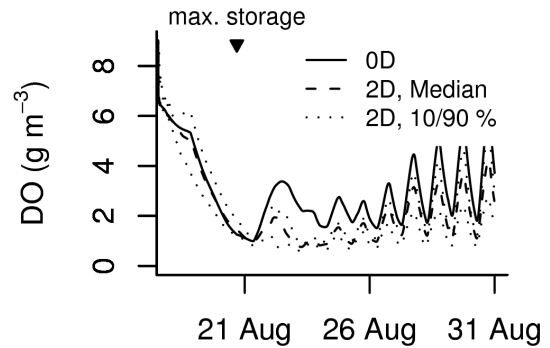


Fig. 7: Concentration of dissolved oxygen in the upper reservoir as simulated by the 0D stirred tank approach and the 2D model (spatial median, 10- and 90-percentile).

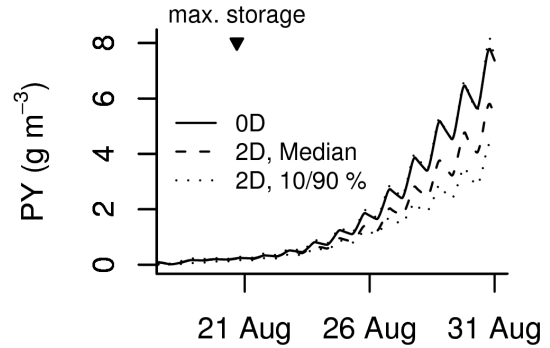


Fig. 8: Concentration of phytoplankton carbon in the upper reservoir computed by the 0D and the 2D model.

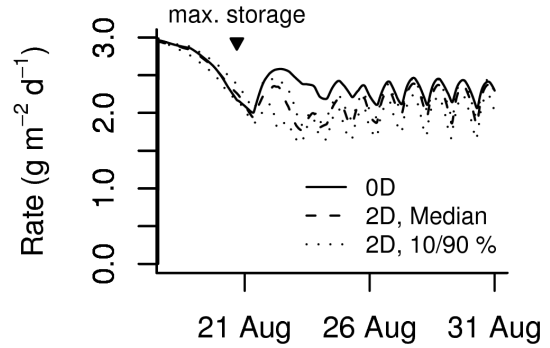


Fig. 9: Rates of the degradation of immobile organic matter (Eq. 7) in the upper reservoir as simulated by the 0D and the 2D model.

The 2D model allows us to directly view the computed spatial heterogeneity of oxygen concentrations at selected time steps (Figure 10). During the filling period, the predicted variability in concentrations is low. At the time of maximum storage on August 21, the simulated DO concentrations are generally

below 1.5 g m^{-3} in both the upper and lower reservoir. When the reservoirs begin to run dry, more or less fragmented water bodies of different depths develop as indicated by the white colors in the plots for the two final days. At this stage, we observe increased spatial gradients in the predicted DO levels.

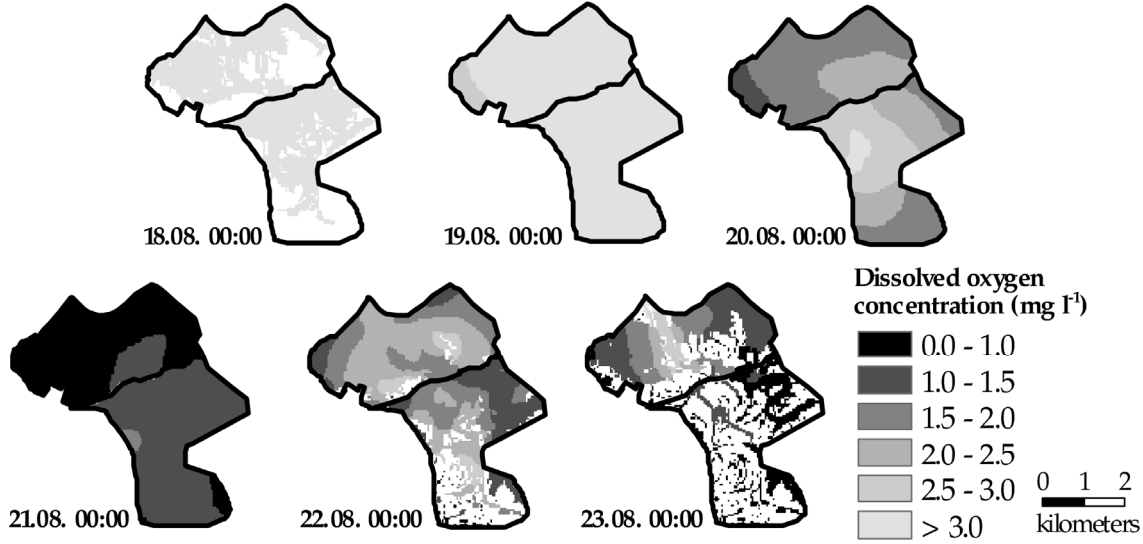


Fig. 10: Dissolved oxygen concentrations in the upper reservoir for the first 6 days of flooding as computed by the 2D model (values at midnight).

4.2 Uncertainty of predictions

Figure 11 illustrates the range of dissolved oxygen concentrations obtained in the Monte-Carlo simulation (Section 3.5). The varied parameters listed in Table 6 control various processes affecting DO consumption, production, and even solubility. While the range between the 10- and 90-percentiles is rather narrow in the period of rising water levels, the span of predictions grows substantially as the reservoir drains and multiple water bodies develop (recall Figure 10). It is worth noting that, in the final period of the simulation, the absolute values but also the range of DO concentrations become particularly large during daytime. The minimum DO concentrations observed at nighttime, however, increase much slower and the spread of the results remains much narrower. Daily minimum values lie between 0.5 and 4 g m^{-3} DO (10- and 90-percentile).

The oxygen dynamics as computed with eight different formulas for wind-dependent re-aeration (see Section 3.5) is shown in Figure 12.

The span of simulated concentrations is surprisingly high with differences of up to 5 g m^{-3} at a time step. Depending on the re-aeration formula, minimum DO levels between 0.3 and 3 g m^{-3} are predicted. With our standard approach underlying all other simulation results presented in this paper (Eq. 16, solid graph in Figure 12), intermediate results are obtained.

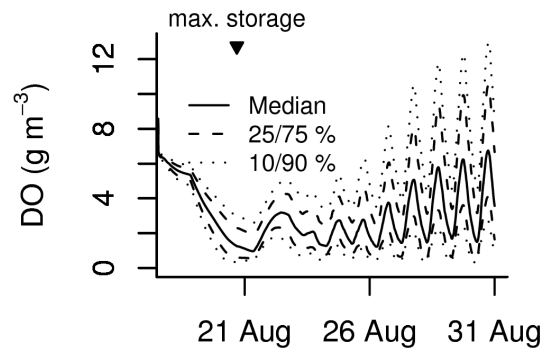


Fig. 11: Quantiles of simulated DO concentrations in the upper reservoir from 250 simulations with randomly modified parameters within the ranges listed in Table 6.

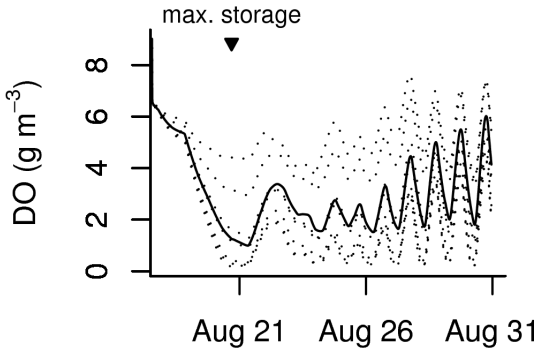


Fig. 12: Dynamics of dissolved oxygen simulated with the 0D model using 8 different empirical formulas for wind-dependent re-aeration. The result obtained with the approach of Banks and Herrera (1977) (Eq. 16) is plotted as solid line. Dashed lines represent the output for the 7 tested alternative formulas listed in Bowie et al. (1985).

5 DISCUSSION AND CONCLUSIONS

5.1 The impact of spatial discretisation

Dissolved oxygen does not only play a central role in the turnover of organic matter (Figure 1), but its concentration also controls the abundance of higher aquatic species such as fish. Hence, we are particularly interested in making good predictions of DO and, consequently, we focus the following discussion on that state variable.

According to Figure 7, the DO concentrations simulated by the two models are very similar in the initial period. However, during the period of drainage starting on August 21, the output of the models deviates more and more. The DO levels in the 0D model permanently exceed the corresponding 90 percentiles computed from the 2D model's results.

To explain the observed differences, we have to consider all processes being directly or indirectly affected by the model's spatial discretisation. Thus, we have to look at those process rates (Eq.s 4-20) and stoichiometry factors (Table 2) that depend on water depth D and/or flow velocity U . These two variables are reservoir-averages in the 0D model, while each grid cell in the 2D model has its individual value.

For example, both U and/or D appear in the expressions controlling re-aeration (Eq.s 16 and 18). Consequently, we observe spatially

variable re-aeration rates in the 2D model (Figure 13). The fact that the rate of flow-induced aeration in the 0D model exceeds the median of the 2D results during the drainage period (Figure 13, bottom) coincides with the higher DO levels predicted by the 0D approach around August 22 (Figure 7). The observed differences in the flow-induced re-aeration rates are not unexpected because of the necessarily simple approach for estimating U in the 0D model (Eq. 19).

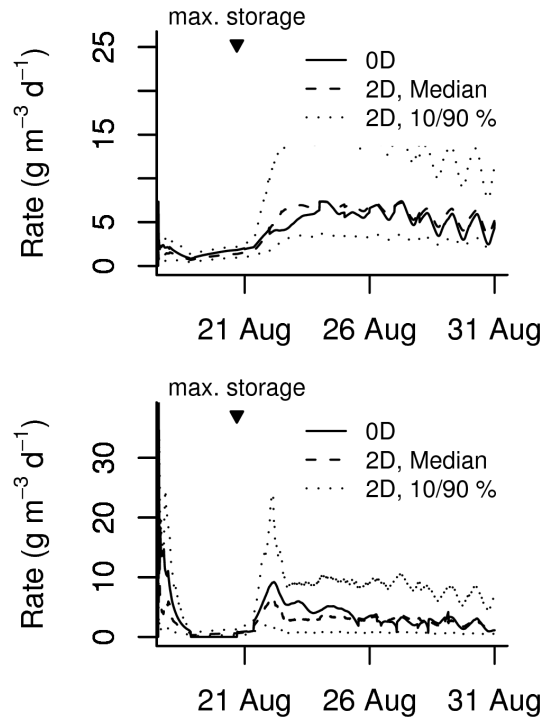


Fig. 13: Rate of wind-induced re-aeration (Eq. 15, top figure) and flow-induced re-aeration rate (Eq. 17, bottom figure) as computed by the 0D stirred tank approach and the 2D model.

Another very important but more indirect link between water depth D and the DO concentration is due to the appearance of D in the light limitation term controlling phytoplankton growth (Eq. 10). Given a total extinction coefficient e_{tot} and a below-surface light intensity I_{srf} , there is a depth D_{opt} , where i_{lim} has a maximum and so has the growth rate. As long as $D > D_{opt}$, phytoplankton growth is limited by light availability. But, according to Eq. 10, phytoplankton growth may also be light-inhibited if $D < D_{opt}$ because of increased photo-respiration and possibly pigment destruction at too high radiation intensities. In

our models, we have the situation $D > D_{opt}$ for the largest part of the simulation period, i.e. growth is mostly light-limited.

As shown in Figure 6, the reservoir's average depth in the 0D model is always close to the median depth computed from the 2D results. Nevertheless, because of the spatially variable depth in the 2D model and the highly non-linear character of Eq. 10, the average phytoplankton growth rates computed by the two models diverge considerably, leading to different phytoplankton levels (Figure 8) and different rates of biogenic DO production (second part of the simulation period in Figure 7).

Finally, when interpreting simulation results for the drainage period, we must take into account the evolution of multiple water bodies in the 2D model (Figure 10). Since these wet patches are only weakly connected or even fully isolated, the leveling effect of mixing becomes more and more negligible. In the 0D stirred tank model, however, the assumption of complete and permanent mixing is inherent.

5.2 Conclusions from the uncertainty analysis

If we want to assess the suitability of either model for practical applications, comparing the spread of results due to the model's discretisation (Figure 7) to the spread of results due to uncertain parameters and mechanisms (Figures 11 and 12) is particularly interesting. Because of the ecological relevance, it is advisable to focus on the state variable DO and the times when the concentration is lowest.

The minimum DO concentrations at the end of the filling period simulated by the two models are almost identical (Figure 7). The prediction of the 0D model coincides with the 2D model's median and the difference between the spatial 10- and 90-percentile is $\leq 0.5 \text{ g m}^{-3}$ only. However, we can conclude from Figure 11 that, due to uncertain rate constants and further parameters of the model, we cannot actually predict the minimum of DO that accurate. For example, the interquartile range of the 250 concentration time series obtained in the Monte-Carlo simulation is in the order of 2 g m^{-3} at the time when the lowest DO levels occur.

In the subsequent days of the simulation, the difference between the prediction of the 0D model and the spatial median of the 2D results is in the order of $1\text{-}1.5 \text{ g m}^{-3}$ (Figure 7). At the same time, the range of concentrations covered by 50% of the Monte-Carlo simulation results is as wide as 2 g m^{-3} and the span between the 10- and 90-percentile amounts to $\sim 3 \text{ g m}^{-3}$ (Figure 11). Thus, the uncertainty in predictions due to insufficient knowledge of the model parameters is, again, larger than the error we make by neglecting spatial variability, i.e. by using the 0D instead of the 2D model.

The uncertainty associated with the simulated DO concentrations becomes even more obvious when we look at Figure 12. Apparently, although empirical re-aeration formulas are part of many water quality models, their use must be considered as a major source of uncertainty. Depending on the selected formula for wind-dependent re-aeration, minimum DO concentrations between about 0.5 and 4.5 g m^{-3} are obtained. This range is larger than the greatest spatial difference computed by the 2D model for any time step.

5.3 Implications and recommendations

Our study shows that the parallel use of a 0D and a 2D model is not just of scientific interest but is also beneficial for practical applications.

The primary advantage of the zero-dimensional approach is the short computing time as well as the minimum effort for post-processing of the model's output. This is a precondition when various flood scenarios with varying boundary conditions need to be examined. Furthermore, only the fast 0D model allows extensive analyses of sensitivity/uncertainty to be carried out. We have shown that, for assessing the reliability of simulation results, such analyses are absolutely essential.

The advantage of the two-dimensional model is its ability to simulate the heterogeneity with respect to the state variables, i.e. concentrations. This is desired if the water body has a complex topography with significant variations in depth, if lateral mixing is ineffective, or when there is a pronounced spatial variation in flow velocities. The advantage of a multi-dimensional simulation is, however, gained by much extra effort for the

preparation, storage, and post-processing of data as well as for running the model (recall Table 1). The long computing times resulting from the spatially explicit solution and the associated restrictions on the length of a simulation time step may severely limit the model's overall applicability.

In Section 5.2 we have shown that knowledge about the consequences of uncertain model parameters may be quantitatively more relevant than a proper representation of spatial heterogeneity. In other words, the exclusive application of a slow-running, highly discretised model, which cannot practically be run in a Monte-Carlo environment, is only reasonable, if the parameter values are very well known. In applied water quality modeling this is a rare case.

For those who aim at modeling water quality in a similar context, the following recommendations may be helpful:

1. Build a simple zero-dimensional model first.
2. Use this lightweight tool to check the sensitivity of results against uncertain parameters and empirical formulas being part of the water quality model. Check whether the range of 'likely' results matches the required accuracy in the target application, e.g. by running a Monte-Carlo simulation.
3. Using the 0D model, examine the sensitivity of those parameters that are spatially variable such as flow velocity and depth and which are, therefore, better represented in a

distributed (e.g. 2D) model than in the 0D approach. (We skipped this step as we aimed at testing the 2D model anyhow.)

4. Build a distributed model if the spread of simulation results obtained in step 3 is significant when compared to the spread of results which is due to uncertain parameters of the water quality model (step 2).

5. For detention areas with deep reservoirs the assumption of vertical mixing may be inappropriate. Based on the experience gained in this study, we recommend testing a 1D-vertical model before building a 3-dimensional one.

ACKNOWLEDGMENTS

The research was funded by the Sixth Framework Program of the European Commission (FLOODsite project, EC Contract number: GOCE-CT-2004-505420). This paper reflects the authors' views and not those of the European Community. Neither the European Community nor any member of the FLOODsite Consortium is liable for any use of the information in this paper.

The authors are grateful to K.-E. Lindenschmidt and M. Baborowski for scientific support and provision of water quality data. Topography and discharge data were kindly provided by the federal and state water authorities LHW Sachsen-Anhalt and WSA Dresden.

Chapter VI

Assessing flood risk for a rural detention area

ABSTRACT:

Flood detention areas serve the primary purpose of controlled water storage during large flood events in order to decrease the flood risk downstream along the river. These areas are often used for agricultural production. While various damage estimation methods exist for urban areas, there are only a few, most often simpler approaches for loss estimation in rural areas. The loss assessment can provide an estimate of the financial provisions required for the farmers' compensation (e.g., in the context of cost-benefit analyses of detention measures).

Flood risk is a combination of potential damage and probability of flooding. Losses in agricultural areas exhibit a strong seasonal pattern, and the flooding probability also has a seasonal variation. In the present study, flood risk is assessed for a planned detention area alongside the Elbe River in Germany based on two loss and probability estimation approaches of different time frames, namely a monthly and an annual approach. The results show that the overall potential damage in the proposed detention area amounts to approximately 40000 € a^{-1} , with approximately equal losses for each of the main land uses, agriculture and road infrastructure. A sensitivity analysis showed that the probability of flooding (i.e., the frequency of operation of the detention area) has the largest impact on the overall flood risk.

Published as: Förster S, Kuhlmann B, Lindenschmidt K-E and Bronstert A. 2008. Assessing flood risk for a rural detention area. Nat. Hazards Earth Syst. Sci., 8, 311–322.

1 INTRODUCTION

Flood risk management measures aim to reduce the negative effects of floods. The designation of detention areas as one of these measures is currently being discussed for the Elbe and many other rivers. Several sites along the middle course of the Elbe River (Germany) have already been proposed as potential locations for flood detention, and were investigated in terms of flood peak reduction potential (IKSE, 2003; Helms et al., 2002). However, stakeholders, such as farmers, are reluctant to allow allocation of agricultural lands for flood detention, because of the negative effects inundated waters have on agricultural lands (crop losses, excessive sediment and contaminant deposition, potential degradation of the soil, etc.). In order to provide decision support for this controversial debate, it is necessary to have an in-depth assessment of the flood risk of the proposed sites.

The objective of the present study is to investigate the effect of time-varying damage in the flood risk assessment of rural flood prone areas. The concept is tested at a proposed flood detention area at the Elbe River. Section 1 gives a short overview of flood loss estimation methods with a focus on rural damage. It shows that agricultural losses have a strong seasonal variation, while the flooding probability also varies with seasons. In order to account for this variability, flood risk that is to be expected for the detention area is assessed based on two loss and probability estimation approaches of different time frames, namely a monthly and an annual approach (section 2). During the large Elbe flood in August 2002, an area of 200 km² on the right side of the Elbe River including the proposed detention site was flooded due to several dike failures (BfG, 2002). This flood event enables a validation of the damage estimation methods using damages recorded at the municipal level (section 3). In a sensitivity analysis the relative importance of the factors crop share, market price and probability of polder operation were investigated (section 4). Finally, the two different flood loss estimation methods, their applicability in other locations, and the potential impact of future developments (i.e., land-use changes, frequency of polder operation) on the results are discussed.

1.1 Damage estimation methods

This study estimates losses associated with the flooding of a detention area in a rural environment. The review of flood loss estimation methods, therefore, focuses on floodwater damage to croplands and grasslands and road infrastructure, which are typical land-use types in such flood detention areas.

Flood damage estimation methodologies are applied in many countries in Europe (Meyer and Messner, 2005) and worldwide (Dutta et al., 2003). These methods are useful in conducting cost-benefit analyses of the economic feasibility of flood control measures. In Germany, responsibility for flood policy lies with the individual federal states and, hence, there are large differences in the character and application of flood estimation methods in these states. The investigated site is located in the federal state of Saxony-Anhalt, where damage evaluation is still rarely used, according to Meyer and Messner (2005). However, with the implementation of the new European Directive on flood risk management (EU, 2007) and the increasing availability of data, it is expected that damage evaluation will gain more importance in flood defence planning in the coming years.

Expected losses in rural areas are typically much lower than those in urban areas. Hence, damage evaluation in rural areas is often neglected or only accounted for by using simple approaches and rough estimates.

Pivot et al. (2002) differentiate between losses due to damage to crops grown at the time of flooding, and damage affecting soil characteristics. The first is mainly due to the anoxia suffered by the crop, the water column pressure and locally the flow of the water. It results in a reduction in yield and crop quality and may require additional expenditures for sowing, tillage, and the application of fertiliser and crop protective agents. The second refers to a potential decrease in the quality of soil due to pollutant deposition and a loss of soil structure due to compaction or erosion.

Main variables that define the flood damage to agricultural lands are the time of year of flood occurrence, water depth, duration of flooding, flow velocity, and deposition of pollutants (DVWK, 1985; LfL, 2005; Citeau, 2003). Many authors point out that the time of occurrence of a flood with respect to crop growth stages and critical field operations plays a crucial role in the magnitude of damage (Penning-Rowsell et al.,

2003; Todorovic and Woolhiser, 1972). This differs significantly from damage evaluation in other damage categories, for example damage to buildings where loss potential does not vary with the seasons. For example, flooding in June/July results in much higher losses for summer grain crops just prior to harvesting than flooding in August just after harvesting. Depending on the time of flooding and the affected crop types, the farmers may decide to undertake measures in order to alleviate overall loss. USDA (1978) lists measures to alleviate flood losses depending on the time of year categorised in half-month periods for pasture and several crop types. For example, it may be possible to replant winter wheat in October with no or low yield reduction, whereas it may be too late for replanting in November, the only option being to plant a substitute spring crop. This saves costs for the harvest-

ing of winter wheat but necessitates additional tillage operations. Generally, loss estimates should be developed for each crop type and period of flooding, making allowance for yield losses due to delayed planting, replanting costs, savings due to costs not incurred, and costs for clean-up.

Table 1 summarises the agricultural damage variables that have been accounted for in selected case studies of flood damage estimation. In most case studies, time of occurrence is considered whereas the flood variables water depth, inundation duration, and flow velocities are only included in a few case studies. This is because the data needed to quantify the impact of these variables on the expected damage are sparse. Citeau (2003) gives a rough estimate of maximum tolerable submersion time, inundation depth, and flow velocity for different rural land-use types.

Tab. 1: Comparison of case studies on flood damage estimation including agriculture losses regarding the considered flood variables.

Reference (case study site)	Submersion period	Water depth	Submersion duration	Flow velocity
Hoes and Schuurmans, 2005 (The Netherlands)	no	stage-damage curve	no	no
Neubert and Thiel, 2004 (Germany)	yes (four periods per year)	no	no	no
Dutta et al., 2003 (Japan)	yes (monthly)	yes (three classes)	duration-damage curve	no
Citeau, 2003 (France)	yes (monthly)	yes (three classes)	yes (four classes)	yes (three classes)
Consuegra et al., 1995 (Switzerland)	yes (15-day period)	no	yes (two classes)	no

The maximum tolerable levels refer to the conditions that plants are expected to withstand without severe damage. The estimates were derived from a survey among farmers in France. According to Citeau (2003), maximum tolerable inundation duration for cropland varies between three days in spring/summer to one month in autumn/winter. Maximum tolerable depth of submersion strongly depends on the type of land use and vegetation height. Examples provided in Citeau (2003) are 1 m for orchards and 0.5 m for vineyards. Maximum flow velocities vary between 0.25 m s^{-1} for field vegetables and 0.5 m s^{-1} for orchards. No velocity values are provided for cropland. High flow velocities can cause direct damage to the plants and to soil degradation from erosion (LfL, 2005).

Another variable causing agricultural losses is the deposition of waste and mud that might contain pollutants. Such losses often necessitate additional clean-up costs, and the inundated crops and vegetables may not be sold due to contamination.

Other agricultural goods that may be susceptible to flood damages are farm buildings, machinery, and infrastructure (e.g. roads). In contrast to crop and grassland losses, damage in these other categories is independent of the season. Usually stage-damage functions are applied which relate the water level to the relative expected damage. In order to obtain an estimate of the total expected loss, the relative damage is related to the maximum damage per area and land-use type (Merz et al., 2004). Indirect losses due to traffic

and business interruptions are usually estimated as a proportion of direct costs (YRFCMP, 2003).

1.2 Study site

The present-day embankments confining most of the German reaches of the Elbe River date back to the 2nd half of the 19th century, although dike construction along the Elbe began as early as the 12th century. The embankments have led to a reduction of the retention area in Germany from 6172 km² to 838 km² (13.6% of original). The reduction of retention areas and the straightening of the main river channel have resulted in an acceleration of flow velocity and an increase of the flood water levels (BfG, 2002).

Today the construction of detention sites in the former inundation area along the Elbe is being discussed. Such sites would enable controlled diversion and storage of excess water during large flood events in order to reduce flood risk adjacent to and downstream from the detention areas.

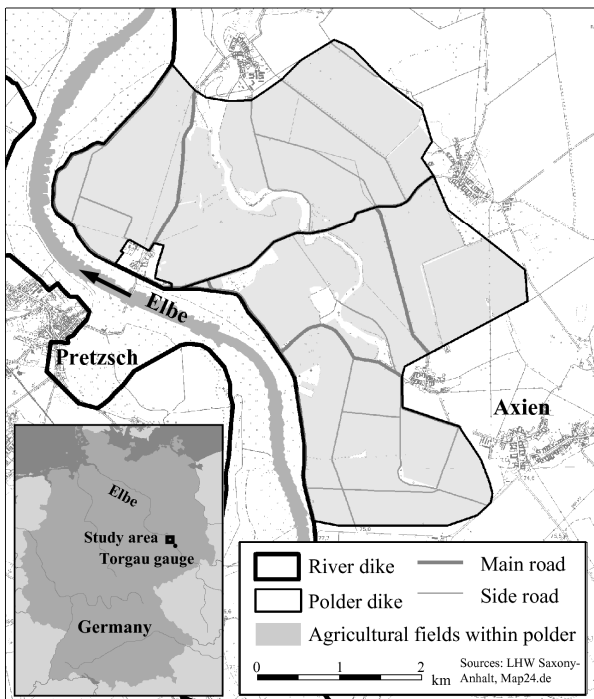


Fig. 1: Detention area with agricultural fields and road system. It is confined by the Elbe main dike to the river and polder dikes to the hinterland.

In the present study, one large controlled detention area was investigated that is already in the early planning stages (Figure 1). It is situated alongside the right bank of the middle course of the Elbe River between the Torgau and Wittenberg gauges and is designed for reducing flood peaks having a 100-years or more recurrence in-

terval. The storage capacity is 40 million m³. The detention area consists of agricultural land with very fertile soils and high agricultural productivity. More than 90% of the land is currently under intensive agricultural use. The remaining 10% of the area consists of watercourses and forest. There are no settlements within the proposed detention area. It is expected that the area will retain its present function as agricultural land even after it has been designated as a detention area.

In order to estimate the expected flood losses on agricultural lands in the detention area, information is needed on the type and mixture of crops typically grown on those lands. The agricultural land-use types for the years 2002 to 2007 were collected by interviewing the local farmers. The farmers' decision about which crops to grow depends on the profit margins for different crops and the farmers' goal, which is assumed to be profit maximization. Grain crops are grown on 51% of the agricultural area due to the good soil quality in the former inundation area (Figure 2). Main grain crops grown in the study area are wheat and barley. Corn (9%) is used for energy production and silage fodder. The share of grassland is comparatively low (7%). Grass is usually cut three times per year and is mainly used for fodder production.

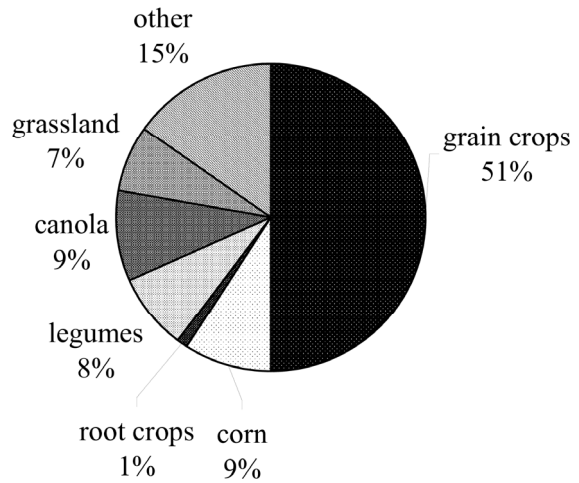


Fig. 2: Land use of the study site (% of agricultural land)

2 METHODOLOGY

Risk is defined as the probability of the adverse effects of a natural process, such as a flood, exceeding a certain magnitude (intensity) from which certain damages and losses occur (vulnerability) (Merz et al., 2007). For the detention area,

the probability of flooding corresponds to the probability of opening the inlet gate for flood water diversion, which would be the case for large floods with return periods exceeding 100 years. The costs are associated with the flood losses on agricultural land and the road system within the detention area. Since loss on agricultural land has a seasonal variation, the flood frequency analysis provides monthly weights on the flooding probability. The annual monetary flood loss in € per hectare per year ($\text{€ ha}^{-1} \text{ a}^{-1}$) on agricultural fields is calculated by weighting the loss from a single flood event occurring in each month with the probability of flooding in that month (Hess and Morris, 1987).

2.1 Damage estimation

Several approaches of varying complexity are available to calculate losses in agricultural production due to flooding. This study applies two approaches, using a monthly and an annual time frame for loss estimation.

A damage estimation model based on a monthly disaggregation of damages to crops and grasslands was developed within the framework of the project “Methods for the evaluation of direct and indirect flood losses” (MEDIS, 2007). The expected damage for each crop is calculated by:

$$ED = MV \cdot \sum_{m=1}^{12} PM_m \cdot DI_m \quad (1)$$

where ED = expected damages (monetary losses in $\text{€ ha}^{-1} \text{ a}^{-1}$), MV = market value (that can be obtained by the harvested crop without flooding in € ha^{-1}), PM = probability of polder flooding every 100 years for a certain month m (a^{-1}) and DI = damage impact on crops for month m (%). The market value MV is calculated by the total yield of a crop harvested multiplied by its selling price. MV differs from region to region since the crop yield is dependent on the climatic and soil conditions and the type of agricultural management practices used. Germany can be

subdivided politically into 38 administrative regions, each of which has different MV values for each crop. The MV values for each region were derived from the standard gross margins provided by the Curatorship for Technology and Construction Engineering in Agriculture (KTBL, 2007). The MV values for the administrative region of Dessau/Saxony-Anhalt, in which the study site lies, are given in Table 2 for selected crops.

The damage impact factor DI depends on the type of crop, the month of the flooding occurrence, and the inundation duration. Table 3 gives an example of damage impact percentages for wheat and grass for each month. The information is based on empirical data from surveys in France and Germany as referenced in LfUG (2005) and expert knowledge. The damage impact factors can reach values of up to 100% indicating a total loss. The impact is particularly dependent on the growth stage of each crop. Root crops and grain crops are harvested once per year and their impact factors have patterns similar to the ones shown for wheat. Their impact factors are differentiated into four classes of inundation duration. Grass is an exception to the other crops because it can usually be harvested three times per year (May, July, and August). The total annual yield of grass is distributed throughout the year in three harvests in May, July, and August with an annual average of 50%, 20% and 30%, respectively. Hence, the impact factors are lower since only a fraction of the total yearly harvest is damaged by a flood. The impact factors are also independent of inundation duration because sediment deposition on grasslands occurs after every flood, regardless how short the inundation period is, making the grass unusable for high value fodder. For inundation times longer than about 10 days, additional costs may be incurred due to structural damage to the grass roots requiring a repair seeding of the grasslands. The costs for the repair seeding of grasslands, which includes seeds, labour and machinery are approximately 45 € ha^{-1} (KTBL, 2006).

Tab. 2: Market value of selected crops for the administrative region of Dessau/Saxony-Anhalt averaged over the years 2000 to 2005.

crop	wheat	rye	barley	corn	canola	potatoes	sugar beets	grassland
market value (€/ha)	704	459	605	883	632	2339	2103	266

Tab. 3: Damage impact factors for wheat and grass for different months of the year grouped by different durations of flooding. Values have been extended from LfUG (2005).

inundation duration	Wheat				Grassland
	1-3 days (%)	4-7 days (%)	8-11 days (%)	> 11 days (%)	1-11 days (%)
January	5	10	20	80	5
February	5	10	20	80	5
March	5	10	20	80	10
April	10	25	40	80	20
May	20	40	70	100	50
June	50	50	80	100	15
July	100	100	100	100	20
August	100	100	100	100	30
September	0	0	0	0	10
October	5	10	20	80	10
November	5	10	20	80	10
December	5	10	20	80	10

Figure 3 shows the expected damage for each crop differentiated into classes of inundation duration. The maximum damage is expected to vary between 10 and 16 € ha⁻¹ a⁻¹ for grain crops and between 32 and 36 € ha⁻¹ a⁻¹ for root crops based on an inundation duration of more than 11 days. Damages for grass are the lowest at approximately 1 € ha⁻¹ a⁻¹.

In addition to the monthly damage estimation model, an annual approach was applied in which only two land-use classes were distinguished and the time within the growing season when the

flooding occurs was not considered. Damages with the annual approach are calculated by:

$$ED = MV \cdot RD \cdot PA \quad (2)$$

where ED = expected damages (monetary losses in € ha⁻¹ a⁻¹), MV = market value (that can be obtained from the agricultural land without flooding in € ha⁻¹), RD = relative damage costs (%) and PA = probability of polder flooding every 100 years (i.e. 0.01 a⁻¹).

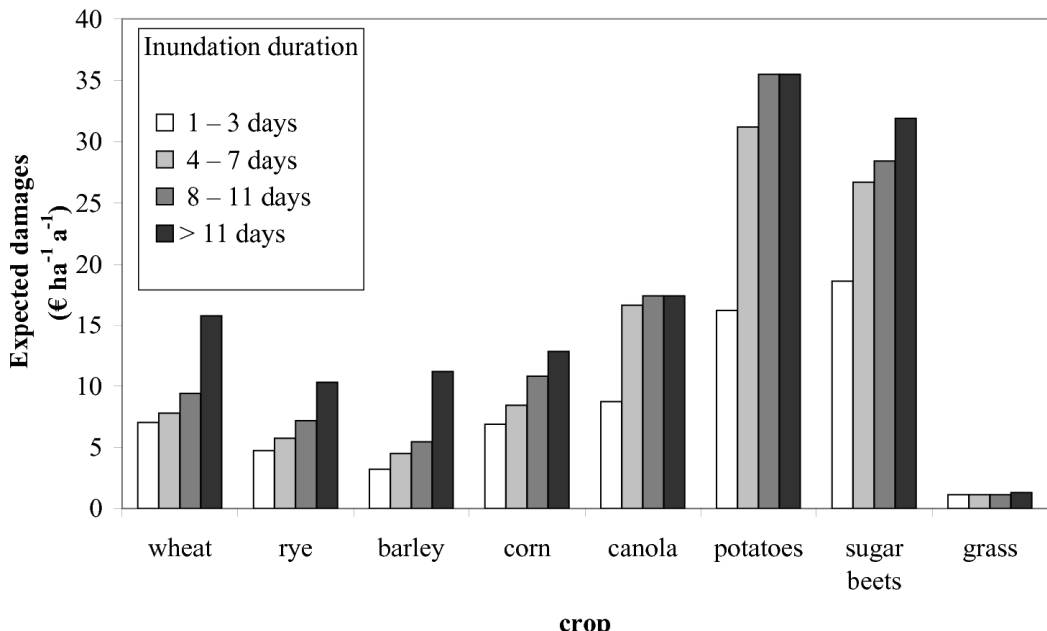


Fig. 3: Expected damages to grain crops (wheat, rye, barley, corn), oilseed plants (canola), root crops (potatoes and sugar beets) and grass based on flooding occurrence categorised on a monthly basis. Data are derived from LfUG (2005), KTBL (2006) and KTBL (2007). It is assumed that the inundation duration of > 11 days classification corresponds to the degree of damage expected to occur within the polders.

The agricultural land was differentiated in arable land and grassland with market values of 4000 and 2000 € ha⁻¹, respectively. These figures are based on damage claims from past extreme flood events in the state of Saxony in Germany (LfUG, 2005). The relative damages to both, regardless of flood depth, inundation duration or the time within the growing season, were set to be 50% and 10%, respectively. According to LfUG (2005), these values were found to fit recorded damages in flat inundation areas best. In comparison, relative damages in mountainous areas with discharges of 1 m² s⁻¹ increase to 75% and 25%, respectively. The damage to be expected when operating the polders to cap floods that exceed discharges with return periods of more than 100 years are 20 € ha⁻¹ a⁻¹ for arable farmland and 2 € ha⁻¹ a⁻¹ for grassland. These damage values are of the same order of magnitude as the damages calculated on a monthly basis (compare Figure 3).

In order to provide a representative picture of the current land-use situation, including crop rotation schemes, the percentage shares of crop types and grassland were averaged over the last 5 years (2003-2007). For the annual approach, this information was aggregated into two classes of arable land and grassland.

During the large flood in August 2002 having a return period of approximately 180 years near the study site the region where the proposed detention basin would be located was flooded as a result of dike failures. Afterwards losses were recorded by the authorities for compensation purpose. Economic loss information for agricultural land on the municipal level was made available for the present study. In order to assess the quality of the results, recorded loss data for one municipality were compared with estimated losses for the same municipality. The municipality was chosen because it has a share of the proposed detention area and was almost completely inundated in 2002, as indicated by satellite imagery. Settlements were less affected because they are built on slightly higher elevated ground. Analogous to the detention area, data on the percentage of crop types and grassland in the selected municipality were collected.

Besides losses in the agricultural sector, infrastructure damage in the form of damage to the road system is considered to be the other major damage component in the study area. Information on length and width of the roads was collected from aerial photographs and field surveys.

The expected damage to the road system was then calculated by:

$$ED = RC \cdot RD \cdot PA \quad (3)$$

where ED = expected damages (monetary losses in € ha⁻¹ a⁻¹), RC = replacement costs (€ ha⁻¹), RD = relative damage (%) and PA = probability of polder flooding every 100 years (i.e. 0.01 a⁻¹). Based on damages recorded during past flood events, damage to the traffic system is given as 200 € m⁻², whereas a relative damage impact factor of 10% is provided for water depths larger than 1 m and flow velocities below 1 m s⁻¹ (LfUG, 2005). This corresponds closely to repair costs of 25 € m⁻² for asphalt roads that were found on the basis of bid prices after the deliberate flooding of a polder system further downstream along the Elbe River (Ellmann and Schulze, 2004). For a probability of flooding of 1%, which corresponds to the operation of the polders every 100 years, the expected damages would amount to 2000 € ha⁻¹ a⁻¹. Although this value is high compared to the expected damages for arable land and grassland obtained with the annual approach, the total road surface area is substantially less than that taken up by agricultural fields.

In the present study loss estimation is restricted to direct tangible damage. Indirect damage such as traffic interruption is considered to be relatively small in the rural study area. Since the detention area is not inhabited and the people will be warned prior to the polder operation, no victims or loss of livestock is expected. Intangible damage is mainly expected in the form of adverse impacts on flora, fauna, and the terrestrial and aquatic ecosystem in the affected area. In particular, the water quality degradation from flooding can have negative effects on the fish fauna as reported in studies on storage basins and floodplains (Knösche, 2003; Howitt et al., 2007). This aspect will be part of future work on the same detention area.

2.2 Flood frequency analysis

As the costs associated with flooding of agricultural land are differentiated on a monthly basis, the expected percentage distribution of damaging floods was also analysed monthly using the discharge recorded from the gauge at Torgau for the time period 1936 – 2004. The Torgau gauge is located approximately 30 km upstream of the

proposed detention area. There are no relevant tributaries on the river stretch between the gauge and the detention site. Figure 4 shows the monthly distribution of all flood peaks in the annual maximum series (AMS) and of the largest 10% of the AMS flood events. 73% of the flood events in the AMS occur during the hydrological winter season from November to April (with more than 30% of the events occurring in March). July and August events constitute 12% of the AMS events, however account for 27% of the largest 10% of the AMS events. Apparently, there are many AMS events with comparatively small peak discharge values in spring, whereas in summer AMS events are less frequent, but typi-

cally larger. This indicates that there is a relation between seasonality of floods and their magnitude, which should be accounted for when determining the monthly percentage distribution of damaging floods. The differentiation into months having different flooding pattern is motivated by the strong dependence of losses on the month of flood occurrence. In Figure 4, the damage impact factors for wheat are included to illustrate this aspect. Extreme flood events with peak discharges relevant for polder operation have a high probability of occurrence during the summer months shortly before harvest, when grain crops are most vulnerable to inundation.

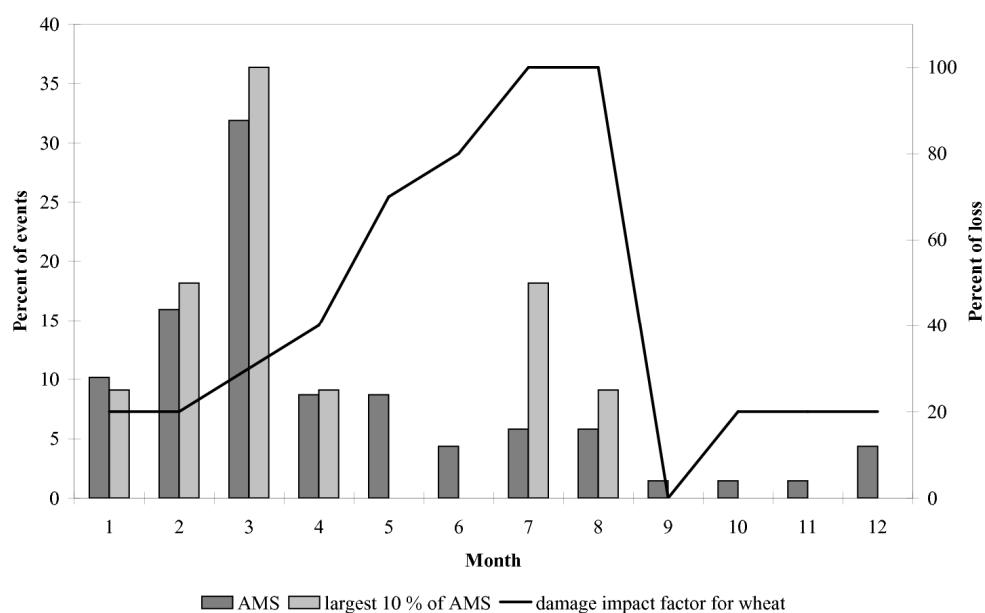


Fig. 4: Seasonality of annual peak flows for all and the 10% largest events based on the discharge AMS for 1936–2004 at the Torgau gauge and seasonality of the damage impact factor for wheat for inundation durations of 8 to 11 days.

The seasonality of flood magnitudes is a result of different flood generating mechanisms that are often dominant during different seasons (Lecce, 2000). If this is the case it is advisable to separate the flood series into seasons of similar generation mechanisms. Petrow et al. (2007) investigated the relation between dominate European atmospheric circulation patterns and annual maximum flood events for a sub-catchment of the Elbe basin. They found that westerly and north-westerly cyclones are responsible for most winter floods, but only play an important role for return periods up to 10 years. Larger floods with return periods larger than 50 years are exclusively generated by a Vb-weather regime, which is characterised by a cyclone system travelling northeastward from the Mediterranean to Central Europe. Sivapalan et al.

(2005) propose a method to isolate the contributions of individual months or seasons to the annual flood frequency curve to account for the intra-annual variability in flood processes.

Since the dikes are designed to retain floods with return periods of up to 100 years and hence the detention area is operated only during very large flood events, it is necessary to determine the probability that this discharge will be exceeded. From the Torgau gauge discharge record for the years 1936 – 2004, the largest flood in the entire year and in each of the 12 months is picked to construct annual and monthly flood frequency curves (Figure 5). A composite of the GEV (Generalised Extreme Value) (Kotz and Nadarajah, 2000) and GL (Generalised Logistics) (Johnson et al., 1994) distributions using L-moments

gave the best fit to the data. Both distribution functions are widely used in flood frequency analysis. The composite distribution function is a combination of the two functions, which were given equal weights (Merz and Thielen, 2005). Figure 5 shows that the discharge associated with the annual return period of 100 years is $4000 \text{ m}^3 \text{s}^{-1}$, while the monthly return periods

corresponding to the discharge of $4000 \text{ m}^3 \text{s}^{-1}$ are larger (for example about 150 years for March), i.e. the occurrence probabilities smaller. This means that the probability of a flood peak of a certain discharge (for example $4000 \text{ m}^3 \text{s}^{-1}$) occurring in a particular month is smaller than its probability of occurrence at any time of the year.

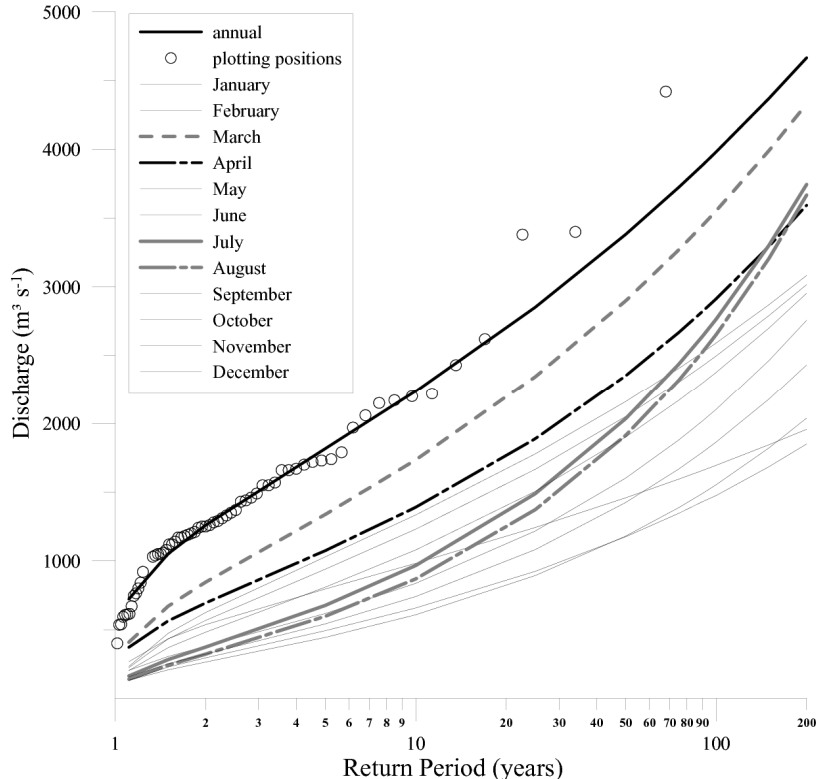


Fig. 5: Flood frequency analyses based on the annual and monthly maximum discharges of the years 1936 – 2004 at the gauge at Torgau. A composite of the GEV and GL distributions is used.

3 RESULTS

The temporal and spatial distribution of flooding variables, such as inundation duration, water depth, and flow velocity were obtained in previous 2D-hydrodynamic simulations of the same detention site based on the large flood event of August 2002 (Förster et al., 2008; Chatterjee et al., 2008; Huang et al., 2007). Simulated water depths in the detention area range from 0.5 m in the higher elevated southern part to 5.7 m in the central part, with a mean water depth of 2.5 m. The entire detention area remains inundated for three days until the start of the emptying process. After day four, the surface water retreats from only 5% of the area, whereas 75% of the area remains in-

undated for more than one week. Maximum flow velocities of 1.4 m s^{-1} are simulated behind the inlet gate. Areas with maximum flow velocities of more than 1 m s^{-1} are restricted to the stilling basin behind the inlet gate and along an already existing stream through the detention area. Figures 6 and 7 show the spatial distribution of the inundation duration and the maximum flow velocity in the detention area, respectively. The results are based on the 2002 flood event, which was characterised by a rather steep flood hydrograph. Inundation duration is expected to increase for flood events having wider flood hydrographs than the 2002 event, because the emptying process will start not earlier than the Elbe water level falls below a level that allows for safe discharge at the downstream river reaches

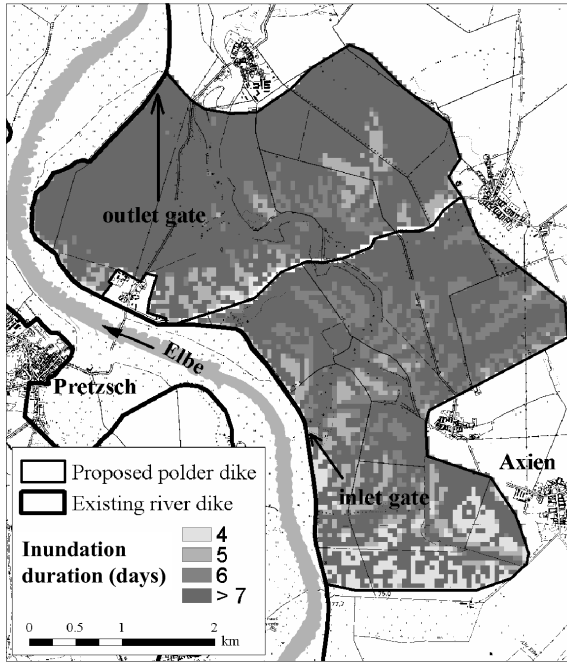


Fig. 6: Simulation results for the flood event of August 2002 (inundation duration in days).

The farmers interviewed stated that most fields were not accessible for machines for several weeks or even months after the August 2002 flood due to high soil moisture and sludge deposition, although the surface flood water had long retreated. Hence, the case of more than 11 days may realistically represent the agricultural damage and was applied in the estimation of the annual damage using the monthly approach.

The estimated annual damage in agricultural fields for the monthly and annual approach amounts to 21400 € a⁻¹ and 14600 € a⁻¹, respectively. The annual damage to the road system was estimated to be 15800 € a⁻¹. Apart from damages to field crops, additional losses to agricultural production due to damages to buildings, machinery, inventory, and clean-up measures occur. They are very site-specific and not easy to estimate. The loss information collected by the authorities for the affected municipalities during the flood in 2002 gives an indication of the magnitude of these additional losses. An average of 11% for building damages, 3% for machinery losses, 7% for inventory losses, and 12% for clean-up costs out of the overall agricultural losses in the flood affected area was recorded. Together, they make up approximately 30% of the overall agricultural losses. Adding these additional costs to the loss estimates obtained with the monthly and annual approaches results in overall losses of approximately 30500 € a⁻¹ and 21000 € a⁻¹, respectively. Together with the esti-

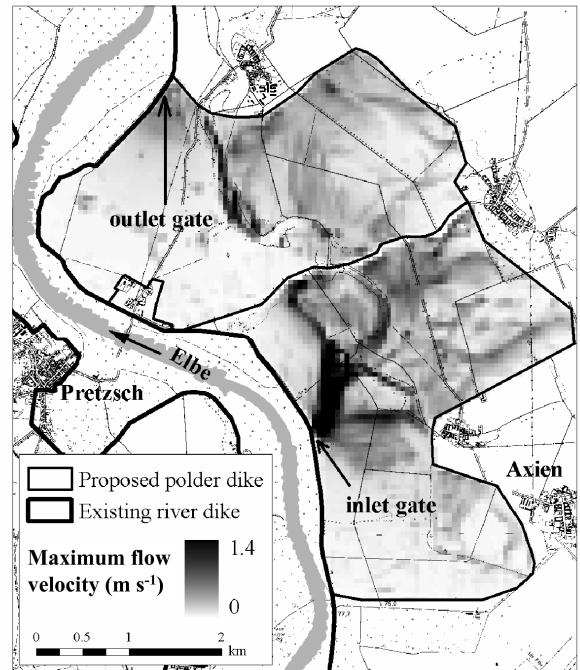


Fig. 7: Simulation results for the flood event of August 2002 (maximum flow velocity in m s⁻¹).

mated loss to the road infrastructure, overall annual damage obtained with the monthly and annual approaches ranges between 46000 € a⁻¹ and 37000 € a⁻¹, respectively. The negative effects on the total production process of the farming operation (e.g., reduction in animal production from diminished fodder quality, changes in crop rotation, non-fulfillment of delivery contracts) were not considered due to the difficulty in quantifying these effects on a regional scale.

In order to assess the quality of the damage estimation methods, recorded and estimated losses for one representative municipality were compared. The agricultural losses recorded for this municipality for the specific flood event of August 2002 amounted to 644000 €. Losses in € were estimated with the monthly and annual approaches for the same flood event. As these are event values, annual or monthly flooding probabilities were not considered. Estimated losses using the annual approach are much higher (3569000 €) than those using the monthly approach (546000 €). This is because in the annual approach, the damage values are independent of when the flood occurs during the growing season (April-October) and therefore constitute an average of the expected losses. In the monthly approach damage impact factors were applied according to the specific month in which the flood occurred. At the time of flooding at the end of August, most of the cereal fields had already been harvested and, hence, estimated losses were com-

paratively low. It illustrates the impact that the time of flood occurrence has on the overall loss. Depending on the time of occurrence, the expected agricultural losses associated with a specific flood event in the detention area vary between 287000 € in January and 994000 € in July.

4 SENSITIVITY ANALYSIS

A sensitivity analysis was performed to determine the relative importance of different factors that are directly influenced by humans. The factors included:

1. crop share of agricultural land use
2. market price for crop types ($\pm 20\%$)
3. probability of polder operation (HQ₈₀)

To account for the sensitivity of the results to different crop shares, four land-use scenarios were considered, which involved allocating the entire land coverage of the polder area to either grain crops, root crops, energy plants, or grasslands:

- *grain crops* – 100% grain crops (wheat, rye, barley)
- *root crops* – 100% root crops (potatoes, sugar beets)
- *energy* – 100% of crops used for biomass energy production or as biofuels (corn, canola)

- *environment* – all of the land is converted to grasslands (grass has a lower oxygen demand on overlying flood waters than do tilled fields and, hence, adverse ecological effects, such as stress on fish populations due to oxygen deficiency, will be reduced).

The actual crop production will be a mixture of the scenarios. Figure 8 shows the results of the four scenarios compared to the current land use in the detention area derived using the monthly damage estimation approach. It is evident that grains, canola and corn (*grain crops* and *energy* scenarios) do not change the expected damages significantly from the current situation because a majority of the land coverage is currently a mix of these crops. However, focusing on the production of root plants (*root crops* scenario) would increase damages by 2½ times. In comparison, expected damages to grasslands (*environment* scenario) are minute.

Changing the market price of the crops in the current situation by $\pm 20\%$ would vary the expected damages by the polder operation by approximately the same degree (17% increase and 22% decrease in expected damages if the crop price is increased or decreased by 20%, respectively). The probability proved to be a sensitive factor with expected damages doubling if the polders were to cap discharge peaks of flood events having a return period of 80 years (i.e., $Q_{peak} = 3300 \text{ m}^3 \text{ s}^{-1}$ as opposed to 100 years with $Q_{peak} = 4000 \text{ m}^3 \text{ s}^{-1}$).

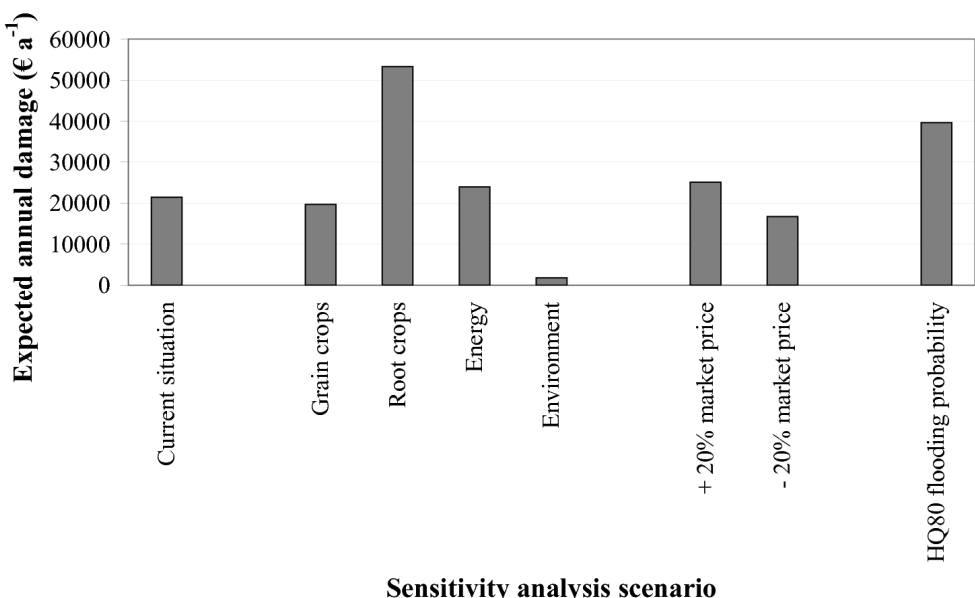


Fig. 8: Sensitivity of land use, market price and probability of polder operation on the expected damage.

5 DISCUSSION AND CONCLUSIONS

Although agricultural damage is often low compared with urban or infrastructure damage, it should be accounted for in areas where agricultural production is a predominant activity (Messner et al., 2007). The proposed monthly damage assessment procedure is applicable to a wide variety of agricultural schemes that are characterised by seasonal variation in plant growth and hence expected losses due to flooding.

The damage to agricultural production that results from flooding during a specific flood event mainly depends on the time of occurrence relative to the growth stages and the share of crop types and grassland in the area flooded. Unfortunately, bibliographic sources only provide little information on the resistance of crops to floods (Citeau, 2003). The market value as a product of total yield and selling price varies greatly between the different agricultural land-use types, while each type exhibits a different seasonal pattern of expected losses.

Other damage variables, such as water depth, inundation duration, and flow velocity, are less relevant in case of flooding of an agriculturally-used detention area. This is due to the fact that the water depths are comparatively high in order to provide a large storage volume compared to the ground surface area. In most cases, a total yield loss has to be assumed because of the combined adverse effect of damages and the restricted accessibility after the flooding due to high soil wetness. The operation of detention areas is a special case of inundation in the sense that the flooding occurs deliberately with warning times long enough to undertake measures that alleviate the losses, such as bringing in the harvest, evacuating livestock, or removing machinery from the flood prone area.

The applied monthly and annual approaches are based on market values of the grown crops in order to estimate agricultural production losses, whereas damages to farm buildings, machinery and inventory as well as clean-up costs were not considered. Hence, both damage results are comparable. The comparatively lower estimated annual damages obtained with the annual approach can be explained by the specific conditions in the study area. The fertile soils allow high yields from the intensive production of crops with high market prices. Furthermore, in the monthly ap-

proach, damage impact factors often reach 100% for arable land because of the long inundation times that are characteristic for detention areas, whereas in the annual approach a uniform damage impact factor of 50% is assumed for arable land. Depending on the specific characteristics of flood prone area with respect to the shares of land-use types and the pattern of flooding probability both approaches may result in different risk assessments. The monthly approach is more desirable as it is likely to provide more accurate estimates. Advantages of the annual approach are, however, the low data requirements and a less time-consuming estimation procedure.

If losses for certain flood events in € instead of annual damages in € per year are to be estimated, the monthly approach seems even more adequate, since the loss estimates strongly depend on the flood occurrence time. The example of the municipality that was flooded in August 2002 demonstrated the large differences in estimated losses between both approaches.

Estimated losses to the road system also constitute a large proportion of the overall expected losses. Damage potential to the road system in the study area has even increased over the past years. This is because after the extensive inundation of the area during the flood event in summer 2002, several formerly unpaved field lanes were reconstructed with an asphalt cover that bears larger reconstruction costs in case of future inundations.

The sensitivity analysis showed that in flood risk assessments of rural areas with low intensive land use it is more important to evaluate the variation in flooding probability than the variation in land use. It is particularly of importance as large summer floods are becoming more likely to occur. According to Kundzewicz et al. (2005), projected increases in temperature and associated increases in potential water content and intense precipitation are expected to increase summer flooding in most of Central Europe. Not only the flood magnitude, but also the seasonal distribution of flood occurrence is likely to be affected by climate change (Sivapalan et al., 2005). Detention basins and other flood management measures are one option to cope with future changes in flooding probability.

ACKNOWLEDGEMENTS

The research was jointly funded by the German Ministry of Education and Research (BMBF) within the framework of the project MEDIS - Methods for the Evaluation of Direct and Indirect Flood Losses (No. 0330688), the Germany Research Foundation (Helmholtz Young Scientists Group "Information and modeling systems for large scale flood situations") and the Sixth Framework Program of the European Commission (FLOODsite project, EC Contract number: GOCE-CT-2004-505420). This

paper reflects the authors' views and not those of the European Community. Neither the European Community nor any member of the FLOODsite Consortium is liable for any use of the information in this paper.

The authors are grateful to the Landesbetrieb für Hochwasserschutz und Wasserwirtschaft Sachsen-Anhalt and the Wasser- und Schiffahrtsamt Dresden for data provision. Dr. Sibylle Itzerott is thanked for her company and support on the field trip.

Chapter VII

Conclusions and recommendations

In this thesis, hydraulic, environmental and economic impacts of flood polder management were investigated using model approaches of different complexities. The research focused on two flood polder systems built for the mitigation of the flood hazard on the Middle Elbe River in Germany.

Based on the research questions posed at the beginning of the thesis, this chapter summarises and discusses the research results and gives recommendations for flood polder management and future research.

1 CONCLUSIONS

1.1 Hydrodynamic modelling

Research Question: How effective are the flood polders in terms of peak reduction for varying flood scenarios and operational schemes?

Hydrodynamic models were applied in both study areas to investigate the peak reduction under different flood scenarios and operational schemes. The study demonstrated that flood peak levels can effectively be capped by temporarily storing excess floodwater in flood polders. However, it also showed that the obtainable flood peak reduction strongly depends on the shape of the flood hydrograph. The event-specific shape is related to catchment characteristics such as basin size, soil permeability or tributary pattern and flood event characteristics such as rainfall pattern and initial soil moisture.

In order to assess the potential effectiveness of flood polders in terms of peak reduction,

Table 1 compares the ratio of storage capacity to basin size and storage capacity to mean annual flood discharge for several flood polders in Germany including the two flood polder systems that were investigated in this thesis. The higher the two ratios, the larger is the general flood peak reduction potential. However, specific conditions such as flood predictability and polder topography have to be considered when evaluating the effectiveness of each single site.

Tab. 1: Comparison of storage indicators of several flood polders in Germany

Flood polder	Storage capacity (million m ³)	Storage capacity to basin size (m ³ /km ²)	Storage capacity to MHQ* (m ³ /(m ³ /s))
Altenheim ¹ / River Rhine	18.0	358	5788
Riedensheim ² / Danube River (planned)	8.3	415	7155
Axien ³ / River (planned)	40.0	724	28369
Havelpolder ⁴ / Elbe River	110.0**	1125	62147
Rösa ⁵ / Mulde River (under construction)	21.5	3484	44792

* MHQ = mean annual flood discharge

** only Havel flood polders without Havel floodplain

Gauge and discharge time series used: ¹ gauge Maxau 1931-2003 (BfG, 2003), ² gauge Ingolstadt 1975-2001 (BfG, 2001), ³ gauge Torgau 1935-2004 (BfG, 2004),

⁴gauge Tangermünde 1961-2002 (BfG, 2002a), ⁵ gauge Bad Düben 1961-2006 (LfUG, 2006)

The timing of opening a flood polder is crucial for a successful operation as pointed out by several authors (Galbáts, 2006; Rátkey and Szlávík, 2001). If the storage is utilised too early, most of the detained volume is taken from the rising limb. If the inlet gate is opened too late, the volume is merely taken from the falling limb. In both cases the peak lowering obtained will be less than potentially possible (Silva et al., 2004). In this study the opening time of the inlet gate was pre-determined for each investigated flood scenario so as to maximise flood peak reduction.

Dividing the inlet gate into separately operable parts has been proved to be a promising strategy for an adjusted gate control. It also allows for the utilisation of the flood polder in case of a gate malfunction.

Flooding characteristics as obtained from the one-/two-dimensional hydrodynamic model showed a large spatial and temporal variation in flow velocity and water depth within the investigated flood polder Axien. These variables are relevant in the subsequent water quality model, which was coupled to the hydrodynamic model.

1.2 Water quality modelling

Research question: How does the long water storage affect dissolved oxygen levels in the flood polders?

During the operation of the Havelpolder system in August 2002, a large number of fish died due to a considerable de-oxygenation of the water in the flood polder reservoirs and the subsequent release of stored oxygen-poor water into the Lower Havel River which is known for its wealth of fish (Knösche, 2003). An environmental risk for fish and other aquatic animals may occur if oxygen-poor flood water is released to a river reach with a small ratio of storage capacity to mean annual flood discharge or if the flood polder itself contains aquatic habitats. The first applies to the Havelpolder system, where water is released to the Lower Havel River, which is a comparatively small tributary of the Elbe River with a mean annual flood discharge of 212 m³/s (based on the discharge series 1981-2002 at the gauge Havelberg (BfG, 2002b)). The second applies to the planned flood polder Axien, where a small stream runs through the flood polder area,

which is home to several protected species and put under protection according to national and European nature conservation legislation.

Numerical water quality simulations in the flood polder Axien showed that under the conditions used in this study oxygen concentration in the flood polder falls below 3 mg l⁻¹. This level is considered critical for fish (Böhme et al., 2005), while Wolter et al. (2003) point out that there are large variations among the species regarding tolerance levels and lethal oxygen concentrations. The low simulated oxygen levels can mainly be attributed to the low flow velocities and large amount of degradable organic matter in the flood polders compared to the river, leading to a strong de-oxygenation of the flood water. Warm and calm weather conditions, as observed shortly after the August 2002 flood event, will even intensify the depletion of dissolved oxygen. Adverse impacts on the water quality of the Elbe River itself when releasing the oxygen-poor stored water are negligible due to the high Elbe discharge compared to the much smaller outflow from flood polder Axien and Lower Havel River, respectively.

1.3 Vulnerability assessment

Research question: How can economic vulnerability be assessed when considering time-varying damage in agricultural areas?

Both study areas are characterised by an intensive agricultural land use with grain crops, corn, canola and grassland being the main crop types. Agricultural fields show a typical growth pattern throughout the year. Losses in case of a flooding therefore strongly depend on the time of flood occurrence relative to growth stages and agricultural field operations. Furthermore, losses vary greatly among the crop types.

Not only the vulnerability of agricultural land, but also the flooding probability varies with seasons. Often the seasonal flooding probability is different for smaller floods than for very large floods which are relevant for flood polder operation. Extremely large floods of the Elbe River have a higher occurrence probability during summer when agricultural vulnerability is highest, compared to lower floods which are most frequent in spring. To account for the seasonal variability in both expected agricultural losses and flooding probability, a monthly differentiation was chosen in this study.

Different from the time of occurrence, agricultural losses in the flood polders do not vary much between floods of different magnitude and duration. However, the potential loss in the benefiting areas, i.e. the areas in which the flood hazard is reduced due to flood polder utilisation, strongly depends on these flood characteristics. This is due to the fact that for the flood polder, the affected land is restricted to the area within the polder dikes, and damage to crops is relatively independent of water depth. In the benefiting area, however, a flood of larger magnitude and duration may result in a larger flood-affected area and higher inundation depths in areas of various land use types. Particularly in urban areas, loss strongly correlates with inundation depth.

Under the current land use, the expected loss per m³ of retained water is estimated for both study areas (Table 2). Mean expected losses on agricultural lands, including crop losses, additional losses due to building and machinery damages and mean losses in the road infrastructure, are considered. Relative losses are significantly higher in the planned flood polder Axien than in the Havelpolder system, although the mean water depth in the Axien flood polder is considerably higher. The differ-

ence in relative losses is mainly attributed to there being less vulnerable land use in the Havelpolder system, in particular the proportion of grassland. While grassland coverage is nearly 70 % in the Havelpolder system, it is only 7 % of the agricultural land in the planned flood polder Axien. Relative losses also vary among the single flood polder reservoirs in both study areas as result of prevailing land use and storage capacity.

Apart from losses that occur in the flood polders during their utilisation, further cost factors have to be considered when assessing cost-efficiency of flood polders, however, they were mostly beyond the scope of this study. These factors include the damage mitigation or reduced expenses for flood management in the benefiting areas, possible land acquisition payments or costs for land use conversion and the expenditures for construction and maintenance of engineering structures such as control gates and dikes. Also the flood polder's location relative to benefiting areas and their vulnerability must be taken into consideration. Flood polders should preferably be located adjacent to or upstream of highly vulnerable areas, but downstream of flood-relevant inflows into the river.

Tab. 2: Comparison of cost-efficiency indicators for both study areas

Case study area	Losses (million €)	Storage capacity (million m ³)	Losses to storage capacity (€/1000 m ³)	Area (km ²)	Losses to area (million €/km ²)	Mean water depth (m)
Havelpolder	6.7	110	61	100	0.07	1.1
Axien	4.6	40	115	17	0.27	2.4

1.4 Model complexity

Research question: Which is the appropriate model complexity to simulate hydraulic and water quality processes in flood polders?

Hydraulic processes in flood plains are often very complex including three-dimensional flow structures (Knight and Shiono, 1996). However, for practical purposes there is a need for simplified spatial representations of the model domain for reasons of limited resources and data availability. All models incorporate certain simplifying assumptions and approximations, which pose specific limitations for certain applications (Shanahan et al., 1998). The appro-

priate spatial discretisation should be chosen according to the system's complexity and the study objective. In this study, hydraulic and water quality models of different spatial discretisation were applied for the simulation of flood polder processes in order to assess the models' suitability in view of performance and modelling effort.

A one- (1D) and a coupled one-/two-dimensional (1D-2D) model approach were applied to simulate the flooding and emptying process in the planned flood polder Axien and the flow in the adjacent Elbe River reach. In both model approaches the river and floodplain geometry was described by a series of cross sections. In the coupled 1D-2D approach the flood polder was represented in the form of a

Digital Elevation Model (DEM), whereas in the 1D approach the flood polder geometry was given solely as a storage function, assuming a horizontal water surface.

Both the 1D and coupled 1D-2D model simulations yield the same flood wave reduction in the Elbe River. However, the 1D-2D model provides additional information such as the spatial variation in flow velocities and water depths. A two-dimensional simulation of the water flow process in the flood polder may be inevitable for certain applications. They include studying the effects of different land use types on water propagation, identifying flow obstacles and preferred flow paths, optimizing the location of control structures, gaining information on the spatial and temporal development of flow velocities or identifying remaining water patches during the emptying process of the flood polder.

The computational time as well as the storage requirements for the 1D model were considerably lower than for the 1D-2D model and even more so when finer resolution DEMs are used. Further, unlike the 1D model, considerable effort was required in setting up and simulating the 1D-2D model. In view of all these factors, it is recommended to use a 1D model for studying the flooding processes of polders, particularly the peak reductions in the main river. However, a 1D-2D approach may be used when the study of flow dynamics in the polder is of particular interest, if a spatial distribution of the flooding parameters such as inundation duration is required for a subsequent damage assessment or if a 2D water quality model is coupled to the 2D hydrodynamic model, as was done in this study.

A 2D vertically averaged model and a zero-dimensional (0D) stirred tank model were applied to simulate the dissolved oxygen dynamics in the flood polder Axien. The same gate inflow and outflow boundary conditions were used in both models as obtained from the previous 1D-2D hydrodynamic simulation. Water quality boundary parameters and water quality processes were chosen to be identical in both models, the spatial discretisation being the only difference between the two approaches. The dissolved oxygen dynamics as simulated with both models were similar in the initial flooding period, but deviated with the start of the emptying process. The deviation can be attributed to

the different approach of determining flow velocities and water depths in the two models.

The 2D model approach required a significantly higher pre- and post-processing effort and longer computation times per simulation run. It is therefore not suitable for the investigation of various different flood scenarios and for testing the model reliability with an extensive sensitivity analysis. However, investigating the impact of the spatial variability within the model domain on the state variables requires a spatially distributed model such as the 2D simulation approach used in this study.

Therefore, for practical application it is recommended to firstly set up a fast running model of lower spatial discretisation like the 0D stirred tank model. Secondly, the parameter sensitivity on the water quality results should be checked with a particular focus on those parameters that are spatially variable and therefore assumed to be better presented in a 2D model. Thirdly, a 2D model should be run if a high spatial variation in water quality results is assumed from the previous runs. Generally, 2D model approaches may be preferred in floodplain areas and flood polders of complex topography and distinct variations in hydraulic variables such as water depth and flow velocities.

2 RECOMMENDATIONS

2.1 Flood polder management

In this section general recommendations and suggestions for flood polder management are drawn from the investigations.

When choosing potential locations for flood polders the most important criteria are (a) a large storage volume compared to the discharge volume of the river flood wave, (b) suitable topographic conditions to allow for an efficient filling and emptying, (c) a suitable location, preferably just upstream or adjacent to the river reaches to be protected, (d) a low vulnerable land use within the flood polder area, and (e) the availability of an accurate and timely flood forecast to adjust the gate control to the predicted flood wave.

The utilisation of flood polders is limited to the flow time of the flood wave in the framework of the available forecast (LAWA, 1995).

The lead time should be long enough to cover the whole flood peak to be capped so as to determine the optimal gate control strategy with reference to the available storage capacity and maximum flow rates through the gates. For operational reliability, it is necessary to divide the inlet into at least two separately operable parts as it allows for the utilisation of the storage area in case of gate malfunction. Separately operable gate parts may also be favourable in view of improving inflow control, as demonstrated in this study.

Apart from optimising gate control, a good flood forecast will also facilitate early communication to residents and farmers so as to allow for loss alleviation. During a flood event, the earlier farmers are informed about the flood polder utilisation, the more time they have to undertake loss-reduction measures, such as bringing in the harvest, evacuating livestock, or removing machinery from the flood-prone area.

Reducing the amount of organic material on the fields by cutting the grass and bringing in the harvest is also advisable in view of water quality. The more easily degradable organic matter remains on the fields, the stronger the oxygen depletion. Particularly under warm and calm weather conditions, oxygen concentration in the water may fall below levels that are lethal for fish and other aquatic and terrestrial animals.

In view of water quality, it is recommended to fully utilise the flood polder storage capacity. Particularly in summer, larger water depths will dampen water warming and hence contribute to higher oxygen saturation levels since cold water can hold more dissolved oxygen than warm water. Furthermore, the possibility of allowing a continuous flow through the flood polder should be considered so as to increase the flow velocity and hence increase oxygenation due to flow-induced re-aeration. Generally, storage times should be kept short by starting the emptying process as soon as possible so as to reduce degradation of biomass and hence deoxygenation of the retained water. However, during the emptying process additional control may be required in cases where catchment management objectives set constraints on the quantity and quality of water release (Hall et al., 1993). In respect of the quantity of water release, the emptying process should not start earlier than when safe discharges at downstream river reaches are assured. Regarding water qual-

ity, the investigations in study area 1 (Havelpolder system) demonstrated that it may be advisable to restrict release of oxygen-poor water into the Lower Havel River with its high fish abundance in order to maintain a sufficient oxygen level in the River.

A controlled emptying process implies the existence of adjustable control structures rather than spillways or an intentional dike opening by dike blasting or excavation. In most cases, adjustable control structures are necessary for safety reasons so as to enable an interruption of the filling process when the flood polder capacity is reached or in unforeseen incidents. Also, they allow for saving storage capacity in the case of a second successive flood wave and for controlling the time of water release during the emptying process. However, control structures are often uneconomic if they are only used for the purpose of flood protection during very rare flood events. Only one of the six reservoirs of the Havelpolder system is equipped with control structures, whereas the others were opened by dike blasting or excavation during the 2002 flood. A comparative analysis showed that the costs for construction and maintenance of the control structures exceed by far the costs for dike blasting and reparation in the case of utilisation during rare flood events (Ellmann and Sauer, 2004). Dike blasting may even be more economically favourable if demolition chambers are installed. The picture may change if additional purposes of the control structures are included, such as frequent use for so-called ecological floodings.

Ecological flooding (also called managed flooding) refers to the periodic flooding of low-lying polder areas during small flood events. It allows for the development of flood-adapted wetland species and therefore reduces future damage in the rare case of flood polder utilisation for flood protection. Ecological flooding often necessitates a permanent land-use change, such as a conversion of intensive arable land to extensive grassland. This involves yearly compensation transfers to the farmers or one-off payments in case of land purchase. In the case of the Havelpolder system, opportunity costs for land use change would by far exceed the damage reduction during rare flood events (Ellmann and Sauer, 2004). In other riverine areas, such as on the River Rhine, ecological flooding schemes, which combine objectives of flood protection and nature conservation, are already

in operation (Bettmann and Bauer, 2005; Armbruster et al., 2006).

According to the German “Act to improve preventive flood control” (BMU, 2005), flood polders are designated as flood plain areas and each federal state is obliged to adopt land use regulations in order to protect or improve ecology of water bodies and their flood areas, prevent and alleviate flood damage and prevent erosion. The water resources laws of the federal states of Brandenburg and Saxony-Anhalt, where the study areas are located, prohibit conversion of grassland to arable land in flood plain areas. Moreover, arable land should be converted to grassland if possible. In the original version of the German preventive flood control act, a strict prohibition of tillage in unspecified “flow regions” of the flood plain areas was proposed. However, this clause was not adopted in the final version of the act as the danger of erosion and pollution of the river was unproven scientifically (Munk, 2005). In fact, in most of the flood plain areas sedimentation processes dominate. Erosion is merely expected to take place in zones and at times of high flow velocities. Therefore considerable erosion in flood polders is mainly restricted to areas near the inlet gates during times of filling. Apart from the construction of stilling basins, erosion may be reduced by filling and emptying flood polders at the lowest lying part if gate location is not restricted by other factors. This study showed that grassland in flooded areas is not generally preferable over arable land in terms of economical vulnerability and oxygen depletion. In fact, there are periods such as shortly after harvest when losses on grassland outweigh crop losses. Similarly, the amount of water deoxygenation due to surface biomass degradation varies considerably throughout the year and is subject to agricultural field operations prior to flooding. Unmown grassland may constitute a larger source of easily degradable biomass than do tilled fields.

The selection of appropriate locations for flood polders often leads to conflicts with farmers and land-owners, although there is a general agreement in the necessity of such measures. Even more opposition is expected in the case of land use restrictions or ecological flooding schemes. The importance of public participation was clearly demonstrated by the case of a planned flood polder designation at the Dutch-German border, where public resis-

tance eventually led to an end of the plans (Roth and Warner, 2007). Stakeholders will accept new proposals that affect their local environment more readily if they are consulted in the early planning stages and are encouraged to make suggestions as to how the project could be modified to meet local requirements (Hall et al., 1993).

Farmers’ acceptance is also raised by assuring financial compensation in the case of flood polder utilisation. After the flooding in 2002 farmers experienced yield losses due to excessive growth of weeds or changes in grassland species assemblage. Grassland in the Havelpolder system only reached its original state after four years (IaG, 2006). However, these long-term effects are usually not compensated nor are they included in vulnerability assessments.

In view of cost-efficiency, an increase in stored volume in the flood polder will hardly affect the expected loss in the flood polder, whereas it may contribute considerably to a decrease in the extent of affected areas, water depth and hence potential loss in downstream areas. If only a portion of the full storage capacity of a flood polder system is required from a hydraulic point of view, it may be considered preferably to utilise only those flood polder reservoirs with the least damage potential and the lowest amount of degradable biomass at the time of flooding. However, hydraulic considerations for an optimization of the peak reduction effect should have first priority. If only selected polder reservoirs are used, dike stability of the unused reservoir dikes must be ensured.

2.2 Future research

In this thesis, it was demonstrated that the analysis of flood risk reduction by means of flood polders requires comprehensive interdisciplinary approaches, including methods from hydraulics, socio-economics and ecology.

It was also stressed that the number of processes considered in the applied models and the models’ spatial discretisation should always correspond to the availability of observation data and appropriate parameter values. While there were few water level and water quality measurement data available in the study area 1, the lack of calibration and validation data in study area 2 made it advisable to keep model complexity low. Nevertheless, there is still considerable improvement potential in the applied hy-

draulic and water quality models so as to better describe the processes that take place during flood polder utilisation. Potential improvements in the hydraulic models include the introduction or refinement of groundwater processes. The water quality model could be further refined by adding more processes than those currently considered, such as de-oxygenation due to sediment oxygen demand or deriving water temperature from solar radiation.

The results of the hydraulic simulations suggest that the shape of a flood wave strongly influences the potential flood peak reduction, while the probability (which in term determines the frequency of flood polder operation) and the seasonality of flooding are of particular importance when assessing costs and benefits of flood polder utilisation. At the same time, changes in flood frequency and timing due to climate change are projected in many studies, e.g., Christensen and Christensen (2003). Taken to extremes, this could mean that the discharge corresponding to a 100 year flood under current conditions may be observed on average every 50 years or even more often. This would necessitate a more frequent flood polder operation and has to be accounted for in the design of flood protection measures in general. Therefore, future research should aim at predicting changes in flooding probability, seasonality and flood wave characteristics as it determines the effectiveness of flood control measures such as flood polders.

In the economic analysis only direct tangible damage was considered. For a comprehensive evaluation of flood management strategies, though, indirect as well as intangible damage should be taken into account. Whereas approaches exist for the inclusion of indirect damage like disruption to traffic, production or trade, an appropriate assessment of intangible damage such as damage to human health and ecological side effects is a major challenge for further research.

The depletion of dissolved oxygen during long flood water storage is a serious adverse ecological side effect. Consequently, it was investigated in this thesis and may contribute to an ecological assessment of flood polder operation. Further environmental indicators to be included when assessing flood polder measures may be the deposition of pollutants (Wurms and Westrich, 2008) or impacts on vegetation growth (Armbruster et al., 2006), which were, however, beyond the scope of this study.

These along with other criteria, including the studied flood peak reduction and economic losses, may contribute to an overall assessment of flood polder measures in a multi-criteria analysis (MCA). MCA techniques may either be applied to evaluate alternative flood protection measures that contribute to the flood risk reduction of a certain area or they may be applied to evaluate alternative variants of a specific flood protection measure. Alternative variants of a flood polder measure may refer to the design and location of polder dikes and control structures, operational strategies or different land use schemes.

MCA methods also allow for the consideration of non-monetary criteria in the evaluation process. After criteria evaluation is completed, weights are assigned to the specific criteria. Weighting is the most crucial part in a MCA. It is often very controversial, especially when several stakeholder groups are involved. In the investigated study areas several objectives such as agriculture, fishery, nature conservation or recreation must be taken into consideration. Currently, most studies comprise social, economic and environmental risk criteria. However, only few examples of real applications of MCA in flood risk management exist (Meyer et al., 2008). Further research should aim at improving MCA techniques for flood risk management to adopt them successfully in real cases involving relevant stakeholders and decision makers.

REFERENCES

- Alphen, J van, Marini F, Loat R, Slomp R and Passchier, R. 2008. Flood risk mapping in Europe, experiences and best practice. Proceedings of the 4th International Symposium on Flood Defence, 6-8 May 2008, Toronto, Canada, 150-1 – 150-8.
- Ambrose R B J, Wool T A Martin J L, Shanahan P and Alam M M. 2001. WASP - Water quality analysis simulation program, Version 5.2-MDEP, Model documentation, Environmental Research Laboratory & ASCL Corporation, Athens, Georgia.
- Antenucci J and Imerito A. 2002. Dynamic reservoir simulation model (DYRESM), Science Manual, Centre for water research, University of Western Australia.
- Armbruster et al. (eds.). 2006. FOWARA. Forested Water Retention Areas. Guidelines for decision makers, forest managers and land owners. http://www.landespflege-freiburg.de/ressourcen/fowara_guideline.pdf. 84 p.
- Aureli F, Maranzoni A, Mignosa P and Ziveri C. 2005. Flood hazard mapping by means of fully-2D and quasi-2D numerical modeling: a case study. In: Van Alphen J, van Beek E and Taal M (eds.). 2005. Floods, from Defence to Management. Taylor & Francis. London.
- Banks R B and Herrera F F. 1977. Effect of wind and rain on surface reaeration, *J. Environ. Eng. Div. Am. Soc. Civ. Eng.*, 103: 489–504.
- Bates P D and De Roo A P J. 2000. A simple raster-based model for flood inundation simulation. *Journal of Hydrology* 236(1-2): 54-77.
- Bates P D, Horritt M S, Hunter N M, Mason D and Cobby D. 2005. Numerical modelling of floodplain flow. In: Bates P D, Lane S N and Ferguson R I (eds.). 2005. Computational Fluid Dynamics. Applications in Environmental Hydraulics. John Wiley & Sons. Chichester.
- Bates P D, Lane S N and Ferguson R I. 2005. Computational Fluid Dynamics: Applications in Environmental Hydraulics. John Wiley & Sons Ltd.
- Bettmann T and Bauer H. 2005. Hochwasserschutz am Rhein durch den Polder Ingelheim (Flood protection at the River Rhine by the flood polder Ingelheim, in German). *Wasser und Abfall* 9: 41-45.
- BfG. 2001. Deutsches Gewässerkundliches Jahrbuch. Bundesanstalt für Gewässerkunde. Koblenz. http://dlr.bafg.de:8086/DGJ/PDF/2001/QBI/10046_003.p.pdf.
- BfG. 2002. Das Augusthochwasser 2002 im Elbegebiet (The August 2002 flood in the Elbe basin, in German). Bundesanstalt für Gewässerkunde. Koblenz. <http://elise.bafg.de/servlet/is/3967/>. p. 49.
- BfG. 2002a. Deutsches Gewässerkundliches Jahrbuch. Bundesanstalt für Gewässerkunde. Koblenz. http://dlr.bafg.de:8086/DGJ/PDF/2002/QBI/50235_0.p.pdf.
- BfG. 2002b. Deutsches Gewässerkundliches Jahrbuch. Bundesanstalt für Gewässerkunde. Koblenz. http://dlr.bafg.de:8086/DGJ/PDF/2002/QBI/58079_0.p.pdf.
- BfG. 2003. Deutsches Gewässerkundliches Jahrbuch. Bundesanstalt für Gewässerkunde. Koblenz. http://dlr.bafg.de:8086/DGJ/PDF/2003/QBI/23700_205.p.pdf.
- BfG. 2004. Deutsches Gewässerkundliches Jahrbuch. Bundesanstalt für Gewässerkunde. Koblenz. http://dlr.bafg.de:8086/index2.php?page=jahreshauptwer-te.php&K1=&K2=12845&jahr=2004&jahr_typ=abflussjahr&MGNAME=QBI.
- BfG. 2006. Wasserstands- und Abflussvorhersagen im Elbegebiet (Water level and discharge forecasting in the Elbe basin, in German). Bundesanstalt für Gewässerkunde. Koblenz.
- BMU. 2005. Act to improve preventive flood control. German Federal Ministry for the Environment. http://www.bmu.de/files/pdfs/allgemein/application/pdf/hochwasserschutzgesetz_en.pdf.
- Böhme M et al. (eds.). 2005. Schadstoffbelastung nach dem Elbe-Hochwasser 2002 (Contaminant loads after the Elbe flood in 2002, in German). 101 p.
- Bowie G L, Mills W B, Porcella D B, Campbell C L, Pagenkopf J R, Rupp G L, Johnson K M, Chan P W H, Gherini S A and Chamberlin C E. 1985. Rates, constants and kinetics formulations in surface water quality modeling (2nd ed.), Report EPA/600/3-85/040, U.S. Environmental protection agency.
- Baptist M J, Haasnoot M, Cornelissen P, Icke J, van der Wedden G, de Vriend H and Gugic G. 2006. Flood detention, nature development and water quality in a detention area along the lowland river Sava, Croatia. *Hydrobiologia* 565: 243-257.
- Bronstert A. (ed.) 2004. Möglichkeiten zur Minderung des Hochwasserrisikos durch Nutzung von Flutpoldern an Havel und Oder (Reducing flood risk by means of flood polders at Havel and Odra Rivers, in German). Brandenburgische Umweltberichte 15. Potsdam. <http://pub.ub.unipotsdam.de/zsr/bub/door/door15.htm>. p. 212.
- Büchele B, Mikovec R, Ihringer J and Friedrich F. 2004. Analysis of potential flood retention measures (Polders) at the Elbe River in Saxony-Anhalt. In: Geller W et al. (Eds.). 2004. 11th Magdeburg Seminar on Waters in Central and Eastern Europe: Assessment, Protection, Management. Proceedings of the international conference 18-22 October 2004 at the UFZ.
- Busch N and Hammer M. 2007. Auswirkungen von geplanten Rückhaltemaßnahmen an der Elbe in Sachsen und Sachsen-Anhalt auf Hochwasser der Elbe (Effects of planned retention measures on floods at the Elbe River in Saxony and Saxony-Anhalt, in German). *Dresdner Wasserbauliche Mitteilungen*. Heft 35. p. 485-494.
- Chapra S C. 1997. Surface water quality modeling, McGraw-Hill.
- Chatterjee C, Förster S and Bronstert A. 2008. Comparison of Hydrodynamic Models of Different Complexities to Model Floods with Emergency Storage Areas. *Hydrological Processes*. Published online, DOI: 10.1002/hyp.7079.
- Chow V T. 1959. Open-channel hydraulics. McGraw-Hill Book Company. New York.
- Christensen J H and Christensen O B. 2003. Severe summertime flooding in Europe. *Nature*, 421: 805.
- Citeau J-M. 2003. A New Control Concept in the Oise Catchment Area: Definition and Assessment of Flood Compatible Agricultural Activities, FIG working week, Paris, France.

- Consuegra D, Joerin F and Vitalini F. 1995. Flood Delineation and Impact Assessment in Agricultural Land using GIS Technology, 177-198. In: Carrara, A and Guzzetti, F (eds.): Geographical Information Systems in Assessing Natural Hazards, Kluwer Academic Publishers.
- DHI. 1997. MIKE11 GIS Reference and User Manual. Danish Hydraulic Institute: Horsholm. Denmark.
- DHI. 2000. MIKE 21 User Guide. Danish Hydraulic Institute, Horsholm. Denmark.
- DHI. 2003. ECO Lab Reference manual, Danish Hydraulic Institute.
- DHI. 2004. MIKEFLOOD 1D-2D modelling package, Danish Hydraulic Institute.
- Dhondia Z and Stelling G. 2002. Application of one-dimensional - two-dimensional integrated hydraulic model for flood simulation and damage assessment. International Conference on Hydroinformatics, UK, Vol. 5: 265-276.
- Dijkman J P M, Ogink H J M, Klijn F and Van der Most H. 2003. Toelichting aanvullend deskundigenoordeel noodoeverloopgebieden. Report Q3570. WL | Delft Hydraulics, Delft, The Netherlands (In Dutch).
- DKKV. 2004. Flood Risk Reduction in Germany. Lessons Learned from the 2002 Disaster in the Elbe Region. Summary of the study. German Committee for Disaster Reduction.
- Dutta D, Srikantha H and Katumi M. 2003. A mathematical model for flood loss estimation, Journal of Hydrology 277, 24-49, 2003.
- DVWK. 1985. Ökonomische Bewertung von Hochwasserschutzwirkungen (Economical assessment of flood protection measures, in German). Deutscher Verband für Wasserwirtschaft und Kulturbau, DVWK Mitteilungen 10.
- Ellmann H and Schulze B. 2004. Schadenpotentiale in Siedlung/Infrastruktur und Ökologie (Damage potential in settlements and infrastructure, in German). In: Bronstert, A (ed.). Möglichkeiten zur Minderung des Hochwasserrisikos durch Nutzung von Flutpoldern an Havel und Oder, Brandenburgische Umweltberichte 15. Potsdam.
- Ellmann H and Sauer W. 2004. Kostenbilanzierung Bauvarianten und Sprengung (Comparison of costs between construction variants and dike destruction, in German). In: Bronstert, A (ed.). Möglichkeiten zur Minderung des Hochwasserrisikos durch Nutzung von Flutpoldern an Havel und Oder, Brandenburgische Umweltberichte 15. Potsdam.
- EU. 2007. Directive 2007/60/EC of the European Parliament and of the Council of 23 October 2007 on the assessment and management of flood risks. Official Journal of the European Union 6 November 2007. L 288/27-34.
- Faganello E and Attewill L. 2005. Flood Management Strategy for the Upper and Middle Odra River Basin: Feasibility Study of Raciborz Reservoir. Natural Hazards 36: 273-295.
- FAS. 1975. Modellversuche für Flutungsbauwerke (Model experiments for flood control structures, in German), Abschlussbericht der Forschungsanstalt für Schiffahrt, Wasser- und Grundbau. Berlin.
- Fischer M, Schindler M and Strobl T. 2005. Controlled Flood Polders - an effective method for reducing floods in middle reaches of rivers. Proceedings of XIIth World Water Congress in New Delhi.
- Förster S, Chatterjee C and Bronstert A. 2008. Hydrodynamic simulation of the operational management of a proposed flood emergency storage area at the Middle Elbe River. River Research and Applications, Wiley InterScience. Published online, DOI: 10.1002/rra.1090.
- Förster S, Kneis D, Gocht M and Bronstert A. 2005. Flood risk reduction by the use of retention areas at the Elbe River. Intl. J. River Basin Management 3(1): 21-29.
- Fread D L, Lewis J M, Carroll T R, Rost A A and Ingram J. 1998. Improving real-time hydrologic services in USA, Part II: Inundation mapping using dynamic streamflow modeling. British Hydrological Society International Symposium on Hydrology in a Changing Environment. UK.
- Galbáts Z. 2006. Flood Control Management with special Reference to Emergency Reservoirs. In: Marsalek J, Stancalie G and Balint G. 2006. Transboundary Floods: Reducing Risks through Flood Management. NATO Science Series IV: Earth and Environmental Sciences. Kluwer Academic Publishers. Springer. Dordrecht, The Netherlands.
- Gocht M and Bronstert A. 2006. Kosteneffizienz von Flutungspoldern (Cost-effciency of flood polders, in German). In: Jüpner R. (ed.). Beiträge zur Konferenz „Strategien und Instrumente zur Verbesserung des vorbeugenden Hochwasserschutzes“. Internationale Konferenz, 23-25 November 2006, Tangermünde, Germany. Schriftenreihe des Instituts für Wasserwirtschaft und Ökotechnologie der Universität Magdeburg-Stendal, Band 6. Shaker Verlag, Aachen: 173-182.
- Hall M J, Hockin D L and Ellis J B. 1993. Design of flood storage reservoirs. Construction Industry Research and Information Association, CIRIA. London.
- Hammersmark C T. 2002. Hydrodynamic modelling and GIS analysis of the habitat potential and flood control benefits of the restoration of a leveed Delta Island, M.Sc. thesis, Hydrological Sciences, University of California. Davis.
- Helms M, Büchele B, Merkel U and Ihringer J. 2002. Statistical analysis of the flood situation and assessment of the impact of diking measures along the Elbe (Labe) river. Journal of Hydrology 267: 94–114.
- Hess T and Morris J. 1988. Estimating the Value of Flood Alleviation on Agricultural Grassland, Agricultural Water Management 15: 141-153.
- Hesselsink A W, Stelling G S, Kwadijk J C J and Middelkoop H. 2003. Inundation of a Dutch river polder, sensitivity analysis of a physically based inundation model using historic data. Water Resources Research 39(9): 1234.
- Hindmarsh A. 1983. ODEPACK, A Systematized Collection of ODE Solvers, in: Stepleman, R.W. et al. (Ed.) Scientific computing, pages 55–64, North-Holland, Amsterdam.
- Hoes O and Schuurmans W. 2005. Flood Standards or Risk Analyses for Polder Management in the Netherlands, ICID 21st European Regional Conference, Frankfurt (Oder) and Slubice, Germany and Poland.
- Horritt M S. 2005. Parameterisation, validation and uncertainty analysis of CFD models of fluvial and flood hydraulics in the natural environment. In Computational Fluid Dynamics: Applications in Environmental Hydraulics, Bates P D, Lane S N and Ferguson R I (eds). John Wiley & Sons Ltd.. 193-213.

- Howitt J, Baldwin D, Rees G and Williams J. 2007. Modelling blackwater: Predicting water quality during flooding of lowland river forests, *Ecological Modelling* 203: 229-242.
- Horritt M S and Bates P D. 2001. Predicting floodplain inundation: raster-based modelling versus the finite-element approach. *Hydrological Processes* 15: 825-842.
- Horritt M S and Bates P D. 2002. Evaluation of 1D and 2D numerical models for predicting river flood inundation. *Journal of Hydrology* 268: 87-99.
- Hosking J R M and Wallis J R. 1997. Regional frequency analysis: an approach based on L-moments. Cambridge University Press: Cambridge, U.K.
- Huang S, Rauberg H, Apel H, Disse, M and Linden-schmidt K-E. 2007. The effectiveness of polder systems on peak discharge capping of floods along the middle reaches of the Elbe River in Germany. *Hydrol-
ogy and Earth System Sciences* 11: 1391-1401.
- Hydrologic Engineering Center (HEC). 2002. HEC-RAS River Analysis System, User's Manual, Version 3.1. U.S. Army Corps of Engineers. Davis. California.
- IaG. 2006. Gemeinsames Gutachten der Länder Brandenburg und Sachsen-Anhalt zur Flutung der Havelniede-
rung bei Hochwasserereignissen. Ökologische Aspekte der Flutung. (Report of the federal states of Brandenburg and Saxony-Anhalt on the flooding of the Havel River lowland. Ecological aspects of the flooding. In German). Institut für angewandte Gewässerökologie. Unpublished report.
- IKSE. 2003. Aktionsplan Hochwasserschutz Elbe (Elbe flood action plan, in German). International Commis-
sion for the Protection of the Elbe River. <http://elise.bafg.de/servlet/is/5130/>. p. 79.
- IKSE. 2004. Dokumentation des Hochwassers vom Au-
gust 2002 im Einzugsgebiet der Elbe (Documentation of the August 2002 flood at the Elbe River ,in German). International Commission for the Protection of the Elbe River. <http://elise.bafg.de/servlet/is/6889/>. p. 207.
- IKSE. 2005. Die Elbe und ihr Einzugsgebiet (The Elbe Ri-
ver and its catchment, in German). International Com-
mission for the Protection of the Elbe. 258 p.
- IWK. 2003. Untersuchung von Hochwasserretentions-
maßnahmen entlang der Elbe im Bereich der Landkreise Wittenberg und Anhalt-Zerbst (Study on flood re-
tention measures along the Elbe River in the counties Wittenberg and Anhalt-Zerbst, in German). Institut für Wasserwirtschaft und Kulturtechnik. Universität Karls-
ruhe.
- Jaffe D A and Sanders B F. 2001. Engineered Levee Bre-
aches for Flood Mitigation. *Journal of Hydraulic Engi-
neering* 127(6): 471-479.
- Johnson N L, Kotz S and Balakrishnan N. 1994. Continu-
ous Univariate Distributions, 2nd ed., Wiley-
Interscience.
- King I P, Donnell B P, Letter J V, McAnalley W H, Thomas W A and LaHatte C. 2001. User's Guide for RMA2 Version 4.5.
- Knight D W and Shiono K. 1996. River Channel and Floodplain Hydraulics. In: Anderson, M G, Walling, des E and Bates P D (eds.). *Floodplain Processes*. John Wiley & Sons Ltd.
- Knösche R. 2003. Fischökologische und fischereiliche Schäden durch Extremhochwasser (Damages to fish ecology and fishery due to extreme floods, in German).
- Naturschutz und Landschaftspflege in Brandenburg 12 (3): 92-94.
- Kotz S and Nadarajah S. 2000. Extreme value distributions - theory and applications; Imperial College Press.
- KTBL. 2006. Betriebsplanung Landwirtschaft 2006/07 (Agricultural engineering, in German), Kuratorium für Technik und Bauwesen in der Landwirtschaft. Darm-
stadt.
- KTBL. 2007. Standarddeckungsbeiträge (Standard profit margins, in German). Online version, Kuratorium für Technik und Bauwesen in der Landwirtschaft. Darm-
stadt. <http://www.KTBL.de>.
- Kundzewicz Z W. 2008. River floods in the changing cli-
mate – Observations and projections. *Proceedings of the 4th International Symposium on Flood Defence*, 6-
8 May 2008, Toronto, Canada, 141-1 – 141-9.
- Kundzewicz Z, Ulbrich U, Brücher T et al. 2005. Summer Floods in Central Europe – Climate Change Track?, *Natural Hazards* 36: 165- 189.
- Kúzniar P, Popek Z and Zelazo J. 2002. The analysis of possibility of flood risk decreasing on the Middle Vis-
tula River reach. 5th International Conference on Hydro -Science & -Engineering, Warsaw. [http://kfki.baw.de/conferences/ICHE/2002-
Warsaw/ARTICLES/PDF/185C2.pdf](http://kfki.baw.de/conferences/ICHE/2002-Warsaw/ARTICLES/PDF/185C2.pdf)
- LAWA. 1995. Guidelines for Forward-Looking Flood Pro-
tection. Länderarbeitsgemeinschaft Wasser.
- Lecce S. 2000. Seasonality of Flooding in North Carolina, *Southeastern Geographer* 21, 2: 168-175.
- LfL. 2005. Veränderte Landnutzungssysteme in hochwas-
sergefährdeten Gebieten (Land use change in flood prone areas, in German). Schriftenreihe der Sächsi-
schen Landesanstalt für Landwirtschaft, Heft 12.
- LfUG. 2005. Hochwasser in Sachsen – Gefahrenhinweise-
karte (Floods in Saxony – Hazard maps, in German). Sächsisches Landesamt für Umwelt und Geologie.
- LfUG. 2006. Sächsisches Landesamt für Umwelt und Geo-
logie. Gewässerkundliche Statistik. [http://www.umwelt.sachsen.de/de/wu/umwelt/lfug/1
fug-internet/documents/560051_Q2006.pdf](http://www.umwelt.sachsen.de/de/wu/umwelt/lfug/1_fug-internet/documents/560051_Q2006.pdf).
- LHW. 2003. Deutsches Gewässerkundliches Jahrbuch. El-
begebiet. Teil I. Landesbetrieb für Hochwasserschutz und Wasserwirtschaft Sachsen-Anhalt.
- Lindenschmidt K-E. 2006. The effect of complexity on pa-
rameter sensitivity and model uncertainty in river water quality modelling, *Ecological Modelling*, 190: 72–86.
- Lindenschmidt K-E, Huang S and Baborowski M. 2008. A quasi-2D flood modeling approach to simulate sub-
stance transport in polder systems for environment flood risk assessment, *Science of the total environment*, 397(1-3): 86–102.
- McCutcheon S C. 1989. Water quality modeling, Vol. 1 - Transport and surface exchange in rivers, CRC press.
- MEDIS. 2007. Methods for the evaluation of direct and indirect losses. In: RIMAX-Risk Management of Ex-
treme Flood Events. [http://www.rimax-
ho-
chwasser.de/fileadmin/RIMAX/download/Allgemeine
s/rimax_broschuere_auflage2.pdf](http://www.rimax-ho-
chwasser.de/fileadmin/RIMAX/download/Allgemeine
s/rimax_broschuere_auflage2.pdf).
- Merz B, Kreibich H, Thielen A and Schmidtke R. 2004. Estimation uncertainty of direct monetary flood dam-
age to buildings, *Natural Hazards and Earth System Science* 4: 153-163.

- Merz B and Thielen A. 2005. Separating natural and epistemic uncertainty in flood frequency analysis, *Journal of Hydrology* 309: 114-132.
- Merz B, Thielen A and Goch M. 2005. Flood Risk Mapping at the Local Scale: Concepts and Challenges. In: *Flooding in Europe: Challenges, Developments in Flood Risk Management*. Kluwer.
- Merz B, Thielen A and Goch M. 2007. Flood risk mapping at the local scale: concepts and challenges. In: *Flood Risk Management in Europe, Advances in Natural and Technological Hazards Research* 25, Springer, 231 – 251.
- Messner F, Penning-Rowsell E, Green, C et al. 2007. Evaluating flood damages: guidance and recommendations on principles and methods. http://www.floodsite.net/html/partner_area/project_docs/T09_06_01_Flood_damage_guidelines_D9_1_v2_2_p44.pdf.
- Meyer V and Messner F. 2005. National Flood Damage Evaluation Methods, A Review of Applied Methods in England, the Netherlands, the Czech Republic and Germany. UFZ-Discussion Papers 21.
- Meyer V, Scheuer S and Haase D. 2008. A multicriteria approach for flood risk mapping exemplified at the Mulde river, Germany. *Natural Hazards*.
- Minh Thu P T. 2002. A hydrodynamic-numeric model of the river Rhine. Dissertation. University of Karlsruhe.
- MLUR (Ed.). 2007. Nutzung von Biomasse als Gärsubstrate (Use of biomass as a substrate for fermentation, in German). 26. Fachtagung Acker- und Pflanzenbau. Landesamt für Verbraucherschutz, Landwirtschaft und Flurneuordnung Brandenburg.
- Munk H-H. 2005. Das Gesetz zur Verbesserung des vorbeugenden Hochwasserschutzes (The act to improve preventive flood control, in German). *Wasser und Abfall* 5: 20-23.
- MURL. 2000. Hochwasserschadenpotentiale am Rhein in NRW (Flood damage potential at the River Rhine in North Rhine-Westfalia, in German). Ministerium für Umwelt, Raumordnung und Landwirtschaft des Landes Nordrhein-Westfalen. Unpublished.
- Neubert G and Thiel R. 2004. Schadenpotentiale in der Landwirtschaft (Damage potential in agriculture, in German). In: Bronstert, A. (ed.) Möglichkeiten zur Minderung des Hochwasserrisikos durch Nutzung von Flutpoldern an Havel und Oder, Brandenburgische Umweltberichte 15. Potsdam.
- O'Brien J S. 2006. FLO-2D: Users Manual Version 2006.01. http://www.flo2d.com/v2006/Documentation/Manual_Main_2006.pdf
- OECD. 2002. Evaluation and Aid Effectiveness - Glossary of Key Terms in Evaluation and Results Based Management. Organisation for Economic Co-operation and Development. <http://www.oecd.org/dataoecd/29/21/2754804.pdf>. 37p.
- Penning-Rowsell E, Johnson C, Tunstall S et al. 2003. The benefits of flood and coastal defence: techniques and data for 2003, Flood Hazard Research Centre, Middlesex University.
- Petrow T, Merz B, Lindenschmidt K-E and Thielen A. 2007. Aspects of seasonality and flood generating circulation patterns in a mountainous catchment in south-east Germany, *Hydrology and Earth System Sciences* 11: 1-14.
- Petzold L. 1983. Automatic Selection of Methods for Solving Stiff and Nonstiff Systems of Ordinary Differential Equations, *Siam J. Sci. Stat. Comput.*, 4: 136–148.
- Peukert V. 1970. Untersuchungen über den Einfluss von überstaute Flächen auf die Wasserqualität von Talsperren (Investigations on the impact of inundated land on the water quality of reservoirs, in German), *Fortschritte der Wasserchemie und ihrer Grenzgebiete*, 12: 66–82.
- Pivot J-M, Josien E and Martin P. 2002. Farm adaptation to changes in flood risk: a management approach, *Journal of Hydrology* 267: 12-25.
- Plate E. 2002. Flood risk and flood management. *Journal of Hydrology*. 267: 2-11.
- R Development Core Team. 2007. R: A Language and Environment for Statistical Computing, R Foundation for Statistical Computing, Vienna, Austria, ISBN 3-900051-07-0, URL <http://www.R-project.org>.
- Rátoky I and Szlávík L. 2001. Perfection of Operation Control for the Emergency Reservoirs in the Körös Valley. *Periodica Polytechnica Ser. Civ. Eng.* 45(2): 93-119.
- Reichert P, Borchardt D, Henze M, Rauch W, Shanahan P, Somlyody L and Vanrolleghem P A. 2001. River water quality model No. 1, IWA Publishing.
- Romero J, Hipsey M, Antenucci J and Hamilton D. 2004. Computational Aquatic Ecosystem Dynamics Model (CAEDYM v.2.1), Science Manual, Centre for water research, University of Western Australia.
- Roth D and Warner J. 2007. Flood risk, uncertainty and changing river protection policy in the Netherlands: The case of “calamity polders”. *Tijdschrift voor Economische en Sociale Geografie* 98, 4: 519-525.
- Rungo M and Olesen K W. 2003. Combined 1- and 2-dimensional flood modeling. 4th Iranian Hydraulic Conference, 21-23 Oct, Shiraz, Iran.
- Schmidt M. 1957. Gerinnehydraulik (Channel hydraulics, in German). VEB Verlag Technik Berlin und Bauverlag GmbH. Wiesbaden.
- Shanahan P, Henze M, Koncsos L, Rauch W, Reichert P, Somlyody L and Vanrolleghem P. 1998. River Quality Modelling: II. Problems of the Art. IAWY Biennial International Conference, Vancouver, British Columbia, Canada, 21-26 June 1998.
- Silva W, Dijkman J and Loucks D. 2004. Flood management options for the Netherlands. *International Journal of River Basin Management* 2(2): 101-112.
- Sivapalan M, Blöschl G, Merz R and Gutknecht D. 2005. Linking flood frequency to long-term water balance: incorporating effects of seasonality, *Water Resources Research* 41. doi:10.1029/2004WR003439.
- Smith K and Ward R. 1998. Floods: Physical Processes and Human Impact. John Wiley & Sons. Chichester.
- Stelling G and Duinmeijer S. 2003. A staggered conservative scheme for every froude number in rapidly varied shallow water flows. *International Journal for Numerical Methods in Fluids* 43: 1329-1354.
- Tayefi V, Lane S N, Hardy R J and Yu D. 2007. A comparison of one- and two-dimensional approaches to modeling flood inundation over complex upland floodplains. *Hydrological Processes* 21 (23): 3190-3202.
- Todorovic P and Woolhiser D. 1972. On the Time When the Extreme Flood Occurs. *Water Resources Research* 8, 6: 1433-1438.

- USDA. 1978. Economics – Basic Data for Evaluating Floodwater Damages to Crops and Pastures in the Northeast, Technical Note, United States Department of Agriculture.
- Werner M. 2001. Impact of grid size in GIS based flood extent mapping using a 1-D flow model. Physics and Chemistry of the Earth, Part B: Hydrology, Oceans and Atmosphere 26: 517-522.
- Werner M. 2004. Spatial flood extent modeling – A performance based comparison. Ph.D thesis, Delft University, Netherlands.
- Werner M, Hunter N M and Bates P D. 2005. Identifiability of distributed floodplain roughness values in flood extent estimation. Journal of Hydrology 314: 139-157.
- Wolter C, Arlinghaus R, Grosch U A and Vilcinskas A. 2003. Fische & Fischerei in Berlin (Fishes and fishery in Berlin, in German). Zeitschrift für Fischkunde, Suppl. 2: 1-156.
- Wurms S and Westrich B. 2008. Targeted Retention of contaminated Sediment in a green Flood Retention Reservoir. Proceedings of the 4th International Symposium on Flood Defence, 6-8 May 2008, Toronto, Canada, 140-1 – 140-8.
- YRFCMP. 2003. Literature Review for the Development of a Socio-Economic Impacts Assessment Procedure to be applied to the flooding of Qianliang Hu Detention Basin, Hunan Province, China, Yangtze River Flood Control and Management Project.

ACKNOWLEDGEMENTS

After the large flood in Central Europe in August 2002 various research projects on flood risk management were initiated. I was lucky to get involved in two interesting projects. In the first project a small enthusiastic interdisciplinary group took up the challenge of producing reasonable results in a very short time. I would like to thank all team colleagues for their engagement, particularly David Kneis and Martin Gocht. The second project gave me the opportunity to gain insights into how a large successful EU project is coordinated, get to know the leading flood researchers in Europe and be a small part of the large FLOODsite family.

I would like to thank all those who supported me during my PhD time. First of all, thanks to Axel Bronstert for giving me the opportunity to work on an interesting and up-to-date topic and letting me have all my freedom in doing so. I am also grateful to the other members of the defence committee, in particular Bruno Merz and Robert Jüpner for taking the time to read this thesis.

I will keep many valuable memories of the PhD time that I don't want to miss, like the exceptional experience of teaching twenty Chinese in Budapest about German flood risk management or of carrying heavy GPS instruments in suffocating heat for many hours to improve an out-dated polder DEM a little bit.

During his one-year stay at our institute I closely co-operated with Chandranath Chatterjee. His thoughtfulness, reliability and heartiness made this time inspiring and enjoyable, both scientifically and personally. Publishing papers can be a long and at times exhausting process. I would especially like to thank Chandranath Chatterjee, David Kneis and Karl-Erich Lindenschmidt for their encouraged work to bring this process to success.

I would like to thank our group at the Institute of Geoecology for creating an enjoyable atmosphere at work and on many other occasions. I also thank Annegret Thieken, Heidi Kreibich and Theresia Petrow and others from the Engineering Hydrology group at GFZ Potsdam for interesting discussions. Special thanks to Sibylle Itzerott for her continuing support, the company on the field trip and nice chats while inline skating.

I am thankful to the Danish Hydraulic Institute (DHI) for providing an evaluation copy of the MIKE software and the German DHI group for giving support when I had urgent questions.

I am most grateful to my family for their love and support and in particular to my parents for many hours of babysitting. Finally, I would like to thank Micha for being a wonderful husband and father, encouraged scientist and lecturer, patient listener, accompanying person, friend and lots more.

CURRICULUM VITAE AND LIST OF PUBLICATIONS

Saskia Förster was born on 5th November 1976 in Potsdam. After completing secondary school in 1996, she studied Geoecology at the University of Potsdam including a two semester stay at the University of Southampton, UK. During her studies she specialised in GIS and remote sensing techniques. After graduating, she started her PhD work at the Institute of Geoecology at the University of Potsdam in 2003. She was involved in two research projects on flood risk management, viz., “Möglichkeiten zur Minderung des Hochwasserrisikos durch Nutzung von Flutpoldern an Havel und Oder” funded by the German Ministry of Education and Research and “Integrated Flood Risk Analysis and Management Methodologies (FLOODsite)” funded under the Sixth Framework Program of the European Commission. Apart from the project and PhD work she gave GIS courses and supervised students in their study projects.

Reviewed journal articles

Kneis D, **Förster** S and Bronstert A. Simulating water quality in a flood detention area using models of different spatial discretisation. Ecological Modelling. (in preparation)

Förster S, Kuhlmann B, Lindenschmidt K-E and Bronstert A. 2008. Assessing flood risk for a rural detention area. Nat. Hazards Earth Syst. Sci., 8, 311–322.

Chatterjee C, **Förster** S and Bronstert A. 2008. Comparison of Hydrodynamic Models of Different Complexities to Model Floods with Emergency Storage Areas. Hydrological Processes. Published online, DOI: 10.1002/hyp.7079.

Förster S, Chatterjee C and Bronstert A. 2008. Hydrodynamic Simulation of the Operational Management of a Proposed Flood Emergency Storage Area at the Middle Elbe River. River Research and Applications. Published online, DOI: 10.1002/rra.1090.

Förster S, Kneis D, Gocht M and Bronstert A. 2005. Flood Risk Reduction by the Use of Retention Areas at the Elbe River. Intl. Journal of River Basin Management, 3 (1), 21-29.

Non-reviewed articles

Förster S, Chatterjee C and Bronstert A. 2007. Investigation on the Operation of a Proposed Emergency Flood Storage Area at the Middle Elbe River in the Context of the Integrated Project FLOODsite. ERWG Letter, Land and Water Management in Europe. 17, 4-5.

Conference proceedings and papers

Förster S and Bronstert A. 2008. Assessment of hydraulic, economic and ecological impacts of flood polder management – A case study from the Elbe River, Germany. Floodrisk2008. 30 September – 2 October 2008, Oxford, UK.

Förster S, Kneis D and Bronstert A. 2008. Sauerstoffhaushalt im Flutungspolder. Tag der Hydrologie, 27. - 28. März 2008, Hannover, Germany.

Förster S, Chatterjee C and Bronstert A. 2007. Reducing flood risk by emergency storage - A case study from the Elbe River. In: Schanze J (Ed.). 2007. Flood Risk Management Research. From ex-

treme events to citizens involvement. Proceedings of the European Symposium on Flood Risk Management Research, 6 - 7 February 2007, Dresden, Germany, 217-219.

Förster S, Chatterjee C and Bronstert A. 2006. Hochwasserüberschwemmungssimulation mittels hydrodynamischer Modellierung für das Management eines geplanten Polderstandortes an der Mittleren Elbe. In: Jüpner R (Ed.). Beiträge zur Konferenz „Strategien und Instrumente zur Verbesserung des vorbeugenden Hochwasserschutzes“. Internationale Konferenz, 23. - 25. November 2006, Tangermünde, Germany. Schriftenreihe des Instituts für Wasserwirtschaft und Ökotechnologie der Universität Magdeburg-Stendal, Band 6. Shaker Verlag, Aachen, 83-92.

Förster S, Chatterjee C, De Medina V, Bateman A and Bronstert A. 2006. Flood Inundation Simulation using Hydrodynamic Models of Different Complexity for the Management of a Potential Polder at the Middle Elbe River, Germany. 3rd International Symposium on Integrated Water Resources Management, 26 – 28 September 2006, Bochum, Germany.

Förster S and Bronstert A. 2005. Benefits and Costs of Using Detention Areas for Flood Risk Reduction at the Elbe River. In: van Alphen J, van Beek E and Tall M (Eds.). 2005. Floods from Defence to Management. 3rd International Symposium on Flood Defence, 25 - 27 May 2005, Nijmegen, The Netherlands, 285.

Förster S, Kneis D, Gocht M and Bronstert A. 2004. Flood Risk Reduction by Use of Detention areas at the Elbe River. EGU General Assembly, 25 – 30 April 2004, Nice, France.

Förster S, Kneis D and Bronstert A. 2004. Untersuchung einer gesteuerten Flutung der Unteren Havelliederung zur Minderung des Hochwasserrisikos an der Elbe. Tag der Hydrologie, 22. - 23. März 2004, Potsdam, Germany.

AUTHOR'S DECLARATION

I prepared this dissertation without illegal assistance. The work is original except where indicated by special reference in the text and no part of the dissertation has been submitted for any other degree. This dissertation has not been presented to any other University for examination, neither in Germany nor in another country.

Saskia Förster

Potsdam, August 2008